RELIABILITY AND INTEGRITY MANAGEMENT OF OCEAN STRUCTURES

By

Jyoti Prasad Bhandari
B.Eng. (Hons) Ocean Engineering

Submitted in fulfilment of the requirements for the Degree of
Doctor of Philosophy
National Centre for Maritime Engineering and Hydrodynamics
Australian Maritime College
University of Tasmania
June 2018

Dedicated to my
Wife-Ganga Bhandari, son-Jayden Bhandari, son-Austin Jyoti Bhandari, my parents
Thagu & Deuki and brothers-Tulsi and Hari

[Page intentionally left blank]

SUMMARY

Corrosion is a major cause of deterioration in marine and offshore structures. It affects the life of process equipment and pipelines. Over the time corrosion can result in structural failure, leakage, product loss, environmental pollution, and the loss of life. Pitting corrosion is regarded as one of the most hazardous forms of corrosion it causes structural failure and its effects on offshore structures are reported to be catastrophic. Hence, significant attention should be given to predict the occurrence of pitting corrosion in offshore structures and the adequate measures should be taken to prevent as well as control the consequences. Pitting corrosion has been studied for several decades and considerable understanding of the pitting phenomenon has been learned. However, in depth knowledge of pitting modelling and pitting measurement is still lacking. This thesis advances these developments by proposing several novel extensions in the areas and provides a complete package. This thesis is also aimed to make a distinctive contribution within the area of safety and reliability of offshore structures susceptible to pitting corrosion.

This thesis contains seven chapters. The first chapter provides the introduction and general structure of the thesis. In the second chapter, a highly systemized and thorough literature review on pitting corrosion was completed and the knowledge gaps were identified. This chapter reviews and analyses the current understanding of the pitting corrosion mechanism and investigates all possible factors that can cause pitting corrosion. Furthermore, different techniques employed by scientists and researchers to identify and model the pitting corrosion are also reviewed and analysed. The third chapter presents a development of a novel methodology for an optimum maintenance programme by integrating a dynamic RBM based reliability approach with risk assessment strategy. The developed methodology is applied to a case study involving an offshore oil and gas production facility. The application of the methodology has proven to be a high degree of prediction capability, which increase the reliability of the equipment and also optimizes the cost of maintenance. A sensitivity analysis proved that pitting corrosion is a predominant and critical factor for structural deterioration. While the fourth chapter proposes a novel probabilistic methodology to precisely predict the depth of pitting corrosion for structural steel in marine and offshore

environments. The propose Bayesian network model combines an understanding of corrosion phenomenological model and empirical model calibrated using real-world data. A case study, which exemplifies the application of methodology to predict the pit depth of structural steel in long-term marine environment, is also presented in fourth chapter. The result shows that the proposed methodology succeeds in predicting the time-dependent, long-term anaerobic pitting corrosion depth of structural steel in different environmental and operational conditions. In the fifth chapter, an accelerated laboratory experiment for pitting corrosion was conducted in order to understand the practical significance of pitting mechanism, and to realistically predict the long-term service life of the steel structures. A series of pitting corrosion tests on stainless steel specimen with different thickness were conducted and data were statistically evaluated. This chapter also presents the modified ASTM G48 procedure. Similarly, the sixth chapter presents an experimental and numerical modelling of the stainless-steel specimen with varying thickness subjected to different level of pitting corrosion deterioration are considered. Numerical investigations using Finite Element Analysis (FEA) were performed using corroded and un-corroded steel specimen to predict the ultimate tensile strength, thereby for casting its prevention for the pitting corrosion degradation. The ultimate strengths for both intact and corroded specimen obtained using numerical method are validated with experimental data. The numerical analysis proved to produce excellent result with minimal difference when comparing with experimental result. Finally, chapter 7 includes the conclusions of the thesis.

Keywords: Reliability, Pitting Corrosion, Risk-based maintenance, Bayesian network, Offshore Structures, Pit Depth, Bayesian Network, Phenomenological model, ASTM G48, Stainless steel, Weibull distributions, Tensile test, Numerical Study

[Page intentionally left blank]

[Page intentionally left blank]

Approvals

Doctor of Philosophy Dissertation
Approved by

Prof. Faisal I. Khan

Vale Research Chair of Process Safety and Risk Engineering
Faculty of Engineering and Applied Science
Memorial University of Newfoundland

Signature: Date: 01/02/2018

Dr. Rouzbeh Abbassi
Senior Lecturer,
School of Engineering, Faculty of Science and Engineering,
Macquarie University, Sydney, NSW, Australia
Adjunct Senior Lecturer,
National Centre for Maritime Engineering and Hydrodynamics
Australian Maritime College
University of Tasmania

Signature: Date: 23/01/2018

Dr. Vikram Garaniya
Senior lecturer, Associate Head Research (AHR)
National Centre for Maritime Engineering and Hydrodynamics,
Australian Maritime College,
University of Tasmania

Signature:

Date: 25/01/2018

Dr. Roberto Ojeda
Graduate Research Coor**d**inator, Senior lecturer
National Centre for Maritime Engineering and Hydrodynamics
Australian Maritime College
University of Tasmania

Signature: Date: 29/01/2018

[Page intentionally left blank]

Declaration and Statements

Declaration of Originality

I declare that this is my own work and has not been submitted in any form for another degree or diploma at any university or other institution of tertiary education. Information derived from the published or unpublished work of others has been duly acknowledged in the text and a list of references if given.

Signature: Date: 29/01/2018

Authority of Access

This thesis may be made available for loan and limited copying in accordance with the Copyright Act 1968.

Statement Regarding Published Work Contained in the Thesis

The publishers of the papers comprising Chapters 2 to 6, inclusive, hold the copyright for that content, and access to the material should be sought from the respective journals. The remaining non-published content of the thesis may be made available for loan and limited copying and communication in accordance with the above Statement of Access and the Copyright Act 1968.

[Page intentionally left blank]

Thesis by Journal Articles

The following four published and one under review journal articles constitutes the content of this thesis.

1) Chapter 2: **Bhandari J,** Khan F, Abbassi R, Garaniya V, and Ojeda R. (2015). Modelling of pitting corrosion in marine and offshore steel structures - A technical review", Journal of Loss Prevention in The Process Industries, 37: 39-62. doi.org/10.1016/j.jlp.2015.06.008.

2) Chapter 3: **Bhandari, J**, Arzaghi, E, Abbassi R, Garaniya V, and Khan F. (2016). Dynamic risk-based maintenance for offshore processing facility. *Process Safety Progress*. doi: 10.1002/prs.11829.

3) Chapter 4: **Bhandari J,** Khan F, Abbassi R, Garaniya V. (2017). Pitting Degradation Modelling of Ocean Steel Structures using Bayesian Network. *Journal of Offshore Mechanics and Arctic Engineering, 139*(5): 2-11. doi: 10.1115/1.4036832.

4) Chapter 5: **Bhandari J,** Lau S, Abbassi R, Garaniya V, Ojeda R, Lisson D, Khan F. (2017). Accelerated pitting corrosion test of 304 stainless steel using ASTM G48; Experimental investigation and concomitant challenges. *Journal of Loss Prevention in the Process Industries, 47*: 10-21. doi: 10.1016/j.jlp.2017.02.025

5) Chapter 6: **Bhandari J,** Khan F, Abbassi R, Garaniya V, and Ojeda R, Experimental and Numerical Strength Assessment of Steel Specimen subjected to pitting Corrosion,

Journal Article and conference proceeding not included in this thesis, but can be accessed as supplementary material.

1) **Bhandari J**, Khan F, Abbassi R, Garaniya V, and Ojeda, R. *Reliability assessment of offshore asset under pitting corrosion using Bayesian Network.* Proceedings of Corrosion 2016, 6-10 March 2016, Vancouver, Canada, pp. 1-15. 2016.

2) Abbassi R, **Bhandari J,** Khan F, Garaniya V, and Chai, S. (2016). Developing a Quantitative Risk-based Methodology for Maintenance Scheduling Using Bayesian Network. *Chemical Engineering Transactions, 48*: 235-240.

3) Pui G, **Bhandari J,** Arzaghi E, Abbassi R, Garaniya V. (2017). Risk-based Maintenance of Offshore Managed Pressure Drilling (MPD) Operation. *Journal of Petroleum Science and Engineering*, 159, 513-521

[Page intentionally left blank]

Statement of Co-Authorship for Journal Articles

The following people and institutions contributed to the publication of the work undertaken as part of this thesis.

- Jyoti Prasad Bhandari, University of Tasmania, TAS, Australia (PhD Candidate)
- Professor Faisal Khan, Memorial University of Newfoundland, St John, Canada (Author 1)
- Dr Rouzebeh Abbassi, Macquarie University, Sydney, NSW, Australia (Author 2)
- Dr Vikram Garaniya, University of Tasmania, TAS, Australia (Author 3)
- Dr Roberto Ojeda, University of Tasmania, TAS, Australia (Author 4)

Performed the case studies: Bhandari
Analysed the data: Bhandari
Wrote the manuscript: Bhandari
Manuscript evaluation and submission: Khan, Abbassi, Garaniya, Ojeda

Paper 1 (Chapter 2): Modelling of pitting corrosion in marine and offshore steel structures - A technical review.
Jyoti Bhandari, Rouzbeh Abbsssi, Faisal Khan, Vikram Garaniya & Roberto Ojeda contributed to conceived idea for this technical review.
Percentage of Contribution: Candidate 70%, Rouzbeh Abbassi 8%, Faisal Khan 8%, Vikram Garaniya 8%, Roberto Ojeda 6%.

Paper 2 (Chapter 3): Dynamic risk-based maintenance for offshore processing facility.
Jyoti Bhandari, Rouzbeh Abbsssi, Faisal Khan, Vikram Garaniya & Roberto Ojeda contributed to conceived idea for development of novel methodology and Application.
Percentage of Contribution: Candidate 74%, Rouzbeh Abbassi 10%, Faisal Khan 8%, Vikram Garaniya 8%

Paper 3 (Chapter 4): Pitting Degradation Modelling of Ocean Steel Structures using Bayesian Network
Jyoti Bhandari, Rouzbeh Abbsssi, Faisal Khan, Vikram Garaniya & Roberto Ojeda contributed to conceived idea for development of novel methodology and Application.
Percentage of Contribution: Candidate 70%, Rouzbeh Abbassi 8%, Faisal Khan 8%, Vikram Garaniya 8%, Roberto Ojeda 6%.

Paper 4 (Chapter 5): Accelerated pitting corrosion test of 304 stainless steel using ASTM G48; Experimental investigation and concomitant challenges.
Jyoti Bhandari, Rouzbeh Abbsssi, Faisal Khan, Vikram Garaniya & Roberto Ojeda contributed to conceived idea for development of design, testing and data interpretation.
Percentage of Contribution: Candidate 70%, Rouzbeh Abbassi 8%, Faisal Khan 8%, Vikram Garaniya 8%, Roberto Ojeda 6%.

Paper 5 (Chapter 6): Experimental and Numerical Strength Assessment of Steel Specimen subjected to pitting Corrosion

Jyoti Bhandari, Rouzbeh Abbsssi, Faisal Khan, Vikram Garaniya & Roberto Ojeda contributed to conceived idea for development of design, testing and data interpretation.

Percentage of Contribution: Candidate 70%, Rouzbeh Abbassi 4%, Faisal Khan 4%, Vikram Garaniya 4%, Roberto Ojeda 18%.

We the undersigned agree with the above stated "proportion of work undertaken" for each of the above published (or submitted) peer-reviewed manuscripts contributing to this thesis
Signed:

Prof. Faisal Khan
Professor Marine and Offshore Engineering
Director, Centre for Risk, Integrity and Safety Engineering (C-RISE),
Canada Research Chair (Tier I) in Safety and Risk Engineering,
Head, Department of Process Engineering,
Faculty of Engineering and Applied Science, Memorial University of Newfoundland,
St. John's, NL, Canada

Signature Date: 28/06/2018

Associate Professor Shuhong Chai
Acting Principal
National Centre for Maritime Engineering and Hydrodynamics,
Australian Maritime College, University of Tasmania,
Launceston, Tasmania, Australia

Signature: Date: 29/06/18

Acknowledgement

I would like to express my sincere and profound sense of gratitude and respect to my supervisor's Professor Faisal Khan, Dr Rouzbeh Abbassi, Dr Vikram Garaniya, and Dr Roberto Ojeda for their expert guidance and untiring support throughout my research at University of Tasmania (UTAS) of Launceston Tasmania. Without their encouragement and advice, this thesis might not have been completed successfully. I am especially thankful to the respected Professor Faisal Khan for his friendship and sharing his vast experience and knowledge over past six years. Professor Khan has been a great supervisor; a good friend and a part of my family members.

Special thanks must go to:

- To Denis Lisson, Jock Ferguson, Michael Underhill, Samantha Lau, and Ehsan Arzaghi from the Australian Maritime College for their support during the experimental work.
- To respected Professor Robert Melchers from University of Newcastle for his expert advice and direction in corrosion studies.
- To AMC, UTAS for its generous scholarship provided along with all the high-quality support programs, workshops and opportunities.
- To the grant, received by Dr Rouzbeh Abbassi from the University of Tasmania (2016) under the Research Enhancement Grants Scheme (REGS) for experimental analysis.
- My friends for their companionship.

Lastly, I would like to take an opportunity to thank my wife (Ganga) for her courageous support and care allowing me to successfully complete my PhD.

[Page intentionally left blank]

List of Abbreviations

WCO	World Corrosion Organization
GDP	Gross Domestic Product
GNP	Gross National Product
HSR	Hydrocarbon Release Statistics
BN	Bayesian Network
RBM	Risk Based Maintenance
AHP	Analytic Hierarchy Process
FTA	Fault tree analysis
ET	Event Tree
CPT	Conditional Probability Table
RN	Root Nodes
ALARP	As low as reasonably possible
USEPA	Dutch acceptance criteria
OREDA	Offshore reliability data
XPS	X-ray Photoelectron Spectroscopy
CPT	Critical pitting temperature
SRB	Sulphate–Reducing Bacteria
PRE_N	Pitting Resistance Equivalent
ROV	Remotely operated vehicles
NDT	Non-destructive testing
VT	Visual and optical Testing
AET	Acoustic Emission Testing

IRT	Infrared and thermal Testing
AES	Auger electrons spectroscopy
XPS	X-ray photo-electron spectroscopy
SIMS	Secondary ion mass spectrometry
ANNs	Artificial Neural Networks
BM	Block Maxima
POT	Peak-Over-Threshold
NHPP	Non-Homogenous Poisson Process
EVA	Extreme Value Analysis
KDE	Kernel Density Estimator
AMISE	Asymptotic approximation of mean integrated squared error
SEM	Scanning electron microscope
EDX	Energy-dispersive X-ray spectroscopy
MLE	Maximum likelihood estimator
GEV	Generalized extreme value
FEA	Finite Element Analysis
USR	Ultimate strength reduction
DOP	Degree of pitting intensity
APDL	ANSYS parametric design language
GUI	Graphical user interface
HPC	High Performance Computing
SMP	Shared-Memory Parallel
MISO	Multilinear isotropic

Table of Contents

List of Figures

List of Tables

[Page intentionally left blank]

1 Introduction

1.1 Background and Research Significance

The scientific exploration and exploitation of the ocean depth is currently proceeding at a greatly accelerated rate [1]. Consequently, there has been particularly rapid progress in the development of infrastructures for deep-ocean investigation and underwater activities. The oil and gas industries have built a large number of offshore platforms, pipelines, ships, and underwater storage and shore facilities. However, the structural reliability of these structures is yet to be fully understood [2]. These marine and offshore structures are typically constructed from steel and have the highest rate of critical incidents due to corrosion deterioration [3]. Corrosion is well defined as the destructive attack on a material by reaction with environment [4-8]. This material degradation results in loss of mechanical properties of the structure such as strength, ductility and impact strength. Material degradation leads to loss of material and, at times, to ultimate failure [4]. Further, corrosion is also of major economic significance. The World Corrosion Organization (WCO) estimates that the annual cost of corrosion worldwide is around $US2.4 trillion (3% of the world's GDP) [9]. The economic cost for all forms of corrosion in advanced economies such as the United States of America was recently estimated at around 4% of gross national product (GNP) [10]. The environmental cost of corrosion can also be high; according to the Offshore Hydrocarbon Release Statistics and Analysis report 2002-2003 (HSR) [11], a total of 2313 hydrocarbon releases were reported from offshore facilities in nine and half years. The most common causes were 'mechanical failure' due to corrosion and other related degradation. A total of 1034 incidents (44.7% of the total incidents) were caused as a result of corrosion [11, 12].

Amongst all types of corrosion, pitting is the most common and damaging form of corrosion in marine and offshore structures [13]. Pitting corrosion is very dangerous, widespread, and difficult to detect; hence, it has been a matter of great concern to marine and offshore industries for several years [14]. Pitting corrosion is defined as a localized dissolution of metals that occurs due to the breakdown of the protective passive film - notably the protective coating and paint on metal surfaces [5, 15-17]. Pitting corrosion can also occur during active dissolution if certain sections of the sample are more

susceptible and dissolve faster than the rest of the surface [18]. Szklarska et al. [17] describes pitting as a form of localized corrosion in which metal is removed preferentially from vulnerable areas of the surface. To be precise, the dissolutions lead to the formation of cavities in passivated metals or alloys, which are exposed to solutions containing aggressive anions. Most pitting failures in the offshore sectors are caused by chloride and chloride containing ions. It is very likely for pitting to occur when protective measures such as paint coating, galvanizing or cathodic protection are ineffective [19]. Pitting is one of the most vicious and insidious forms of corrosion; the attack is extremely localized resulting in holes in the structure and thereby causing failures [19].

History shows that pitting corrosion is a dominant cause of structural failure in marine and offshore sectors. The reason for this is due to the well-known fact that seawater is an aggressive corrosive environment and the structures are generally fabricated with alloy steel which favours pitting corrosion. The pitting in these structures is often very severe, not only under sustained immersed conditions, but also under general exposure to atmospheric conditions [14]. The effects of pitting corrosion can be catastrophic, as illustrated by several incidents reported in the offshore oil and gas sectors. In March 1965, a natural gas pipeline exploded in Louisiana killed 17 people including 9 children. The heat from the explosion was very intense; 6 cars and 3 trucks melted, and 5 houses were scattered over a large area. In July 1988, there was a massive leakage of gas condensate on Piper Alpha due to pitting corrosion which, when it ignited, caused an explosion leading to large oil fires. The scale of the disaster was enormous, killing 167 people on board, and it is regarded as the deadliest accident in the history of the oil and gas industry [3]. In April 1992 a sewer explosion in Guadalajara, Mexico killed 215 people. In this incident a series of blasts damaged 1600 buildings and injured 1500 people [20]. Roberge et al. [20] described it as being one of the most catastrophic accidents resulting from a single pit. A recent example of pitting corrosion-related failure is the BP ULA accident in Norway. In September 2012, an estimated 125 barrels of oil and 1,600 kilograms of gas leaked at the North Sea platform due to pit in a valve; despite there being no injuries, production was stopped for 67 days [3]. Similarly, in December 2012 a buried, half a meter diameter, high-pressure natural gas pipeline operated by Columbia Gas Transmission ruptured due to pitting corrosion. There were

no fatalities; however, several houses were damaged and about 2 million standard cubic meters of natural gas was released and burned. The total cost was expected to be about $9 million dollars [21]. Consequently, significant attention should be given to predict the occurrence of pitting corrosion in offshore structures and adequate measures should be taken to prevent and control the consequences.

Pitting corrosion in offshore steel structures has particular importance where containment is critical, such as for pressure vessels, boilers, turbine blades and for metallic containers for toxic materials. It is also significant for localized structural strength in piping, tanks, ships and marine structures [22, 23]. Melchers et al. [23] stressed the importance of pitting corrosion knowledge as being crucial for the marine and offshore sectors. They recommended a deep knowledge of pitting corrosion - its effects, and the application of preventative methods - as this will assist in reducing material losses resulting from same [24]. This will also improve the safety of operating equipment [22]. Pitting corrosion has been studied for several decades and considerable understanding of the pitting phenomenon has been generated. However in depth knowledge of pitting modelling and pitting measurement is still lacking [18]. There is also a limited understanding of why the pitting corrosion rate is not constant over time and why data tends to be scattered. Hence, it is necessary to review what actually happens when a steel surface is exposed to natural seawater and how this process progresses with time [10].

Many researchers have studied factors affecting pitting corrosion in marine and offshore environments [5, 15, 25-30]; however, the factors investigated are very limited and there is still a potential to study them more thoroughly. Traditional corrosion models are of poor quality. Although the conventional models provide a strong understanding of corrosion process, they are often hard to test in real-world engineering applications. These models are useful for specific site or operating conditions, they still carry high uncertainty associated with each data points as some data point might be wrong owing to errors in observation or data processing [24]. Hence it is essential to use a Bayesian statistics to develop corrosion loss/pitting depth model considering ‘prior’ knowledge of the corrosion process involved together with data used to calibrate them in the real world. Melchers [24] also emphasized on the importance of developing probabilistic models such as Bayesian statistics in the future model for predicting corrosion

loss/pitting depth. In this context, this project aims to increase the safety and reliability of ocean structures by studying all possible factors that can cause pitting corrosion and by developing dynamic risk based maintenance strategy for pitting corrosion, a probabilistic model for predicting the pit depth, laboratory based experimentation for pitting corrosion and destructive testing and computational analysis is also carried out to better understand the practical perception of pitting corrosion process. The further improvement of this work could be analysing effect of pitting corrosion on systems such as the structural elements of marine and offshore structures, Static process equipment and Rotating machinery. The influence of mechanical loads on pit growth kinetics as well as a criterion of transformation of pit into fatigue crack is also considered as a further improvement of this work.

The output of this research project will contribute to knowledge enhancement in the academic research community and also to offshore industrial society

1.2 Research Overview

1.1.1 RESEARCH AIM

"*To improve the safety and reliability of the ocean structures susceptible to pitting corrosion by developing a predictive model and applying risk-based methodology to assess the remaining life of the offshore asset."*

1.1.2 RESEARCH QUESTIONS

This research question is divided into several sub-questions as follows:

- How to identify wheather the existing offshore structures are still safe? If it is safe how many years before it becomes unsafe?
- How often and at what cost the offshore structure should plan for the maintenance in order to prevent the structural failure due to pitting corrosion?
- How can future deterioration of the offshore structures be predicted to increase the safety and remaining life of the offshore asset?
- How can a probabilistic/mathematical model be developed to predict the long-term pit depth/pit density in marine and offshore environments?
- How to precisely estimate the failure and strength performance of steel specimens subjected to pitting corrosion?

1.1.3 RESEARCH OBJECTIVES

This research focuses on the reliability and integrity management of the offshore steel structures under the attack of pitting corrosion. An understanding of the contributing factors of pitting corrosion and how these factors can make the expected behaviour predictable. Developing a model to predict pitting behaviour in marine environments is a need to reduce failure probabilities, optimize maintenance and inspection schedules, and to aid in material selection for this type of application. The purpose of the research is to study the pitting mechanism in detail, to investigate how pitting characteristics

such as rate, depth, density and interfacial distance cause structural failure. Developing and validating the predictive models using existing and newly developed data are also considered. Both experimental and numerical testing procedures are conducted to investigate the structural failure due to pitting. The experimental and Finite Element Analysis (FEA) are conducted for steel specimens exposed to marine environments to evaluate the failure and strength performance. This research project is conducted in five stages: detail literature review on pitting corrosion degradation mechanism, development of risk–based maintenance and case study, pit depth modelling using probabilistic approach, experimental studies, finite element modelling and validation to destructive testing. This study is performed based on following objectives:

- To achieve an in-depth understanding of the pitting corrosion mechanism in marine environments.
- To develop a novel risk-based maintenance strategy for the offshore structures susceptible to pitting corrosion.
- To develop a novel probabilistic methodology to predict the pitting corrosion and future deterioration of offshore structures.
- To design the laboratory experiment to better understand pitting mechanism and to realistically predict long-term service life of steel structure in different environmental conditions.
- To develop failure model and to study ultimate strength performance for steel specimens subjected to pitting corrosion using Finite Element Analysis (FEA).

1.3 Thesis Organization Scope and Contribution

The summary of the thesis outline is provided in below section. These chapters are, to a large extent, self-contained and can be read independently. While several novel aspects are expected to be developed from this project, the major novel components this work are:

Chapter 2: Modelling of Pitting Corrosion in Marine and Offshore Steel Structures - A Technical Review

Chapter 2 is a detail and technical review work and it reviews and analyses the current understanding of the pitting corrosion mechanism and investigates all possible factors that can cause pitting corrosion. Furthermore, different techniques employed by scientists and researchers to identify and model the pitting corrosion are also reviewed and analysed. Future work should involve an in-depth scientific study of the corrosion

mechanism and an engineering predictive model are recommended in order to assess failure, and thereby attempt to increase the remaining life of offshore assets. A thorough revision and discussion of the wide spectrum of factors that can cause pitting corrosion and their respective effects is made available to the corrosion research community. This has already been accomplished and the outcomes of the revision have been published in the Journal of Loss Prevention in the Process Industries.

Chapter 3: Risk-based Maintenance (RBM) of an Offshore Process Facility using Bayesian Network

This chapter introduces a developed methodology for the risk-based maintenance planning using probabilistic approach. This methodology helps to maximize the reliability of the equipment and reduces the total cost of the maintenance of offshore oil and gas structures susceptible to pitting corrosion. Risk-based maintenance strategy provided a tool for maintenance planning and decision-making to reduce the failure probability of equipment and the associated consequences.

This article discusses a novel methodology for the design of an optimum maintenance programme integrating a dynamic RBM based reliability approach and a risk assessment strategy. In this study, Bayesian Network (BN) is employed to develop a new dynamic RBM methodology for the design of an optimum maintenance programme for offshore production facility. The application of this methodology has high degree of prediction capability which increases the reliability of the equipment and also optimizes the cost of maintenance. The developed methodology is applied to a case study involving an offshore oil and gas production facility. A sensitivity analysis is also conducted to study the critical equipment based on the risk levels. This component of the work has been published in the Journal of Process Safety Progress.

Chapter 4: Pitting Degradation Modelling of Ocean Steel Structures using Bayesian Network

Chapter 4 develops the novel probabilistic methodology to predict the longer term pitting corrosion depth of structural steel will be made available to the industrial society. This methodology can be adopted for the future design of the offshore structures to predict the pitting depth as a function of exposure time using the corresponding operating conditions. The detail development of the methodology and the application

of proposed methodology is published in the Journal of Offshore Mechanics and Arctic Engineering.

Chapter 5: Accelerated Pitting Corrosion Test of 304 Stainless Steel using ASTM G48; Experimental Investigation and Concomitant Challenges

Chapter 5 is the experimental investigation of the challenges associated with the ASTM G48 standard for accelerated pitting corrosion test. This investigation improves the ASTM G48 standard for pitting immersion test on 304 stainless steel specimens by modifying testing regime and implementing some extra measures. A series of pitting corrosion tests on stainless steel specimen with different thickness were conducted and data were statistically evaluated. The generalized extreme value distribution, such as Weibull, provides adequate statistical descriptions of the pit depth and pit diameter distributions. The modified ASTM G48 offered advantages in the extraction and interpretation of the data for pit characteristics in the accelerated pitting corrosion test simulating actual marine environment. This chapter is been published in the Journal of Loss Prevention in the Process Industries.

Chapter 6: Experimental and Numerical Strength Assessment of Steel Specimen subjected to pitting Corrosion

Chapter 6 developed a computational technique to analyses the failure of steel structure under pitting corrosion attack. It is also equally important to determine the remaining strength of the corroded structure in order to maintain its reliability and survivability. This paper presents the experimental and numerical modelling of the stainless-steel specimen with varying thickness subjected to different level of pitting corrosion deterioration. The surface of 24 corroded specimens with differing pit characteristics was studied to investigate the strength reduction due to pitting degradation.

Chapter 7: Conclusions

This final chapter summarizes the major findings of this PhD research.

[Page intentionally left blank]

2 *Modelling of Pitting Corrosion in Marine and Offshore Steel Structures-A Technical Review*

Abstract

Corrosion is a major cause of structural deterioration in marine and offshore structures. It affects the life of process equipment and pipelines, and can result in structural failure, leakage, product loss, environmental pollution and the loss of life. Pitting corrosion is regarded as one of the most hazardous forms of corrosion for marine and offshore structures. The total loss of the structure might be very small, but local rate of attack can be very large and can lead to early catastrophic failure. Pitting corrosion is a localized accelerated dissolution of metal that occurs as a result of a breakdown in the protective passive film on the metal surface. It has been studied for many years; however, the structural failure due to pit characteristics is still not fully understood. Accurate pit depth measurements, precise strength assessment techniques, risk analysis due to pitting, and the mathematical relationship of the environmental factors that causes pitting failure are also factors, which need further understanding. Hence this paper focuses on these issues. It reviews and analyses the current understanding of the pitting corrosion mechanism and investigates all possible factors that can cause pitting corrosion. Furthermore, different techniques employed by scientists and researchers to identify and model the pitting corrosion are also reviewed and analysed. Future work should involve an in-depth scientific study of the corrosion mechanism and an engineering predictive model is recommended in order to assess failure, and thereby attempt to increase the remaining life of offshore assets.

Keywords: Pitting Corrosion, Offshore Structures, Prediction, Corrosion Modelling, Safety Assessment, Steel

2.1 Introduction

The scientific exploration and exploitation of the ocean depth is now proceeding at a greatly accelerated rate [1]. Consequently, there has been particularly rapid progress in the development of equipment for deep-ocean investigation and underwater activities. The oil and gas industries have built a large number of offshore platforms, pipelines, ships, and underwater storage and shore facilities. However, the structural reliability of these structures is not fully understood [2]. These marine and offshore structures are typically constructed from steel and have the highest rate of critical incidents due to corrosion deterioration [3]. Corrosion is well defined as the destructive attack on a material by reaction with its environment [4-8]. This material degradation results in loss of mechanical properties of the structure such as strength, ductility and impact strength. Material degradation leads to loss of material and, at times, to ultimate failure [4]. Further, corrosion is also of major economic significance. The World Corrosion Organization (WCO) estimates that the annual cost of corrosion worldwide is around $US2.4 trillion (3% of the world's GDP) [9]. The economic cost for all forms of corrosion in advanced economies such as the United States of America was recently estimated at around 4% of gross national product (GNP) [10]. The environmental cost of corrosion can also be high; according to the Offshore Hydrocarbon Release Statistics and Analysis report 2002-2003 (HSR) [11], a total of 2313 hydrocarbon releases were reported from offshore facilities in nine and half years. The most common causes were 'mechanical failure' due to corrosion and other related degradation. A total of 1034 incidents (44.7% of the total incidents) were caused as a result of corrosion [11, 12].

Amongst all types of corrosion, pitting is the most common and damaging form of corrosion in marine and offshore structures [13]. Pitting corrosion is very dangerous, widespread, and difficult to detect; hence, it has been a matter of great concern to marine and offshore industries for several years [14]. Pitting corrosion is defined by Szklarska [17] as a localized dissolution of metals that occurs due to the breakdown of the protective passive film - notably the protective coating and paint on metal surfaces [5, 15-17]. Pitting corrosion can also occur during active dissolution if certain sections of the sample are more susceptible and dissolve faster than the rest of the surface [18]. Szklarska et al. [17] describes pitting as a form of localized corrosion in which metal is

removed preferentially from vulnerable areas of the surface. More specifically, the dissolutions lead to the formation of cavities in passivated metals or alloys, which are exposed to solutions containing aggressive anions. Most pitting failures in the offshore sectors are caused by chloride and chloride containing ions. It is very likely for pitting to occur when protective measures such as paint coating, galvanizing or cathodic protection are ineffective [19]. Pitting is one of the most vicious and insidious forms of corrosion; the attack is extremely localized resulting in holes in the structure and thereby causing failures [19]. History shows that pitting corrosion is a dominant cause of structural failure in marine and offshore sectors. The reason for this is due to the well-known fact that sea water is an aggressive corrosive environment and the structures are generally fabricated with alloy steel which favours pitting corrosion. The pitting in these structures is often very severe, not only under sustained immersed conditions, but also under general exposure to atmospheric conditions [14]. The effects of pitting corrosion can be catastrophic, as illustrated by several incidents reported in the offshore oil and gas sectors. In March 1965 a natural gas pipeline exploded in Louisiana, killing 17 people including 9 children. The heat from the explosion was very intense; 6 cars and 3 trucks melted and 5 houses were scattered over a large area. In July 1988 there was a massive leakage of gas condensate on Piper Alpha due to pitting corrosion which, when it ignited, caused an explosion leading to large oil fires. The scale of the disaster was enormous, killing 167 people on board, and it is regarded as the deadliest accident in the history of the oil and gas industry [3]. In April 1992 a sewer explosion in Guadalajara, Mexico killed 215 people. In this incident a series of blasts damaged 1600 buildings and injured 1500 people [20]. Roberge et al. [20] described it as being one of the most catastrophic accidents resulting from a single pit. A recent example of pitting corrosion-related failure is the BP ULA accident in Norway. In September 2012, an estimated 125 barrels of oil and 1,600 kilograms of gas leaked at the North Sea platform due to pit in a valve; despite there being no injuries, production was stopped for 67 days [3]. Similarly, in December 2012 a buried, half a meter diameter, high-pressure natural gas pipeline operated by Columbia Gas Transmission ruptured due to pitting corrosion. There were no fatalities; however, several houses were damaged and about 2 million standard cubic meters of natural gas was released and burned. The total cost was expected to be about $9 million dollars [21]. Consequently, significant attention should

be given to predict the occurrence of pitting corrosion in offshore structures and adequate measures should be taken to prevent and control the consequences.

Pitting corrosion in offshore steel structures has particular importance where containment is critical, such as for pressure vessels, boilers, turbine blades and for metallic containers for toxic materials. It is also significant for localized structural strength in piping, tanks, ships and marine structures. [22, 23]. Melchers et al. [23] stressed the importance of pitting corrosion knowledge as being crucial for the marine and offshore sectors. They recommended a deep knowledge of pitting corrosion - its effects, and the application of preventative methods - as this will assist in reducing material losses resulting from same [24]. It will also improve the safety of operating equipment [22].

Pitting corrosion has been studied for several decades and considerable understanding of the pitting phenomenon has been generated. However in depth knowledge of pitting modelling and pitting measurement is still lacking [18]. There is also a limited understanding of why the pitting corrosion rate is not constant over time and why data tends to be scattered. Hence, it is necessary to review what actually happens when a steel surface is exposed to natural seawater and how this process progresses with time [10].

Many researchers have studied factors affecting pitting corrosion in marine and offshore environments [5, 15, 25-30]; however, the factors investigated are very limited and there is still a potential to study them more thoroughly. In this study, all possible factors that can cause pitting corrosion will be discussed and the effects of a number of factors in initiating the pitting corrosion will be summarized. In addition different techniques employed by scientists and researchers, to identify and model the pitting corrosion, are focused on in subsequent sections.

2.2 General Description of Pitting Corrosion

Pitting corrosion is defined as localized corrosion of a metal surface, confined to a point or small area that takes the form of cavities [22]. Major consequences of pitting are the breakdown of passivity; in general, pitting occurs when there is a breakdown of surface films exposed to the pitting environment. Pitting corrosion occurs when discrete areas

of a material undergo rapid attack while most of the adjutant surface remains virtually unaffected [31]. The attack leads to characteristic forms of cavity, such as pits or crevices in the metal surface [23]. Research shows the common factors contributing to the initiation and propagation of pitting corrosion are [20]:

- Localized chemical or mechanical damage to the protective oxide film
- Factors that can cause breakdown of a passive film, such as acidity, low dissolved oxygen concentrations and high chloride concentrations; these are likely to turn a protective oxide film less stable, and thereby initiate pit
- Localized damage to, or poor application of, protective coating
- Presence of non-uniformities in the metal structure of the component such as non-metallic inclusions.

Pitting corrosion can produce pits with their mouth open (uncovered) or be covered with a semi-permeable membrane of corrosion products. Pits can be either hemispherical or cup-shaped. In some cases they are flat-walled, revealing the crystal structure of the metal but they may also have a completely irregular shape. Figure 2-1 shows the common pit shapes divided in two groups namely: trough pits (upper) and sideway pits (lower):

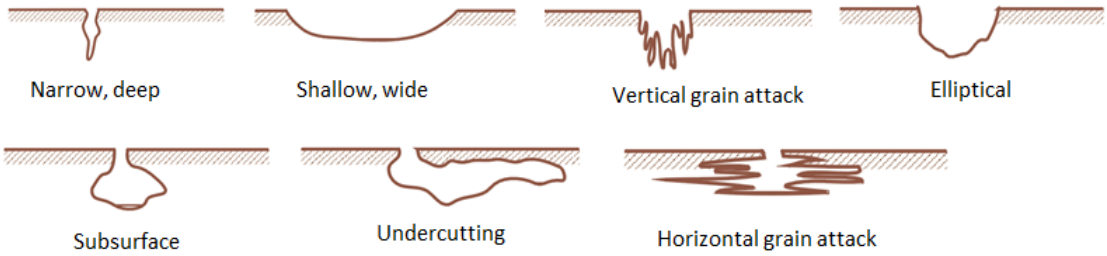

Figure 2-1. Sketch of common pit shapes.

Pitting cavities may fill with corrosion products and form caps over the pit cavities, sometimes creating nodules or tubercles. While the shapes of the pits vary widely, as evidenced in Figure 2-1, they are usually roughly saucer-shaped, conical, or hemispherical for steel and many associated alloys [20].

Pitting corrosion is complicated in nature; according to Abood et al. [22] the oxide films that form on different metals vary one from another in electronic conduction, porosity, thickness and state of hydration [22]. Zaya et al. [30] studied pitting theory and stages

of pit development; the schematic of different stages for the development of an individual pit can be seen in the Figure 2-2. Zaya et al. [30] distinguished various stages of the pitting corrosion process and divided them into four stages (see Figure 2-2). Stage 0 represents an un-attacked metallic surface which is completely covered with the passive films. Stage 1 involves the rupture of the passive layer; the substrate is still protected except for a small patch in contact with the electrolyte. The dimension of the small patch in stage 1 can be smaller or comparable to the thickness of the passive film. Subsequently, the dissolution of the substrate begins. Stage 2 is reached when the conditions for pit growth are met and repassivation cannot occur anymore i.e. the pit begins to grow. Therefore, in stage 3 the dissolution of the substrate begins to grow and the pit becomes about 1 to 10 μm which can be seen under optical microscope. Pits have a shape of hemisphere or of a polyhedron by stage 3. At the final stage 4 the pits can be seen with the naked eye. The pit can have an irregular shape if partially covered around the mouth with solid corrosion products [1, 17, 23, 30].

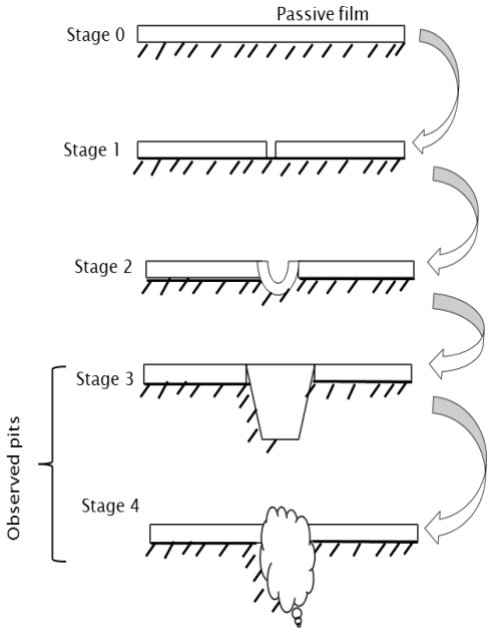

Figure 2-2. Schematic stages of pit development (adopted from Zaya, 1984 **[20]**

Many researchers, starting with Evens and Bannister in 1931 [32, 33], and later Richardson in 1973 [34], claim that local weak spots or defects are always present in the passive films. Therefore stage 0 never exists and, immediately after immersion, the process starts at stage 1, i.e. metal and solution are in contact [32-34]. The induction period only corresponds to the rate time necessary for the corrosion to be well developed

and detectable. Additionally, the corrosive attack is highly localised and the precise location of pits appears to be unpredictable [23, 30].

Steel alloys, such as stainless steel and aluminium alloys, are commonly used in marine and offshore sectors. These alloys are comprised of passive films which are thin (nanometre-scale) oxide layers that can form on the metal surface in marine environments [20, 35]. However, such passive films are often susceptible to localized breakdown resulting in accelerated dissolution of the underlying metal [36]. If the attack initiates on an open surface it is called pitting corrosion. This form of localized corrosion can lead to accelerated failure of structural components by perforation or by acting as an initiation site of cracking [23]. Figure 2-3 shows an example of the deep pits on a metal surface.

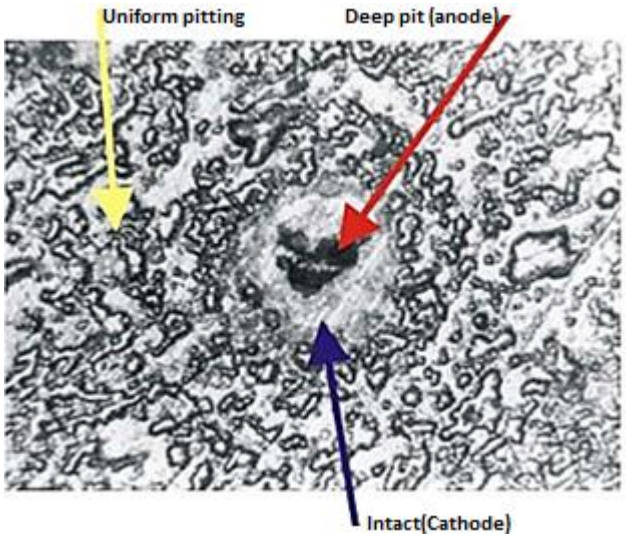

Figure 2-3. Deep pit in the metal **[22, 31]**

Roberge et al.[20] reported that the practical importance of pitting corrosion depends on the thickness of the metal and on the penetration rate. In general, it was found that the rate of penetration decreases if the number of pits increases. This is attributed to closely spaced pits having to share the available adjacent cathodic area which controls the corrosion current that can flow [17, 20, 31]. Abood et al. [22] studied different parameters that influence pitting corrosion. The parameters investigated were limited to environment, metal composition, pitting potential, temperature and the surface conditions. Within these, environmental parameters were found to be the most critical factors. They include aggressive ion concentration, pH, and inhibitor concentration [17,

20, 22]. Similarly, Frankel et al. [18] provided an overview of the critical factors that influence the pitting corrosion of metals. They found that the effects of alloy composition, environment, pitting potential and temperature are critical for pitting to occur. These critical factors are further reviewed in the following section.

2.2.1 Stages of Pitting Corrosion

Pitting can consist in various stages: passive film breakdown, pit initiation, metastable pitting, pit growth and pit stifling. Any of these stages may be considered to be critical [17, 22, 37]. Pitting corrosion capitalizes on breakdown in the protective layer, either natural or applied, and provides a nucleation point for the formation of pits in the presence of an electrolyte containing an aggressive anion [25]. Once the passive film breaks down and a pit initiates, there is a possibility that a single pit will grow. The passive state is required for pitting to occur; however some researchers believe that the minutiae of passive film composition and structure play a minor role in the pitting process [22]. Regardless, pit growth is critical in practical applications of failure prediction in marine and offshore structures.

2.2.1.1 Passive film breakdown

A passive film breaking theory was originally proposed by Hoar et al. [38] in 1967 and was later extended on by many researchers [30]. Hoar et al. [38] suggested that the absorption of the damaging ions on the surface of the passive film produces mutual repulsion which lowers the interfacial surface tension. It was reported that when the repulsive force is sufficient, the passive film cracks [30, 38]. The breakdown of the passive film and the details of pit initiation comprise the least understood aspect of the pitting phenomenon. Breakdown is a rare occurrence that happens very rapidly and on a very small scale, making direct detection of the breakdown difficult [22, 23, 30, 38].

Caines et al. [25] described passive film breakdown in stainless steel alloys commonly used in offshore installations. In these alloys, the breakdown of the passive film provides sites for pit nucleation and, consequently, these breakdown sites are susceptible to pitting corrosion. Passive films are present on the surface of the stainless steels in the presence of oxygen. At low temperatures, a true oxide layer is not formed;

instead a thin passive film is formed and acts as a barrier and thereby provides corrosion resistance [25].

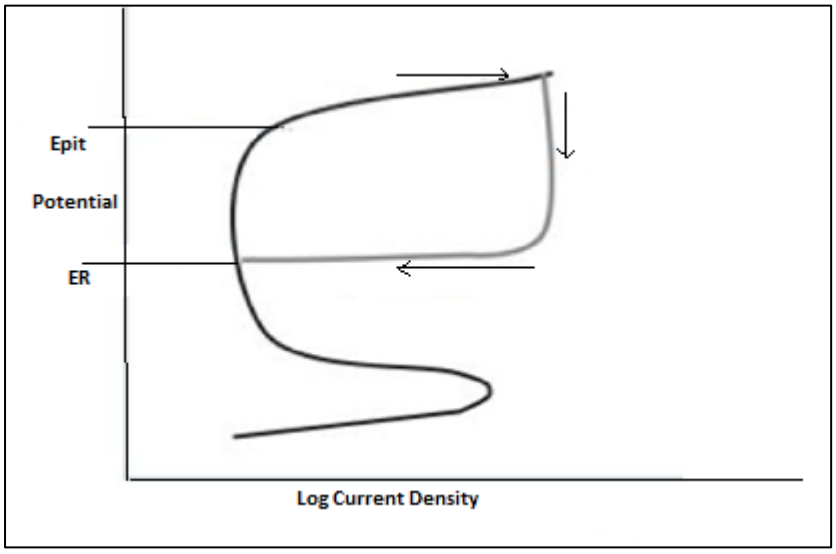

Figure 2-4. Schematic of anodic curve for a metal immersed in a solution containing aggressive ions (Adopted from Caines et. al **[17, 18, 25]**

Figure 2-4 illustrates the polarization curve [10, 17, 18, 22, 25, 39] to estimate the susceptibility of the metal alloy to pitting corrosion [25]. The curve is used to find E_{pit} and repassivation potential (E_R). Higher E_{pit} for a material in a given environment indicates greater resistance to pitting [17, 25, 40]. Similarly, if the potential is reduced below E_{pit}, the surface may repassivate and pit growth can stop. However, if the potential is between E_{pit} and E_R, pitting can be expected [17, 25, 40].

2.2.1.2 Pit Initiation

The initiation stage of pitting is generally agreed to be of very short duration. Melchers et al.[23] reported that the duration of pit initiation can be as short as micro-seconds and that pitting initiation is strongly dependent on the surface conditions of the material. This is important in setting the overall areal pattern for subsequent localised corrosion [23]. Caines et al. [25] postulated that the initiation of pits is influenced by surface defects which may be due to manufacturing issues such as installation problems, improper maintenance procedures and environment changes[25]. Caines et al. [25] also studied different factors that cause the site of pit initiation. Some of these are:

- Damage to protective chemical or mechanical oxide layer

- Environmental factors such as low pH, high chloride concentration causing protective layer breakdown
- Damage to applied protective coating
- Discontinuities in the protective coating

Strehblow et al. [40] and Frankel et al. [18] represented pit initiation by categorizing it in three different mechanisms: (a) penetration (b) adsorption and thinning and (c) film breaking mechanisms [18]. Penetration mechanisms for pit initiation involves the transport of the aggressive anions through the passive film to the oxide interface where aggressive dissolution is promoted [18]. This mechanism is aided by the induction time for pitting and the presence of chloride in an electrolyte. An adsorption theory of pitting initiation is based on the material's adsorption of chloride and oxygen. Strehblow et al. [40] described an aspect of pit adsorption, based on X-ray Photoelectron Spectroscopy (XPS) measurements, as being the exposure of Fe to chloride and other halides which cause the thickening of the passive films, even under conditions where pit has not formed. This is as a result of the catalytically enhanced transfer of cations from the oxide to the electrolyte [18, 40]. The film breaking may occur due to mechanical stress at weak sites, or flaws, causing local breakdown events; however these can also rapidly heal in nonaggressive environments [18, 40].

2.2.1.3 Metastable Pitting

Metastable pits are those that initiate and grow for a limited period before repassivating, or before dying [18, 41]. Pits which cease growing and repassivate in this manner are described as metastable [22, 41, 42]. The metastable pits may survive and become stable growing pits depending upon the composition of the material, the critical solution, mass-transport and the pitting potential at the bottom of the pit. Stable pitting corrosion occurs when the corrosion potential, E_{corr}, exceeds the pitting potential, E_{pit} [18, 41]. The measure of a material's ability to undergo stable pitting corrosion in a certain environment is defined as the pitting potential (E_{pit}) [42]. Galvele et al. [43] described E_{pit} as a limit where the growth of pits happens above the surface, however a passive surface is maintained below [43].

Wika et al. [41] described metastable pits as the incipient growth of initiated pits, and which must survive in order to become stable growing pits. These are small pits, of only few microns in size, which normally last only a few seconds before the surface repassivates [41].

Pistorius et al. [42] investigated the development of highly aggressive anolyte inside the metastable pit which has low pH as a result of hydrolysis of the dissolving metal cations. The anolyte also carries an enhanced concentration of anions because these migrate into the pit to maintain analytic charge neutrality. Hence, the pit growth becomes self-sustaining due to the development of the aggressive anolyte in the pit.

2.2.1.4 Pit Propagation (stable Pitting)

The pit propagation is the stage where the development of some of the initiated pit occurs and, in particular, where its rate of growth increases [23, 25, 44]. Caines et al. [25] defined this as the stage where pits grow and have the potential to increase beyond wall thickness, thereby leading to leaks [25]. They also reported that certain conditions must be met for pits to propagate:

- E_{pit} must be exceeded and remain above E_R (repassivation potential)
- An aggressive ion must be present
- Localized breakdown of passive or applied film.

Melchers et al. [23] reported that the precise mechanics of pit propagation is not fully understood; however it is known that highly acidic conditions (i.e. low pH) is associated for pit to be propagated [23]. Angal et al. [45] described pit growth in the marine environment as an autocatalytic process [45]. Fe^{2+} ions attract negative Cl^- ions and, through the hydrolysis, creates a porous $Fe(OH)_2$ cap over the pit. This process creates a self-propagating system where the increased acidity in the pit cavity increases corrosion of the steel walls of the pit [25, 45]. Some researchers [18, 22, 40, 44, 46] reported that pit propagates at a rate that depends on material compositions, pit electrolyte concentration, and pit-bottom potential. It was suggested that, in order to understand pit growth and stability, it is essential to ascertain the rate-determining factors such as electrochemical reactions which include charge-transfer process, ohmic effects, mass transport and the combinations of these factors. Smialowska et al. [17]

explained how the pit growth at low potential (i.e. below the range of limiting current densities) is controlled by a combination of ohmic, charge transfer, and concentration over potential factors [17, 23]. They suggested that pit growth is nonlinear at higher chloride ion concentration. Additionally, nonlinear growth of the high chloride concentration t^n with n in the range of 0.33 to 0.5 has been suggested by Melchers et al. [23], Smailowska et al. [17] and Abood et al. [22].

2.3 Mechanism of Pitting Corrosion

Pits almost always initiate due to chemical or physical heterogeneity at the surface such as inclusions, second phase particles, solute-segregated grain boundaries, flaws, mechanical damage, or dislocations [17]. Most engineering alloys have many or all such defects and a pit tends to form at the most susceptible sites first. For example, pits in stainless steels are often associated with manganese sulphide (MnS) inclusions which are found in most commercial steels. The role of MnS inclusions in promoting the breakdown and localized corrosion of stainless steels has been recognized for some time [14, 17, 18]. Abood et al.[22] acknowledge that the pitting corrosion caused by passive film breakdown only occurs in the presence of aggressive anionic species, and that chloride ion is usually the cause. The severity of the pitting tends to vary with the amount of chloride concentration. The reason for the aggressiveness of chloride has been considered for some time and a number of investigations and examinations were carried out in marine and offshore installations [18]. Chloride is an anion of a strong acid and many metal cations exhibit considerable solubility in chloride solutions. Hence, the presence of the oxidizing agent (oxide) in a chloride-containing environment is extremely damaging and it can further enhance localized corrosion [36]. Szklarska et al. [17] presented an experiment by means of ASTM G48, which is a common procedure when testing pitting corrosion, with the specimens immersed in 6% of $FeCl_3$. The results showed that the increase in potential associated with oxidizing agents enhances the likelihood of pitting corrosion [17, 18, 22]. Refer to Equation 1.1:

$$Me^{2} + 2H_2O \rightarrow Me(OH)^{+} + H^{+} \qquad (1.1)$$

Pitting corrosion normally starts with chloride rapidly penetrating the protective oxide film which covers the metal surface. These points act as initiation sites for pitting

corrosion [23, 36]. Selective dissolution is another way that pitting corrosion can initiate and this occurs when one of the components dissolves faster than other components [17].

Abood et al. [22] considered pitting to be autocatalytic in nature; once a pit starts to grow, the local conditions are altered such that further pit growth is promoted. Figure 2-5 shows that the anodic and cathodic electrochemical reactions that comprise corrosion separate spatially during pitting. The local pit environment becomes depleted in cathodic reactant (e.g. oxygen) which shifts most of the cathodic reaction to the surface outside of the pit cavity. Refer to Equation 1.2:

$$O_2 + 2H_2O + 4e^- \rightarrow 4OH^- \qquad (1.2)$$

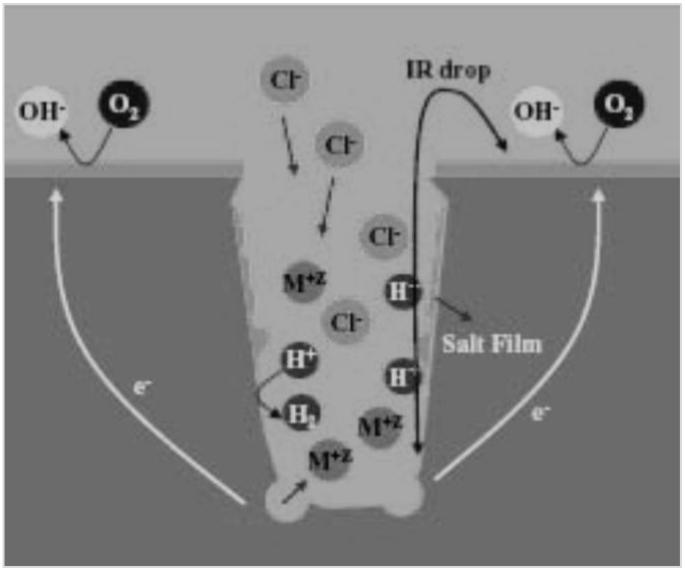

Figure 2-5. Autocatalytic process occurring in a corrosion pit (adapted from Abood et al **[22]**

In Figure 2-5 the metal, M, is being pitted by an aerated NaCl solution. Rapid dissolution occurs in the pit while oxygen reduction takes place on the adjacent metal surfaces.

The pitting phenomenon can be summarized as the local pit environment depleted in the cathodic reactant, such as dissolved oxygen, and enriched in metal cation including anionic species. This acidic chloride environment is aggressive to most metals and tends to prevent repassivation, thereby promoting continued propagation of the pit. It was

suggested that removal of oxidizing agents, e.g. removal of dissolved oxygen, is one powerful approach for reducing susceptibility to localized corrosion [17, 18, 22].

A number of researchers [18, 22, 23, 30, 43, 44, 47] have studied the local chemistries that form in pits using a range of techniques. Wong et al. [44] described a way to isolate the pit solution by rapid freezing of the electrode in liquid nitrogen, removal of the surface excess, and subsequent thawing [18, 44]. This approach is mainly used to study the pH in Aluminium pits and the chloride concentration in pits for stainless steel. Likewise, Frankel et al. [18] considered a way to isolate the pit solution by using artificial pit electrode methods. This is also known as one dimensional pit, or lead–in-pencil electrode, which is a wire imbedded in an insulator such as epoxy [18]. This technique allows a considerable volume of pit electrolyte to be analysed [44]. Another way to isolate the pit solution is by inserting microelectrodes into pits, cracks and cervices [18]. With this technique, once the local solution composition is fully characterized, it is possible to reassemble the local environment by reconstituting it in bulk form from reagent grade chemicals, and then determining the electrochemical behaviour of a normal-sized sample extracted from a local environment.

Frankel et al.[18] also studied the electrochemistry of pitting corrosion and have found that different characteristics potentials exist within pitting corrosion [18]. It was found that metastable pit formation can occur below the E_{pit}, however this cannot be seen as initiation points of pitting [17, 18, 41]. Metastable pits are those pits that initiate and grow for a limited period before repassivating. Materials exhibiting higher value of pitting potential (E_{pit}) and repassivating potential (E_{rep}) are more resistant to pitting corrosion therefore cyclic polarization experiments are generally used to measure the pitting resistance of metals [18]. The value of E_{pit} can be used to determine under what conditions pitting corrosion occurs [17, 41].

The environment (chemistry) and the material (metallurgy) factors determine whether an existing pit can be repassivated or not [31]. Sufficient supply of oxygen to the reaction site may enhance the formation of oxide at the pitting site and thus repassivate or heal the damage to the passive film. An existing pit can also be repassivated if the material contains a sufficient amount of alloying elements such as Cr, Mo, Ti, W, N,

etc. [48]. Amongst these elements, Mo can significantly enhance the enrichment of Cr in the oxide and thus repassivate the pit. A detailed analysis of the influence of pit chemistry on pit growth and stability has been provided by Galvele et al. [43]. The concentration of various ionic species at the bottom of modelled one-dimensional pit geometry is discussed by many researchers [18, 22, 41, 43]. The concentration of various ionic species is determined as a function of current density based on a material balance that considered generation of cations by dissolution, outward diffusion, and thermodynamic equilibrium of various reactions such as cation hydrolysis [18] (refer to equation 1). Galvele et al. [43] found that a critical value of the factor $x \cdot i$, (where x is pit depth and i is current density), correspond to a critical pit acidification for sustained pit growth [18]. Current density in a pit is a measure of the corrosion rate within the pit and thus a measure of the pit penetration rate. The value "$x.i$" can be used to determine the current density required to initiate pitting at a defect of a given size [22]. Increasing the pit density increases the ionic concentration in the pit solution, often reaching supersaturation conditions. Frankel et al.[18] demonstrated an example of a solid salt film that may form on the pit surface. When the solid salt film is formed on the pit surface, the ionic concentration drops to the saturation value and the pit growth rate is limited by mass transport out of the pit [18, 22, 44].

Although many researchers claimed that salt films are required for pit stability, Frankel et al. [18] disagreed. These authors suggest that salt films will only enhance stability by providing a buffer of ionic species that can dissolve into the pit to reconcentrate the environment in the event of failures such as the sudden loss of a protective pit cover [18, 22]. The shape of the pit varies on the environmental conditions, and on whether the pit contains a salt film or not. Abood et al. [22] and Frankel et al. [18] both agreed that, under mass-transport-limited growth, pits can be hemispherical with polished surfaces. In the absence of a salt film, pits can be crystallographically etched or irregularly shaped [18, 22].

2.4 Characteristics of Pitting Corrosion

In 1984, Zaya et al. [30] reported the following characteristics of metal that should be studied to characterise the pitting corrosion:

- Existence of a threshold value of the anodic potential below which pitting does not occur in the given electrolyte system or the potential of the metal must exceed a certain threshold [30].
- Some aggressive anion must be present. These ions correspond to strong acids and they tend to form complex and very soluble salts with the metal they attack [49].
- Some other ions inhibit the effect of the aggressive ions as pitting agents. The relationship between the potential necessary for pitting and the concentration of aggressive and inhibiting ions is given in Equation 1.3 [17, 30].

$$E = E_0 - a.\log[Agg.] + b.\log[Inh.] \tag{1.3}$$

- The delay (induction time), between the fulfilment of the necessary conditions for pitting, and the detection of the first pit, is due to the detection not taking place until the pit has reached stage 3 (Figure 2-2) [30].
- The corrosive attack is highly localized on the surface but otherwise still passive. The precise location of a pit is unpredictable but the probability of occurrence is higher at grain boundaries, inclusions and other surface discontinuities [30, 50].
- Inside the pit the aggressive ions reach concentrations much higher than in the bulk of the solution. This is accompanied by changes in the concentration of the other components of the solutions - usually a drop in the pH [30, 44].

These properties were selected after extensive observation of pitting in combinations of several metal-solutions [17, 30].

2.4.1 Passive Films

It is generally acknowledged that the susceptibility of metals, and the rate at which the corrosion processes take place, are closely related to the quality of the passive film which normally occurs on the metal surface [17]. Many researchers have studied susceptibility of metals for many years. Amongst these, Smialowska [17] and Melchers [23, 51-53] applied both theoretical and experimental knowledge to estimate the susceptibility of metals for pit to initiate in marine and offshore structures. Smialowska

et al. [17] described different ways to estimate the susceptibility of the metal alloy to pitting:

- Determination of characteristic pitting potential
- Determinations of a critical temperature of pitting
- Measurement of the number of pits per unit area, weight loss and, if possible, the size and depth of pits formed in a suitable standard solution
- Determination of the lowest concentration of chloride ions causing pitting [17]

Although the nature of the passive films is not fully understood, many researchers acknowledge that pitting susceptibility is related to local imperfections or discontinuities [23, 41, 54]. Smialowska et al.[17] listed the following understanding on the formation of weak spots in passive film [17, 23]:

- Boundaries between the metal matrix and non-metallic inclusions where differences exist in the coefficient of thermal expansion, causing either cracking or localised compression zones.
- Boundaries between the metal matrix and second phase precipitates, as these often have the ability to draw from the alloy some components responsible for the passive state (e.g. Cr impoverishment of Cr-Ni stainless steels as a result of chromium carbide formation).
- Inclusions of greater chemical reactivity than that of the alloy or metal itself.

In addition to non-metallic inclusions, the following features can create weak spots in the passive films:

- Grain boundaries at which some impurities segregate (i.e. not purely physical defects)
- Flaws
- Various kinds of mechanical damage
- Three phases of metal (solid, liquid and gas)
- Exit point of dislocations.

Melchers et al. [23] and Smialowska et al. [17] propose various ways in which the susceptibility of an existing structural materials to pitting can be assessed under experimental conditions [23]. Among these, measuring susceptibility to pitting by using pitting potential and/or by temperature is commonly used ways and is discussed in the following sections.

2.4.1.1 Measuring Susceptibility of Pitting Potential

Electrochemical studies of pitting corrosion reported that pitting potential is related to the electrochemical process associated to corrosion [18, 23]. When the electronic potential is measured for a given metal electrolyte system, it was observed that there exists a threshold value of the anodic potential below which pitting does not occur [23]. Smialowska et al. [17] discussed various electrochemical methods used to determine characteristics pitting potentials and a detailed description is available [17]. Different methodology used to determine characteristics pitting potentials are:

- Measurements of the anodic polarization curve using a potentiostatic device [55]
- Measurements of the anodic polarization curve by galvanostatic methods [56]
- Measurements of current density vs. time at constant potential [57]
- Measurements of potential vs. time at constant current [58]
- Repassivation time methods (Scratch Methods) [17]
- The pit propagation rate test [59]
- The critical pitting temperature test [60]
- The scanning reference electrode technique [61].

Malik et al. [58] used these methods to conduct electrochemical tests to investigate the pitting corrosion behaviour of AISI 316L in Arabian Gulf Sea water and reported that the pitting potentials vary for the same materials under identical conditions depending upon the methods used [58].

2.4.1.2 Measuring Susceptibility of Pitting using Temperature

According to DNV-RP-G101 [62], temperature is the main reason for pitting corrosion attack on offshore steel structures [62]. The reported experimental work on temperature often focused on finding the critical pitting temperature (CPT) which is defined as the

lowest possible temperature where pitting occurs [41]. Moayed et al. [54] defines CPT as " the lowest temperature at which the growth of stable pits is possible" [54]. ASTM G 150 is a standard test method for electrochemical CPT testing of stainless steel.

Several authors [18, 23, 25, 41] reported that, with an increase in temperature, the E_{pit} decreases and the damage caused by corrosion increases. Melchers et al. [23] reported that, for Carbon Steel, it appears that the passive film becomes less protective with higher temperature and that this is related to the behaviour of chloride ions [23]. Wika et al. [41] found that the increasing temperature causes higher current transients and promotes the conversion of metastable pits into stable growing pits [41]. Bohni et al. [60] carried out electrochemical studies in micro and large scale - both in chloride free and in chloride solutions. In chloride free solutions, the increase in temperature caused an increase in dissolution of MnS inclusions, while in a chloride environment the growth of pits increases [60].

2.5 Factors Affecting Pitting corrosion in Marine and Offshore Steel Structures

Steel alloys are used in numerous and diverse applications in marine and offshore industries [50]. Stainless steel grade 316 alloys are commonly used in offshore applications because of their corrosion resistant nature. It is regarded as safe for design life when choosing a material in an aggressive environment [2, 50, 63, 64]. Nevertheless, even though these alloys offer a better resistance to general corrosion, they are still susceptible to pitting corrosion [65]. The most common causes of failure of stainless steel in marine environments is pitting corrosion because the material can quickly be penetrated despite that its general corrosion rate is very low [58].

Several findings on pitting corrosion of steel alloys, accomplished by using numerical and experimental techniques, have been published by different investigators. Salh et al. [66] studied the pitting corrosion of carbon steel in sodium molybdite solution. They found that the sodium molybdite is a good pitting inhibitor in solutions of moderate and low concentration of chloride, and that the corrosion potentials shifted to more positive value in the presence of molybdite [22, 66]. Malik et al. [58] investigated the pitting behaviour of 316L stainless steel in Arabian Gulf seawater. The immersion test and electrochemical techniques were utilized to study different factors affecting the pitting

corrosion [58]. Similarly, Melchers et al. [10] investigated the corrosion wastage in aged offshore structural steels. They summarized the progress in the development of the mathematical models for corrosion loss and maximum pit depth under in-situ conditions of steel as a function of time[67]. Several published materials [4, 68-72] are widely available.

The phenomenological factors which influence pitting corrosion in marine and offshore environments are generally similar to those of uniform corrosion. The influence of these factors differ depending on the types of marine environments, such as atmospheric, splash zone, tidal zone and shallow water immersion [23, 39]. The different types of exposure can be sub-classified as illustrated in Figure 2-6. A summary of all the possible factors involved in pitting corrosion is given in the Figure 2-7. These factors are categorised into four different types: (1) Physical factors (2) Chemical factors (3) Biological factors and (4) Metallurgical factors.

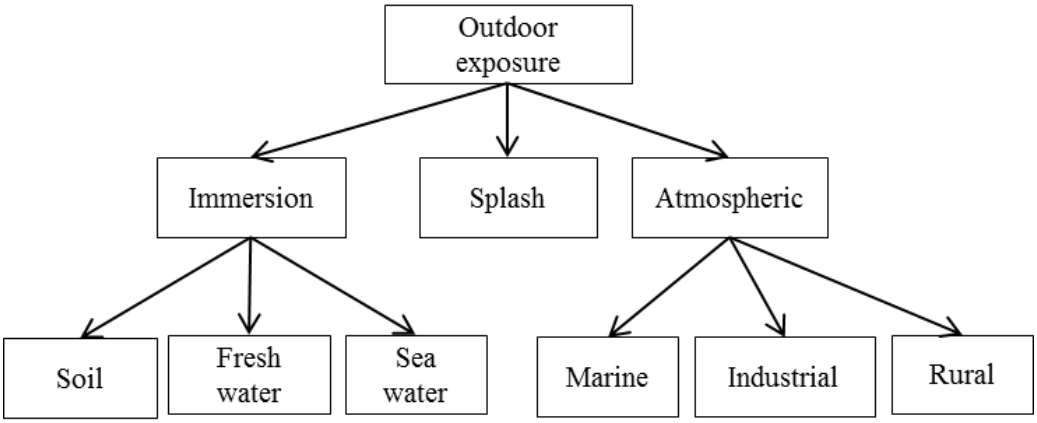

Figure 2-6. Classification of environments encountered by pitting corrosion **[73]**

A summary of the different types of exposure in marine environments is shown in Table 2-1. Factors which can affect pitting corrosion given in the Figure 2-7 are composed from all types of exposure zones. Attention is not limited to just stainless steel; mild steel and low alloy steels are also considered because literature indicates that the corrosion behaviour is similar to all [5, 15, 23, 39, 74].

Table 2-1. Classification of Marine Environments **[10, 23, 39]**

Marine Zone	Description of Environments	Characteristics of steel corrosion behaviour

Interior Spaces	High humidity, higher than ambient temperature, periodic wetting possible.	Particularly aggressive in areas where moisture can accumulate.
Atmosphere	Minute salt particles present, corrosivity varies with height above water, wind direction and velocity, dew cycle, rainfall, temperature, pollution etc.	Sheltered surface may deteriorate more rapidly than those boldly exposed. Corrosion decreases rapidly with distance from sea.
Splash	Wet, well aerated surface, no fouling.	Most aggressive zone for steel. Protective coating is difficult to maintain.
Tidal	Well oxygenated, marine fouling likely to occur, oil coating from polluted harbour water may be present.	High attack for steel, however oil coating may reduce corrosion attack. Some protection on continuous steel pile.
Immersion	Usually saturated with oxygen. Pollution, sediment, fouling, velocity etc. have key roles in the degree of corrosion.	Biofouling restricts oxygen supply rate to surface, reducing corrosion. Protective coatings may be effective for limited corrosion control.

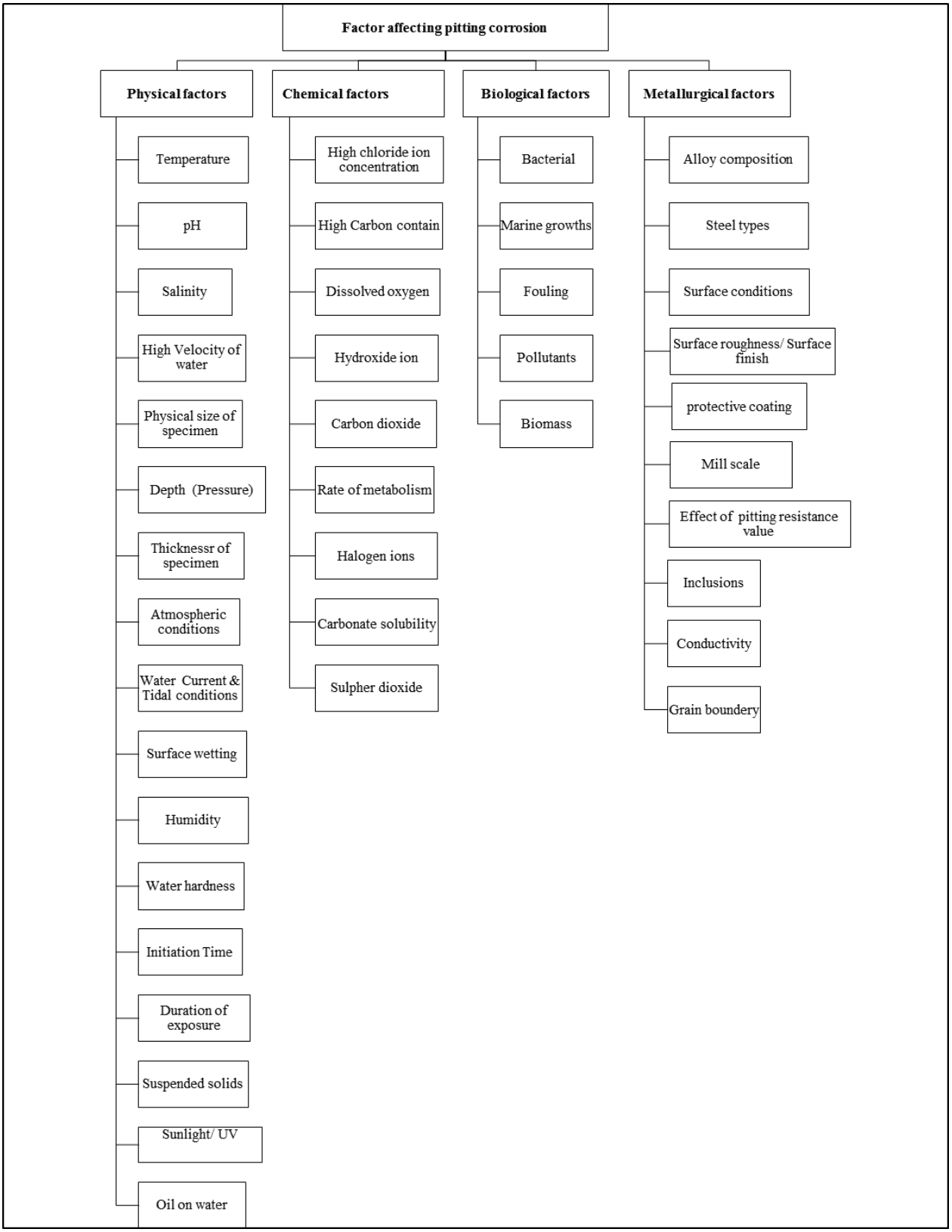

Figure 2-7. Factors affecting pitting corrosion in marine and offshore environments.

Table 2-2. Environmental factors as shown in the flowchart Figure 2-7 and its effect on the corrosion rate **[1, 23, 39, 75]**

Type	Factor	Effect on initial state corrosion	Effect on steady state corrosion	Influenced by
Biological	Bacteria	Little effect	Controls rate	Seawater temperature
	Biomass			NaCl concentration
	Pollutants	Varies	Varies	Little known about
	Marine growth	Little effect	Controls rate	Pollutant type/ level
Chemical	O_2	Directly proportional	None	
	pH	Little effect	Uncertain	Little effect at sea
	CO_2	Little effect	Little effect	
	NaCl	Inversely proportional	Uncertain	Little effect at sea
	Ca	Little effect	Varies	Little known about
	Carbonate solubility	Little effect	Little effect	
Physical	Temperature	Proportional >10°C	Proportional	Geographical locations
	Pressure	Uncertain	Not none	Oxygen effect
	Water velocity	Little effect	Uncertain	Geographical locations
	Suspended solids	Uncertain	Uncertain	Geographical locations
	Surface wetting and wave action	Proportional for tidal/splash zone	Proportional	Location, weather patterns
	Oil in the water	Reduces for tidal zone	Reduces for tidal zone	Industrial development/shipping

Environmental factors which influence marine immersion corrosion are shown in the Table 2-1. Classification of Marine Environments [10, 23, 39]. Not all of these factors are well understood although some have become clearer through recent investigations [75]. The main factors governing pitting corrosion in a marine and offshore environment are described in subsequent sections.

2.5.1 Physical Factors

2.5.1.1 Temperature

Temperature is one of the critical factors in pitting corrosion, because it greatly influences the corrosion behaviour of steels in seawater [5, 17, 18, 22, 29, 40, 44, 76, 77]. Many materials do not pit at a temperature below a certain value which may be extremely high and reoccurring [48]. Pitting potential of stainless steel alloy is measured in the temperature range of $25-90^{\circ}C$ [76]. The majority of chemical and electrochemical reactions proceed more rapidly at higher temperature. Therefore it might be anticipated that the rate of pitting would increase with increasing temperature [17]. Almarshad et al. [48] experimentally studied the effect of temperature on pitting by either varying the temperature at a range of fixed applied potentials, or by varying the potential for a range of constant temperature experiments. They provided a plot of pitting and repassivation potentials for three different stainless steels in 1M NaCl as a function of solution temperature [22, 78]. From these experiments it was observed that extremely high breakdown potentials occur at low temperature corresponding to transpassive dissolution - but not with localized corrosion. However, just above the critical pitting temperature (CPT), pitting corrosion occurs at a potential that is far below the transpassive breakdown potentials [48].

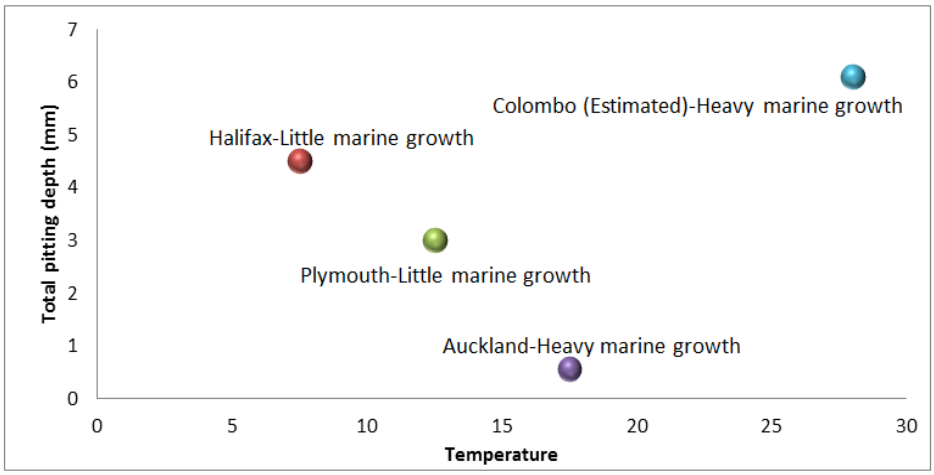

Figure 2-8. Pitting depth for tidal conditions as a function of annual mean water temperature **[23].**

Hadfield et al. [79] reported metal losses for ordinary steels over a 5 year exposure. Figure 2-8 shows the pitting depth for tidal conditions as a function of annual mean temperature for different experimental cities. It can be seen that pitting is inconsistent as a function of temperature for tidal conditions, whereas there is an increasing trend of pitting with temperature for general corrosion conditions [10, 23, 39].

The specimens were despatched to testing stations at Auckland, Colombo, Halifax (Canada), and Plymouth. Observations suggest that, despite the differing sea and atmospheric conditions, immersion corrosion of carbon steel is very similar when comparing all five locations. The effect of temperature on atmospheric corrosion was also thoroughly examined and showed that atmospheric corrosion was generally consistent with temperature. Melchers et al. [23, 39, 80] stated that the reaction process for corrosion becomes faster with higher temperatures after the initial phase, suggesting that the corrosion rate increases with increase in temperature. However, in immersion conditions, oxygen concentration decreases with increase in temperature while biological activity increases with increase in temperature [23, 39, 80].

2.5.1.2 pH

The pH of seawater may vary slightly depending on the photosynthetic activity. Plant matter consumes carbon dioxide and affects the pH during daylight hours [1, 81]. The carbon dioxide content in seawater (close to the surface) is influenced by the exchange with carbon dioxide in the atmosphere [1]. It is reported that the usual daily fluctuations of pH (of between 8.0 to 8.2) has little direct effect on corrosion rate. However it can be a factor in calcium carbonate deposits which does affect the corrosivity [1, 23]. Comparable conclusions were made by Melcher et al. [23]. Chandler et al. [82] did not consider pH of seawater to be one of the main physical factors that influences pitting corrosion rate on steel [82]. Revie et al. [83] stated that, within the range of pH of about 4-10, the corrosion rate is independent of pH and depends only on how rapidly oxygen diffuses to the metal surface [71, 83].

Many experiments were carried out to understand the effect of pH on pitting corrosion in marine environments. Malik et al. [76] performed electrochemical tests on metal and found that corrosion rate increases with increasing acidity of the solution. They stated that corrosion rate increases with rising pH between 4 and 9 [76]. Similarly, Carpen et

al. [63] carried out potentiodynamic experiments with distilled solutions containing chlorides. They found that a pH of 3 contributes a little lower pitting potentials than solutions of pH 5 with low chloride content. No effect of pH was observed at higher chloride content. It was therefore suggested that pH has little effect on pitting potentials in chloride solutions and does not much change the susceptibility to pitting corrosion in the pH range 3-7 [41, 63]. The effect of pH on the breakdown potential was not understood well [22]. Pistorius et al. [84] found that the breakdown potential (E_b) value is almost constant within a large range of pH values [22, 66, 84].

2.5.1.3 Salinity

Seawater Handbook [1] defines salinity as the total weight in grams of solid matter dissolved in 1000grams of water [1]. The effect of seawater salinity is conventionally considered to be a very important factor with regard to pitting corrosion [85]. The composition of seawater for salinity is given in Table 2-3. It can be appreciated that the salinity of seawater is composed of about 90% sodium chloride (NaCl). The dissolved salt leads to a low resistivity so that the sea water acts as a good electrolyte, thereby enabling pitting corrosion [39].

Table 2-3. Composition of seawater and ionic constituents and total solids in Ocean waters **[1]**

Constituent	**G/kg in 1000 grams of water**	**Cations, Precent**		**Anion, Precent**		**Body of water**	**Salinity ppm**
Chloride	19.353	Na++	1.056	Cl-	1.898	**Baltic Sea**	8,000
Sodium	10.76	Mg++	0.127	So_4-	0.265	**Black Sea**	22,000
Sulphate	2.712	Ca++	0.040	HCO_3-	0.014	**Atlantic Sea**	37,000
Magnesium	1.294	K+	0.038	Br-	0.0065	**Mediterranean Sea**	41,000
Calcium	0.413	Sr++	0.001	F-	0.0001	**Caspian Sea**	13,000
Potassium	0.387	**Total**	**1.262**		**2.184**	**Irish Sea**	32,5000
Bicarbonate	0.142						
Bromide	0.067						
Strontium	0.08						
Boron	0.004						
Fluoride	0.001						

Variations on salinity in open surface water appears to range from 32000 to 37500 ppm (3.2-3.75%) with deep water mean around 35000 ppm (3.5%) [39] . A great variation in salinity is observed in some of the more isolated seas (see Table 2-3) and, because the salinity variations are accomplished by other changes, the total effect on the pitting corrosion has to be established in each case [1].

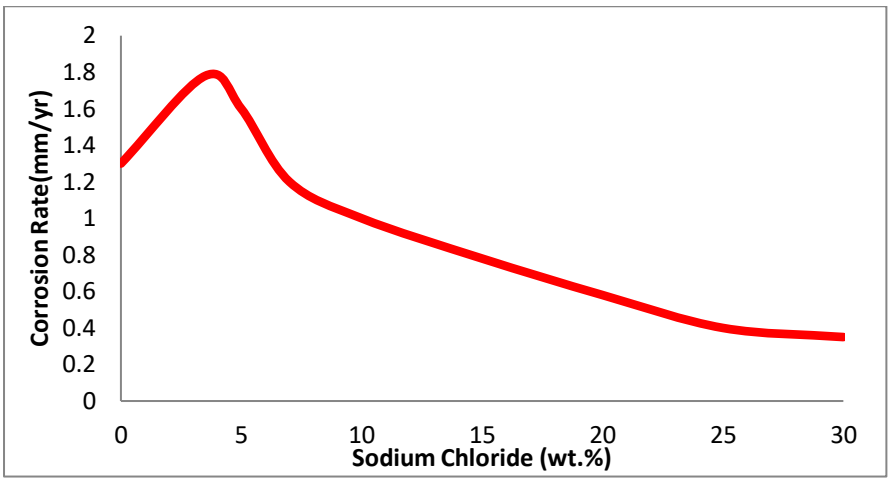

Figure 2-9. Combination of sodium chloride concentration versus the rate of corrosion in seawater **[86]**

Figure 2-9 shows how the combination of chloride concentration and dissolved oxygen concentration results in the maximum pitting corrosion rate. The highest oxygen concentration can be achieved at 3.5 weight precents sodium chloride [86]. Melchers et al [39] reported that, in immersed conditions, the corrosion rate is expected to increase due to higher dissolved oxygen concentration with reducing salinity (Figure 2-9) [39]. However, some researchers reported that, in the longer term, the pitting corrosion rate effect of salinity may be less because the increased oxygen has a greater tendency to form protective deposits (scale) or protective biofouling containing calcium carbonate [39].

Some researchers [71, 75, 82, 87] reported that, for sea water conditions, salinity is of little practical importance to marine corrosion. This is because corrosion of metals is not appreciably affected due to the salinity variations in open-ocean surface water range from 32000 to 37500ppm per thousand gram of water [71, 75, 82, 87]. According to the experimental work of Mercer et al. [87], the effect of change in salinity appears to be marginal for stainless steel in calm conditions. Chandler et al. [82] also did not

consider sea water salinity as one of the main environmental factors that influences corrosion rate of steel [82].

2.5.1.4 High Velocity of Water

Many metals are sensitive to velocity effects in seawater [1]. For metals like iron or copper, there is a critical velocity beyond which corrosion becomes high. However, for steel structures in marine environments, the little effect of water velocity can be ignored [88]. Melchers et al [75] reported that, with the possible exception of the effect on marine biological growth and the influence of the continuous supply of oxygen, the effect of low and moderate water velocity on the rate of corrosion can be ignored [75, 88]. However Melchers et al [5] found that water velocity does increase the rate of pitting corrosion nonlinearly. They indicated that when corrosion products and/or marine growth is disrupted or removed (as through erosion or abrasive action) the effect of water velocity on pitting corrosion can be more severe [52, 71].

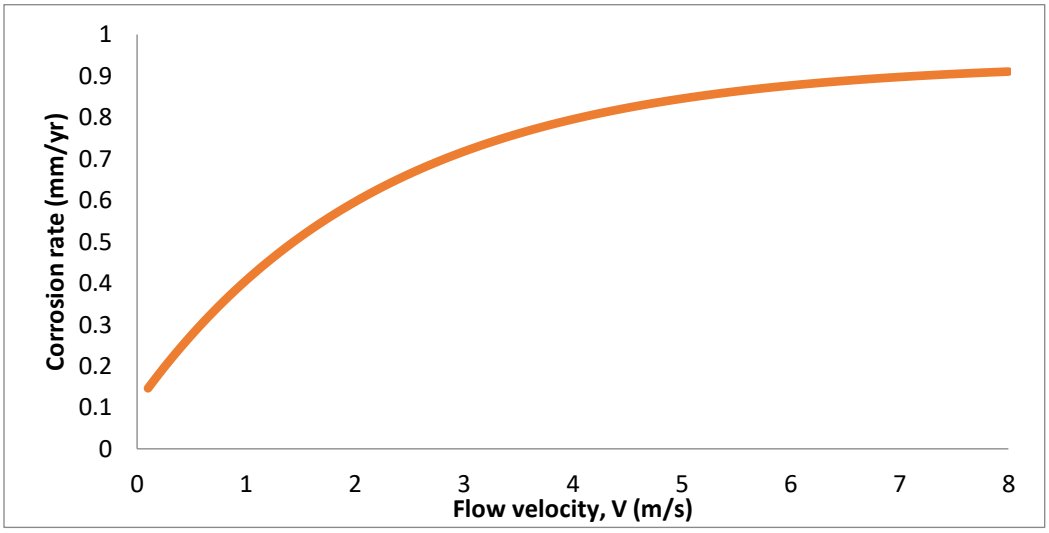

Figure 2-10. Effects of velocity of sea water on the corrosion rate of steel **[71]**

The effect of higher water velocity on marine pitting corrosion should be considered. Soares et al. [71] reported that the corrosion of steel by seawater increases as the water velocity increases. The effect of water velocity at higher levels is shown in Figure 2-10 and illustrates that the rate of corrosion attack is a direct function of the velocity until critical velocity is reached [22, 71]. Special forms of corrosion associated with higher seawater velocity are:

- Erosion-corrosion caused by high-velocity silt bearing seawater

- Impingement attack - where air bubbles are present
- Cavitation - where collapsing vapour bubbles cause mechanical damage and often corrosion damage as well [1].

2.5.1.5 Physical Size

Pitting corrosion in seawater is influenced by the size of the sample. The pitting susceptibility depends on marine environments such as tidal and/or splash zones; however, the size of the specimen may alter the rate of pitting corrosion. The effect of physical size on marine pitting is not yet fully understood. Melchers et al. [23] recommended that consideration be given to the physical size of specimen in order to model metal loss and pitting for realistic structures [23, 39]. They also advised that a comparative study be performed with the available observations on steel pylons in a marine environment and the results from isolated test specimens [23].

2.5.1.6 Water Depth (Hydrostatic Pressure)

The water depth (hydrostatic pressure) is also considered to be a factor that increases the rate of pitting corrosion in marine environments. The effect of depth of exposure in seawater on the average corrosion rate of steels has been studied by some researchers [63, 74, 89-92]. Melchers et al. [74] studied the corrosion rate for mild steel coupons exposed at variable immersion depths and at various geographical locations. Analysis of the data showed that there is not an obvious effect of water depth on short-term corrosion behaviour. Nevertheless, oxygen concentration and water temperature are important parameters influencing weight loss as a function of time in different immersion depths. The effects of immersion depth for long-term corrosion behaviour may not be limited to just these parameters however, as it will also be governed by anaerobic conditions [39, 74, 93].

Saleh et al. [94] conducted a laboratory test to evaluate the effect of seawater level on the corrosion behaviour of different alloys [94]. Specimens were fixed at three locations, namely: above sea water surface, semi-submerged in seawater and fully submerged in seawater. The experimental results show that, in a splash zone, the stainless steel usually has satisfactory performance but that the carbon and low alloy steels do not. The stainless steels are susceptible to pitting corrosion in the submerged zone because of

factors such as oxygen concentration, biological activities, pollution, temperature, salinity and velocity. Similarly the pitting corrosion rate for 316L stainless steel is higher above the water level than when compared to submerged conditions. This is due to the higher oxygen concentration above the seawater. However it is just the opposite for 304 stainless steel; the pitting density and pit depth resulted in an increased rate of corrosion for this alloy when in a submerged location. Conversely from these experiments, it was found that the pitting corrosion rate of metals at semi-submerged conditions is higher than for submerged and atmospheric conditions [94, 95].

2.5.1.7 Atmospheric Effects

In atmospheric conditions, the intensity of the corrosive attack is influenced greatly by the amount of salt particles or mist which collects on the metal surface [96]. Salt deposition varies with wind and wave conditions, the height above sea level, and exposure etc. [1]. Schumacher et al. [1] reported that several other factors which affect the atmospheric corrosion behaviour in marine environments can include solar radiation, the amount of rainfall and fungi.

Melchers et al. [23, 39] reported that macro biological activity is basically absent in atmospheric corrosion, but that it may have some influenc**e.** Additionally, the air temperature and exposure will have a direct influence on rate of corrosion [23, 39]. Newton et al. [97] conducted an experiment to investigate the variation of atmospheric corrosion as a function of length of exposure in various locations. They reported difficulties in drawing conclusions because of the variation in several factors like exposure, humidity and distance from the sea. Additionally, there were significant differences in air temperature and annual rainfall [23, 39, 97].

2.5.1.8 Water Current & Tidal conditions

Water current may have an effect on marine biological growth through the provision of an adequate rate of food supply. It also has an influence on the continuous supply of oxygen [1, 39]. Lewis et al. [98] reported that the effect of water current is difficult to quantify as it doesn't have a direct effect on pitting corrosion; however it can be a subsidiary factor for pit initiation. For example, it may increase the marine biological growth by dissolving the impurities in the ocean which could then lead to pit growth

[39, 98]. Melchers et al. [23] suggested that the effect of low to moderate water currents on the rate of pitting corrosion can be ignored [23].

The pitting susceptibility is higher in the tidal zone compared to pitting susceptibility in a fully immersed zone [39, 99]. Melchers et al. [39] gathered experimental observations and data, performed in cities such as Halifax, Colombo, Panama, Auckland, and Plymouth, which investigated the extent of corrosion loss as a function of length of immersion exposure [39, 99]. The plot for pitting depth in tidal conditions as a function of annual mean temperature for different experimental cities is shown in Figure 2-8.

2.5.1.9 Surface Wetting

The degree and continuity of surface wetting is particularly important for atmospheric, splash and tidal zone corrosion. The surface wetting depends on the location of the structural specimen relative to the sea water [39, 100]. In the tidal and splash zone, wetting may be controlled by the local tidal range and climatic conditions such as water, air and temperature. The effect of surface wetting is still not fully understood but the pitting due to surface wetting is believed to be minimal. Melchers et al. stated that no general rule exists to describe functional relationships between surface wetting and climatic conditions [23, 39, 100].

2.5.1.10 Initiation Time

Initiation time is often called induction time and pertains to the elapsed time before pitting corrosion begins [9]. Schumacher et al.[1, 76] described an experiment conducted in different stainless steels at $50^{\circ}C$ which were immersed in chloride solutions under open circuit potential measurements [1, 41, 76]. It was found that pitting potential could be presented as a linear function of initiation time, t_i, where A and B are constants that depend on temperature. Refer Equation 1.4):

$$E_{pit} = A + B.\log(t_i) \tag{1.4}$$

Malik et al.[101] conducted electrochemical measurements of the open circuit potential and found that the logarithm of the induction time decreases linearly with increasing

chloride contained and at increasing temperatures. These test temperatures were conducted at 30, 50 and $80^{\circ}C$ [101].

2.5.2 Chemical Factors

2.5.2.1 High Chloride Ion Concentration

The presence of certain aggressive anions, such as chloride concentration (Cl^-), can migrate to the active corroding area and stabilize pitting corrosion [102]. The influence of Cl^- on the susceptibility to pitting corrosion has been studied in numerous metals and alloys and particularly in stainless steel. Pardo et al. [102] stated that the presence of alloyed elements, such as Cr, Mo, and N, improve the resistance to localized corrosion of the stainless steel. However, the presence of chloride ions can easily penetrate the film due to its high diffusivity [41, 102]. Frankel et al. [18] explained that pitting corrosion will only occur in the presence of aggressive anionic species, which are usually chloride ions, and that the severity of pitting corrosion tends to vary with the logarithm of the bulk chloride concentration [18].

Figure 2-4 shows the curves plotted for two different chloride concentrations. It can be seen that E_{pit} increases with decreasing chloride content. Many researchers [18, 101, 103, 104] have published studies describing the relationship between E_{pit} and the chloride content. Different polarization measurements [18, 101, 103, 104] demonstrated that the pitting potential was a linear function of the logarithm of the chloride concentration. High alloyed stainless steels are less affected by increasing chloride content, and therefore E_{pit} changes only slightly for these alloys. [41].

2.5.2.2 Dissolved Oxygen

Dissolved oxygen content is a major factor affecting the corrosivity of seawater. For many common metals, a higher oxygen content is accomplished commensurate to the increase in the rate of pitting attack [1]. The corrosion rate of local anodes is dependent on the cathode reaction and, therefore, depolarization is more rapid with the increase of oxygen at the cathode. The depolarization is a function of the amount of dissolved oxygen in the seawater and the velocity of flow at the surface [22, 29].

Various authors commented that there is a good correlation between dissolved oxygen and corrosion mass loss [18, 58, 71, 105]. Melchers et al. [52] stated that the corrosion rate usually has a linear relationship with the concentration of dissolved oxygen [52, 71]. They further stated that the dissolved oxygen levels in open ocean conditions reduce with depth around 5-7 ml/l at surface, mainly as a result of increased pressure [23, 39]. Hence, the oxygen concentration is critical in the immersion corrosion process during the early stage of seawater corrosion [23, 39]. Schumacher et al. [1] mentioned that the oxygen level in seawater may range up to 12ppm. The factors that increase seawater oxygen could be photosynthesis of green plants and wave action etc. Conversely, the biological oxygen demand of decomposing dead organisms will reduce seawater oxygen level [1, 23]. Regional variation exists in surface water temperature; hence, salinity and locally mixed conditions occur due to the regional variations of oxygen level [39].

In waters containing high salt concentration, corrosion is proportional to the amount of oxygen dissolved in the water. If the salt concentration in the water increases, then the solubility of oxygen decreases and, consequently, the corrosion rate is reduced [92]. Therefore, oxygen dissolved in water is probably the most troublesome corrosion-producing substance. An exception to this statement is metals which depend on a passive film for corrosion protection. Nevertheless, stainless steel often corrodes rapidly where the oxygen supply to the metal is restricted [1, 39, 50].

2.5.2.3 Carbon Dioxide

The dissolved carbon dioxide in seawater produces carbonic acid and, after ionisation, it forms bicarbonate and carbonate ions[39]. Few effects of carbon dioxide are known for pit initiation in marine steel structures. However, Melchers et al. [39] did report that the presence of undissolved boric acid in oppositely charged ions such as carbon dioxide may provide a constant and fairly high pH level [1, 39].

2.5.2.4 Effects of Halogens Ions

Pitting corrosion can be caused by different halide anions [22]. The anodic process associated with metal passivation is strongly affected by the presence of halide ions in the electrolyte. With large concentration of halide ions the passive film on a metal is

susceptible to pitting and also suffers local damage; however, low concentration produces only an increase of anodic current in the passivity range [17]. Smialowska et al [17] described chloride as the most aggressive anions to produce pitting in several metals [17, 22]. The three main reasons for the specific effect of chloride ions is explained by Abood et al. [17, 22] as:

- Its ability to increase the activity of hydrogen ions in the pit electrolyte
- Ability to form complexes with cations and hydroxide
- Its ability to form a salt layer at low pH at the bottom of the pit.

2.5.3 Biological Factors

2.5.3.1 Bacterial

The corrosion of metals by sulphate–reducing bacteria (SRB) is well recognized as one of the factors that increase rate of pitting corrosion in marine environments [106]. Recent studies show that the hydrogen sulphide produced by these organisms can have a serious effect on mechanical failure processes by increasing a metal's susceptibility to corrosion - especially pitting corrosion [106]. Thomas et al.[106] stated that the effect of bacteria is particularly important for offshore structures; here it is envisaged that the combination of bacteria activity under marine fouling conditions, wave loading and an aggressive environment can result in the premature failure of metal components by pitting corrosion fatigue [106].

Melchers et al. [39] explained that bacteria is most commonly associated with marine corrosion of steel. *Desulfovibrio* is one of the most common; it is a genus of gram negative sulphate reducing bacteria. When this bacteria attached to the surface of a metal with other bacteria, they may not grow when there is a presence of oxygen [23, 39]. However Melchers et al. [23, 39] reported that, where anaerobic conditions are more conducive, they can grow well in the temperature range of 25°C- 44°C and with pH ranging from 5.5 to 9.0 [39].

2.5.3.2 Fouling

Marine fouling in offshore structures can have serious consequences on their integrity, enhancing both the corrosion and stress components of corrosion fatigue [106]. Fouling

is commonly considered to be growth beyond the bacterial stage. Algal growth may include seaweeds, coral, aurelias, barnacles, mussels etc. Melchers et al.[39] reported that common fouling can tolerate a range of temperature and light intensities, with growth most productive in the range of 15°C- 20ºC [75].

2.5.3.3 Marine Growths

Marine growth can affect the rate of pitting corrosion in immersion conditions [98]. Although the amount of marine growth varies considerably from location to location, it does not have an initial effect for short term immersion corrosion. It also appears that an initial effect is not reflected in fouling growth [23, 98]. Melchers et al.[23, 39, 98] reported that, despite local and regional geographical differences, the overall fouling pattern is somewhat similar. Moreover, the presence of local warm currents with adequate food supply appears to be the major factors for marine growth. It was also assumed that marine growth may be affected adversely by high currents and suspended solids [23, 39, 98].

2.5.3.4 Pollutants

Water pollution, particularly in harbours, may result in the increase of corrosion rate. Under these conditions the water may be more aggressive because of the greater concentration of ammonia or sulphide which is also combined with lower oxygen levels [107]. Due to the pollutants, water is less able to support marine growth of protective bacteria and bio fouling [23, 71]. Harbours and coastal regions may be susceptible to nutrient pollution from sewage or agriculture run-off. Offshore oilfields are also known to provide sources of nutrient pollution [23, 71]. Schiffrin et al. [23, 107] reported the effect of nutrient-based pollution on the corrosion of mild steel coupons. It was found that pollutants like oils and grease lower the corrosion rate due to their inhibiting the rate of oxygen transfer for the oxidation process. The effects of pollutants for marine pitting corrosion is not fully understood; however, for coastal and harbour areas, the effect of pollutants for pitting corrosion is expected to be higher than that for uniform corrosion [10, 23, 39, 107].

2.5.4 Metallurgical Factors

2.5.4.1 Alloy composition

The effect of alloy composition acts on the tendency for an alloy to initiate pit and also affects rate of corrosion [17]. This influence appears to be related to the quality of the magnetite layers found on the surface of steel and appears to be a function of the alloying elements [39]. Schultze et al.[108] provided a summary of the effect of steel composition on corrosion loss. It was reported that a particular alloy may have a favourable effect in corrosion resistance under some exposure conditions but have an unfavourable effect on others [39, 108].

Table 2-4. Effects of alloying elements on corrosion resistance of steels **[39, 108]**

Alloy	**Immersion Zone**	**Tidal Zone**
Aluminium	Not conclusive, but perhaps beneficial long term effect	Not conclusive, but perhaps beneficial long term effect
Chromium	Favourable initially (<5 years) therefore undesirable	
Copper	Probably detrimental long term	-
Manganese	Slight beneficial effect	Probably detrimental
Molybdenum	Unfavourable short-term, however favourable long term	-
Nickel	Little effect	Beneficial effect
Phosphorus	Very detrimental long term, low concentration in steels	-
Silicon	Not important	
Sulphur	May be detrimental even in small quantities	

Table 2-4 summaries the main effects of alloying elements. The influence of steel composition on pitting corrosion susceptibility and uniform corrosion susceptibility is similar in marine corrosion. However, the pitting resistance of low alloy steel may be less than that of carbon steel [23].

Ting et al. [109] reported that the small changes (say <0.5%) in the alloying elements used in steel composition should have zero or negligible effect on the degree of corrosion that occurs while oxygen diffusion controls the corrosion process [109]. More specialized steel with larger alloy compositions will have a lower initial rate of corrosion. This is particularly so for alloying elements such as chromium, molybdenum

and aluminium and, to a lesser extent, for nickel, silicon, titanium and vanadium [53, 109]. Smialowska et al. [17] studied the effect of small increases in molybdenum in steel composition and it was found that only a small increase can greatly reduce pitting corrosion susceptibility. In addition to this, a small increase in elements such as nitrogen and tungsten also have a strong influence on the pitting resistance of stainless steels [17, 22].

2.5.4.2 Steel Types

Steels differ in their relative corrosivity under different conditions. ASTM [89] and Melchers et al. [39] categorised steels as: 1] ordinary steels, such as mild steel, 2] low alloy steels, or high strength steels and 3] stainless or chromium steels [39, 89].

Stainless steels are obtained by the addition of chromium (around 3%) to steel. This alloy is usually used for applications in marine atmospheric conditions for maintaining the passivity protective surface film. Melchers et al. [39] stated that, when local perforation of the stainless steel passive film occurs, active passive cells are formed and heavy local corrosion such as pitting occurs. For immersed conditions, the addition of chromium to stainless steel is beneficial for short term exposure (a few years); however, it is not agreed if this is also the case for long term exposure. The resistance to corrosion of low alloy steels may range from two to ten times that of ordinary carbon steel. This is because, due to the formation of basic salts on the surface, low alloy steels form a tighter rust coating at a faster rate than that of coronary carbon steels. [39, 80, 110].

2.5.4.3 Surface Conditions & Surface Roughness

The state of the metal surface is known to affect pitting susceptibility [17, 29]. The more homogenous the surface is, both chemically and physically, the higher is the potential for pitting. Consequently the number of pit is expected to be lower and metal resistance to pitting will increase [17, 22, 58]. Surface roughness is caused by local 'weak' points in the protective oxide film where a critical Cl^- concentration can attend, or by homogeneities resulting from surface preparation; either can increase the number of active sites for pit nucleation [17]. Isaacs et al. [64] studied the effect of exposure time on active pit propagation on AISI 304 stainless steel in 0.4M $FeCl_3$ solution of pH 0.9, using a scanning reference electrode to measure the number of active pits. Both the

number of active pits and the rate at which their growth was decreased (because of passivation) depended on the steel surface treatment [17, 64].

The roughness of a material's surface depends on the surface preparation. This preparation is done to ensure proper adhesion of the coating. The coating is used to protect the materials from the environment by making a smoother surface and, thereby, reducing the possibility of localized corrosion occurring [41]. Moayed et al. [54] reported, and it is well established, that at temperature above the CPT, the pitting potentials tend to decrease as the sample surface roughness increases. The surface roughness offers advantages to change the characteristic of sites for pit initiation. Pits initiate at specific sites on the surface and a rougher surface generally provides the site with more passage geometry [17, 41, 54]. Moayed et al. [54, 111] studied the relationship between CPT and surface roughness. They found that, with an increase in surface roughness, the CPT decreases and standard deviation of the test result increases. The higher chance of stable pitting in rough surfaces is attributed to the longer length of diffusion and larger micro-crevices surrounding the inclusions [54, 111]. Manning et al. [112] established a similar correlation on the effect of surface roughness on pitting potential for single-phase and duplex stainless steel.

2.5.4.4 Protective Coating

Protective coating systems, also known as anticorrosive coating, is one of the methods developed to protect external surfaces against corrosion [41]. The protective coating systems is highly recommended by classifications society rules such as DNV-RP-G101 [113] and NORSOK M-501 [114]. Protective coatings are critical for marine structures mainly because the environment is very aggressive and corrosive [62, 73, 114]. Marine structures require applications consisting of primer, one or several intermediate coats, and a topcoat. The function of the primer is to protect the substrate from corrosion and to ensure good adhesion to the substrate [73].

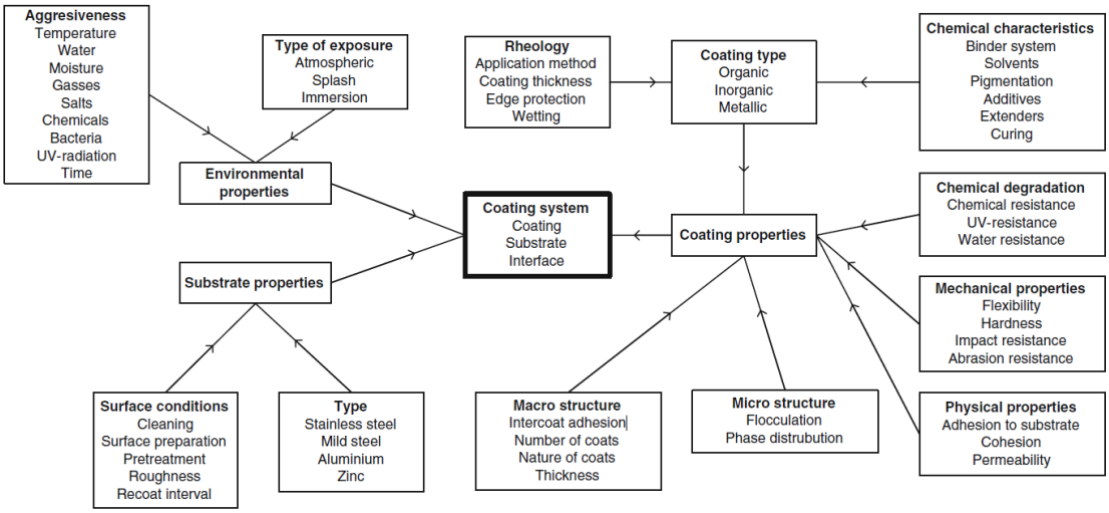

Figure 2-11. Factors affecting the durability of an anticorrosive coating system [73]

Figure 2-11 shows the factors that affect the durability of an anticorrosive coating system [73]. Sorensen et al. [73] stated that the coating provides the required colour and gloss for surfaces exposed to external marine environment. The protective coating should have a high resistance to ultraviolet radiation [73] as well as adequate resistance to altering weather conditions and impact from objects. Bayer et al.[115] reported that environmental degradation caused by moisture, temperature and ultraviolet radiation will reduce the lifetime of the coating. These authors reported six primary causes of the majority of paint and coating-related failures: 1] Improper surface preparation, 2] Improper coating selection, 3] Improper application, 4] Improper drying, curing and over-coating times, 5] Lack of protection against water and aqueous systems, and 6] Mechanical damage [115].

2.5.4.5 Mill Scale

The presence of mill scale on structure's appears to lead to greater pitting corrosion [39]. The effect appears to be most significant for atmospheric corrosion and less for tidal and immersed corrosion conditions. Melchers et al. [39] stated that the intensification of rate of pitting attack caused by mill scale is thought to occur due to electrochemical action between the mill scale and the undecorated metal. Generally, mill scale tends to protect the metal underneath, except at cracks. At these points the scale becomes anodic and, because of the relatively large cathodic area, the rate of attack caused by

electrochemical action between mill scale and the bare metal at local anodes is instantaneous [23, 39].

2.5.4.6 Effect of PRE_N Value

Pitting Resistance Equivalent (PRE_N) is the capacity of an alloy to resist pitting. A higher potential is needed to initiate pitting in alloys with large PRE_N values than with alloys which have low values [41, 76]. PRE_N is represented by the Equation 1.6:

$$PRE_N = \%Cr + 3\%Mo + 16\%N \quad (1.6)$$

PRE_N is mentioned in several studies when assessing whether an alloy can resist pitting corrosion [18, 22, 25, 35, 41, 76, 116, 117]. Lorentz et al. [118] initially established a good correlation between the pitting potential of a wide range of stainless steels. It was found that the sum of %Cr+3.3×(%Mo), indicating molybdenum additions, were three times more effective than chromium additions in increasing pitting resistance [117, 118]. Malik et al. [76] reported that, PRE_N >38 conditions should be satisfied to provide pitting corrosion resistance to seawater-immersed conditions [41, 76]. Johnson et al. [119] studied CPT as a function of PRE_N. His research demonstrated that the CPT increases almost linearly with increasing PRE_N. The experiment involved testing of stainless steel alloy samples in seawater at $50^{\circ}C$ with the corrosion rate dependent on the PRE_N value. The results showed that the PRE_N value decreases with an increase in temperature [41, 118, 119]. Malik et al [103] suggested that E_{pit} is also a linear function of the PRE_N value [41, 103].

2.6 Corrosion-Related Accidents in Marine and Offshore Sectors [3, 11, 89, 95, 120-122].

Table 2-5. Historical offshore accidents reported due to pitting corrosion

Accident	Year	Fatalities	Cost	Descriptions
Umm Said Qatar (Weld Failure, Gas Processing Plant)	April 1977	3 killed	US$ 179 million	A tank containing 236,000 barrels of refrigerated propane at 45 °F failed at weld. The possible cause of weld failure was corrosion due to the influence of sulphate reducing bacteria that remained inside the tank after hydro test with seawater. The wave of liquid propane swept over the dikes before igniting a nearby tank containing 125,000 barrels of buthane. It took eight days to completely extinguish the fire.
Ekofisk Norway (Weld Failure, Offshore Platform)	March 1980	123 killed		Alexandra L Kielland Platform, a semi-submersible oil-drilling platform located at Ekofisk field North Sea, capsized during a storm. The platform was supported by five columns standing on five 22-meter diameter pontoons. The five 8.5 diameter columns on the pontoons were interconnected by a network of horizontal bracings. A cracked bracing made five other bracings break off due to overload, and the vertical column connected with the cracked bracings became separated from the platform. The platform subsequently became unbalanced and capsized. The investigation showed that a corrosion fatigue crack had propagated from the double fillet near the hydrophone mounted to one of the horizontal bracings.
Mexico Pipe Leaking (LPG)	November 1984	650 killed 64000 injured	US$ 29 million	A 12-inch pipeline between cylinder and sphere storage ruptured. Initial blast caused a series of BLEVEs (boiling liquid expanding vapour expansion). The outstanding cause of escalation was the ineffective gas detection system and, due to this, of lack of emergency isolation. This explosion and fire is perhaps the most devastating incident ever. The high death toll was due to the proximity of the LPG terminal to a residential complex. The accident is not fully understood however; researchers claim that this accident occurred due to the pitting corrosion in the pipe.
Piper Alpha North Sea (UK)	July 1998	167 killed	US$ 1.27 billion	This was predominantly an operational error. Gas leaked from two blind flanges due to localized corrosion - then the gas ignited and exploded. A pump from two available pumps was tripped, and an operator accidentally changed the backup pump with a pressure relief valve, which had been removed, for maintenance. Severity damage of the explosion was due largely to the contribution of oil and gas pipelines connected to Piper Alpha.
Sinking of the Erika	Dec 1999	8 Killed		Erika broke into two near the coast of France whilst carrying approximately 30,000 tons of heavy fuel. 19,800 tons of fuel spilled along the coast of Brittany and France. This single oil spill was equal to the total amount of oil spilled worldwide in 1998. A corrosion problem, which had apparently existed on the Erika since 1994, led to this devastating accident in 1999.
Roncador Brazil	March 2001	2 Killed 8 missing	US$ 515 million	Investigation report of the fire, explosion, and sinking to P-36 (the largest offshore production facility) revealed a sequence of events started from the failure of the starboard emergency drain tank (EDT). Excessive pressure in Starboard EDT, due to a mixture of water, oil, and gas, caused a rupture and leaking of EDT fluids into the fourth level of the column. The leaks were believed to have occurred due to corrosion.

2.7 Methods of Identification of Pitting Corrosion

The first stage in understanding pitting corrosion of steel is to correctly identify the phenomenon. Pitting corrosion is characterized by small flaws in the surface of a material as shown in the Figure 2-3 [25]. There are many techniques that can identify the presence of pitting [25, 120]

2.7.1 Visual Inspection

To identify pitting corrosion, visual inspection can be done in ambient light to determine location and severity of pitting. Cairns et al. [25] stated that photographic imaging is often used to document the difference in appearance of pits before and after removal of corrosion products [25]. Roberge [20] describe this technique as easiest to employ as it does not require specialized equipment and is relatively economical [20]. Recently, the use of remotely operated vehicles (ROV) and autonomous underwater vehicles (AUV) replaces dangerous human effort for deepwater inspection and underwater work. They increase safety, reduce costs and increase efficiency. These technologies utilize visual imaging and produce high resolution photographs of the corrosion susceptibility in structures [123].

2.7.2 Metallographic Examination

Metallographic examination is an investigative technique that can be used to determine the size, shape and density of corrosion pits [25]. Jana et al. [124] stated that metallographic examination is typically a destructive analysis technique as the specimen must be cut from the component and examined with a microscope [124]. Power et al. [61] studied the simultaneous electrochemical analysis and in situ optical microscopy for 316L stainless steel samples submerged in sulphuric acid based solutions. They reported that this technique provides both a detailed visual account of the corrosion process as well as a standard electrochemical analysis of the pitting potentials and corrosion rate [61]. A brief discussion on the metallographic examination is provided by Caines [25].

2.7.3 Non-Destructive Testing (NDT)

Non-destructive testing (NDT) is a key technique used in industry to evaluate the current state of component and equipment in service and to aid in maintenance planning. It plays an important role in the continued safe operation of physical assets [25, 122, 125]. American Society for Non-destructive Testing (ASNT) defines NDT as “the determination of the physical

condition of an object without affecting the object's ability to fulfil its intended function. NDT techniques typically use a probing energy form to determine material properties or to indicate the presence of material discontinuities" [125]. ASTM G46-96 [122] stated that NDT technique is applicable to identify pitting corrosion however, it is not effective at characterizing pitting as a destructive method . Additionally, specialized training is required to ensure realistic results [25, 122]. A brief description of each NDT method is presented by Forsyth et al. [125] and Caines et al. [25].

An NDT method is classified according to its underlying physical principle [25, 124-126] and common methods are:

- Visual and optical Testing (VT) [125]
- Radiographic Testing (RT) [127]
- Electrochemical and Electromagnetic Testing (EC, ET) [17]
- Ultrasonic Testing (UT) [128]
- Liquid Penetrant Testing (PT) [25]
- Magnetic particle Testing (MT) [25, 125]
- Acoustic Emission Testing (AET) [25, 95] and
- Infrared and thermal Testing (IRT) [25]

2.7.4 Surface Analysis Technique

Methods of surface analysis are increasingly being used to detect and quantify elements present inside the passive layer [30, 92]. Auger electrons spectroscopy (AES) is a common analytical technique used in the study of the composition of the outer 1-5 atomic layer of the surfaces of solids [129]. During AES, the sample is attacked with 1 to 10 KeV electrons and the instrument analyses the emitted auger electrons. The sensitivity to individual elements is about 0.1%, however the accuracy of the result is fairly poor [30, 129].

X-ray photo-electron spectroscopy (XPS) consists of subjecting a specimen to X-ray photons and analysing the ejected electrons. The main advantage of this technique is that the energy of these electrons varies with the chemical state of the sample element. The depth sampled, and the sensitivity, is approximately the same as for AES. The main disadvantage of XPS is the poor lateral resolution obtained due to the absence of focus by the incoming energy [130].

Secondary ion mass spectrometry (SIMS) is a technique for surface and thin-film analysis. SIMS has been extensively reviewed from various instrumental aspects such as analytical applications, comparison with other surface analytical techniques, application of surface studies and fundamental aspects of ion emission [131]. Usually, these techniques are

associated with ion sputtering (ejecting the atom from a solid) to allow for in-depth analysis of the sample. However, sputtering has various disadvantages because it destroys the chemical bonding which may have been present on the surface, as well as at the original find topography. It may also form a cavity when sputtering is uneven, and some elements may sputter more slowly than others creating a new distribution in the removed sample [30, 58, 129, 130].

2.7.5 Probabilistic Approach for Pit Identification

Pitting corrosion has long been known to be a particularly inconsistent and unpredictable process [30, 132]. More precisely, it is challenging to forecast when a pit will initiate and where this is going to take place, therefore researchers have tried to extract data from the distributions during times of pit nucleation events [28, 30]. Shibata et al. [133] were the first to postulate that the critical potential necessary to induce pitting, and the induction time elapsed before pits become observable, are both statistically distributed quantities [134]. They asserted that the nucleation of a pit is a statistical process similar to the development of a crack in brittle material. They conjectured that the pit generation process has the Markov property, i.e. that the future probability of pit nucleation is uniquely determined once the state of the system at the present stage is known [30, 133]. Henshall et al. [134] found that the stochastic model of pitting corrosion was useful in predicting corrosion damage of high-level radioactive waste containers. They stated that the model includes simple phenomenological relationships describing environmental dependence of stochastic parameters, and that it can simulate pit initiation and growth under various environments, including those that change during exposure [134]. Similarly, Valor et al. [27, 135] used a new stochastic model for pit initiation and pit growth [27, 28, 135].

Spatial distribution models are commonly used in locational analysis, including spatial location of activities among the zones of a region and measure of interaction between zones [136]. In the case of pitting corrosion models, spatial distributions is used when the pits on the sample do not exactly follow a poisson distribution [30]. Several researchers have modified the spatial distributions to model pitting corrosion [9, 12, 27, 135-141]. In addition, Aziz et al. [137] introduced exponential distribution of the pit depth to calculate the maximum depth by the statistic of extreme values [137].

2.8 Corrosion Modelling

The quantitative understanding (i.e. a model) of how the corrosion process operates as a function of exposure time and under various environmental influences is necessary. It is also required to predict the likely amount of corrosion in the future for defined conditions [70]. Prediction and identification of pitting corrosion in marine and offshore structures is a difficult problem for a number of reasons [46]. Firstly, the events take place on a very small scale, with passive film nanometres in thickness and with initiation sites of similar sizes. Immediately after initiation, the rate of pit growth can be extremely high, even tens of A/cm^2 [18, 23, 46]. Frankel et al [46] considered the pitting location as an extremely dynamic one with rapidly moving boundaries and rapidly changing chemistries.

The modelling of pitting corrosion in marine and offshore conditions has been study of interest for some time. The effect of the main factors in pitting corrosion modelling, such as temperature, bacterial community, oxygen concentration, pH, and velocity, has been considered in the past by several researchers [47, 54, 60, 80, 81, 101, 102, 142].

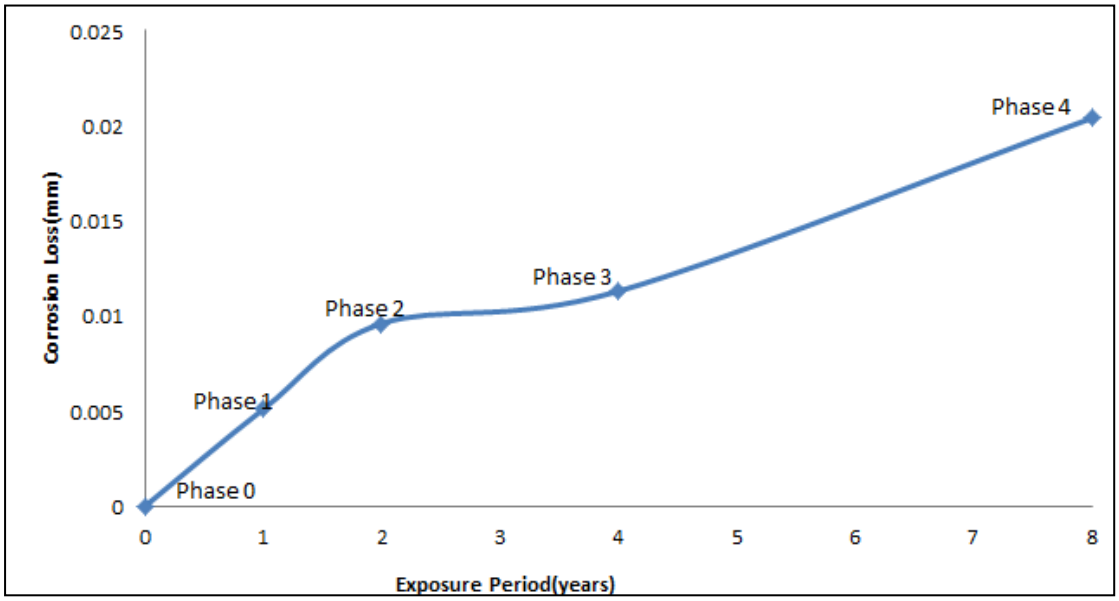

Figure 2-12. General schematic of model for corrosion loss showing the changing behaviour of the corrosion process as a series of sequential phases, Adapted from **[110]**

Researchers [8, 15, 47, 67, 75, 110, 140, 143-145] proposed a widely accepted multiphase phenomenological model for corrosion loss as a function of exposure period. As shown in Figure 2-12, the model was developed based on corrosion science philosophy. The model has several phases, including kinetic, diffusion, transition, and anaerobic, and each of these phases is believed to control the corrosion process [6, 110, 146]. This model is based on theoretical

and empirical corrosion mechanics. In Figure 12, phase 2 indicates the theoretical point at which anaerobic conditions is reached [6, 7, 15, 24, 51]. This condition tends to encourage rapid marine growth and, by inference, conditions favourable for sulphate- reducing bacteria (SBR) including activation and growth. [145]. From Figure 2-12, the number of sequential phases which correspond to the different processes controlling the (instantaneous) rate of corrosion for 'at sea' conditions is summarised as below [6, 52, 110, 146-148] :

Phase 0 – a very short period of time during which corrosion is under 'activation' or kinetic control. This is governed by the rate at which local chemical reactions can occur unhindered by external diffusion or transportation limitations [74, 93, 110].

Phase 1 – a period of 'oxygen concentration' control; the corrosion rate is governed by the rate of arrival of oxygen through the water and the corrosion product layer to the corroding surface. It can be seen in the multiphase model that this phase can be modelled, to an approximation, as a linear relationship between depths of corrosion vs. time [39, 67].

Phase 2 – in this phase the corrosion rate is controlled by the rate of oxygen diffusion to the corroding surface through the increasing thickness of the corrosion product. This phase is therefore a non-linear function of time - the reason being is that, when the corrosion products build up, the oxygen flux will decline and eventually anaerobic conditions will be established in the zone between the corrosion product and the corroding metal [144, 145, 149].

Phase 3 – in this phase the rate of corrosion is controlled by the metabolic rate of sulphate reducing bacteria (SRB) under anaerobic conditions. Often, this phase 3 is a period of rapid growth of SRB resulting from the conditions now being suitable for their increased metabolism and from the plentiful supply of nutrients [149]. The high rate of metabolite production initially produces a high rate of corrosion, but this reduces to a quasi-steady state situation in equilibrium with the rate of supply of nutrients and energy sources from the bulk water [24, 144, 147, 149, 150].

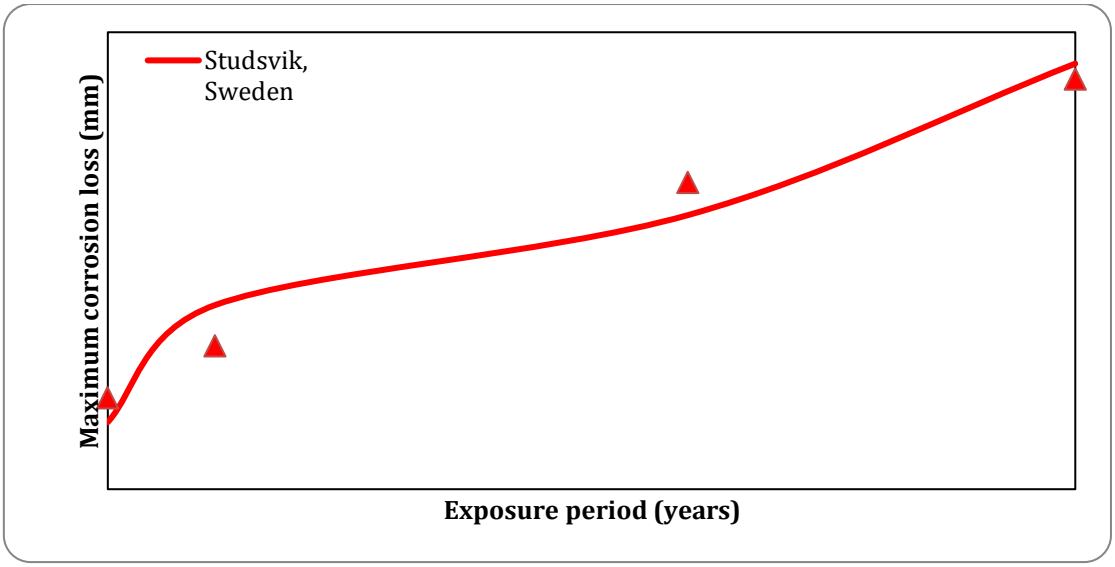

Figure 2-13. Corrosion loss model and data fitting for long term corrosion data accessed from ASTM worldwide corrosion data.

Phase 4 – this represents the quasi-steady state situation reached at the end of phase 3 and is presumed to continue indefinitely. Melchers et al. [149] stated that presently there is insufficient understanding of the precise mechanisms involved in this phase; however, the long term data for pitting corrosion suggests that it is closely linear with time (Refer Figure 2-13). Observations for a variety of steels also suggest that the corrosion rate is largely independent of the actual activity levels of SRB and of the type of steel [144, 149, 150].

Modelling of the uniform/general corrosion in marine and offshore structures is reviewed in the subsequent sections; however, the focus is on modelling the pitting corrosion in marine and offshore structures [5, 6, 9, 10, 12, 15, 24, 27, 28, 52, 71, 74, 105, 109, 135, 138, 140, 141, 146, 147, 151-162].

2.8.1 Modelling the General Corrosion in Marine Environments

Statistical and stochastic aspects of pitting corrosion were first developed in the late 1970s [158]. In large-scale engineering structures, the measurement of pit depth and frequency is considered to be time-consuming and expensive. Therefore, only the deepest pits are studied since they are likely to be the cause of failure in these structures [9, 28, 158]. The extreme value statistics developed by Gumbel are widely used in the application of the maximum pit depth distributions. Extreme value distributions include three types of asymptotic distributions for an infinite number of samples:

Type I : *Gumbel distribution* $F(x) \sim \exp(-\exp[-x])$ (1.7)

Type II : *Cauchy distribution* $F(x) \sim \exp(-x^{-K})$ (1.8)

Type III : *Weibull distribution* $F(x) \sim \exp(-\exp[\omega - x]^{k}$ (1.9)

Where x is a random variable representing the maximum pit depth, and k and ω are constants.

Melchers et al. [162] studied the assessment of the remaining safe and serviceable life of deteriorating structures. A probabilistic model for immersion corrosion loss with time on mild and low alloy steels was developed based on the fundamental physiochemical model [52, 146]. They stated that, for structural reliability assessment using probability theory, the structural strength at any point in time t can be represented by $R(t)$ with probability function $f_R(r,t)$, where $R(t)$ is a random variable and r is a discrete, deterministic value. The generic form of the proposed model has material loss due to corrosion as a function of time and is expressed by:

$$c(t, E) = b(t, E).f(t, E) + \varepsilon(t, E) \quad (2.0)$$

Where $c(t,E)$ is the average depth of penetration from one side of steel plate (mm); $f(t, E)$ = mean value function; $b(t, E)$ = bias function which should be unity when $f(t, E)$ represents $c(t, E)$ exactly under all conditions; $\varepsilon(t,E)$ = zero mean uncertainty function; and E = vector of factors which characterize the exposure environment, steel composition, and the surface finish factors. From this analysis Melchers et al.[162] stated that the rate of pit growth is not a linear function of time [162]. Additionally, Melchers et al. [146] proposed a similar probabilistic modelling based on corrosion mechanics and environmental factors. The environmental factors included were: temperature, dissolved oxygen, salinity, calcium carbonate, pH, water velocity and marine growth. The probabilistic model divided the corrosion into four particular stages: initial corrosion; oxygen diffusion controlled by corrosion product and micro-organic growth; aerobic activity with limited food supply; and anaerobic activity [110].

Neither of the previous studies attempted to include the effects of the different operational or environmental factors on the corrosion degradation expected through the lifetime of the structures. Melchers et al. [74] stated that in order to improve corrosion models it is necessary to not only account for time but also include contributing variables [74]. They also identified the main corrosion mechanisms that can be found in steel structures as well as the main environmental factors that affect them [52, 146]. Conversely, other studies tried to extend the previously developed, time-dependent corrosion models to include the effect of additional

different environmental factors. These studies were mainly based on statistical analysis of field and experimental data [52, 105, 146].

Using literature field data as well as new field observations; Melchers et al. [5, 15, 110] calibrated the parameters of multiphase time-to-corrosion models on mild and low alloy steel under fully aerated immersion conditions. They proposed a phenomenological model for general corrosion of mild, low alloy steel under near-surface conditions; this was adapted from a model of at-sea immersion conditions which had already been proposed [154]. They utilized literature data from the previous work [110, 154] and applied a similar probabilistic framework (refer to Equation 1.7) [151]. The calibrated parameters were then used to predict the corrosion degradation as a function of time and sea water temperature [5, 15, 110].

Melchers et al. [105] proposed examples of mathematical modelling for long term general corrosion of structural steels in sea water. Consideration was given to the early corrosion controlled by oxygen concentration which then later evolves to anaerobic conditions. The model was calibrated using extensive field data received from an offshore oil platform site located in Haloong Bay, Vietnam, and from coastal sites along the China Coast [105]. Furthermore, Melchers et al [147] proposed the probabilistic model for atmospheric corrosion of structural steels in ocean environments [147]. However, they disagree with some of the assumptions previously made such as that corrosion is the linear function of time, i.e. that there is a constant corrosion rate and the assumption that the corrosion rate is a monotonically decreasing function of time [147].

2.8.2 Modelling the Pitting Corrosion in Marine Environments

Katano et al. [156] proposed a predictive model for pit growth on underground pipes. They relied on the theory that the pitting corrosion rate for metal depends on environmental factors. They established the relationship between pitting depth and environmental factors. This relationship was explored through regression analysis, with pitting depth as dependent variables and on environmental factors as independent variables. Pitting depth was expressed as a power of time *t*.

$$\eta = \gamma t^{a} \qquad (2.2)$$

Where, γ and *a* are constant. From the above relationship, they derived a statistical model of pitting depth *(y)* as a dependent factor and environmental factors (x) as independent factors. A regression model is expressed as:

$$y = \eta \exp(\varepsilon)[\varepsilon \square N(0,\sigma^2)],\ \eta = t^{\alpha} \exp\left(\beta_0 + \sum_{j=1}^{p} \beta_j x_j\right) \quad (2.3)$$

Where, α and β are regression coefficient.

Melchers et al. [74] extended the model previously developed[139] to include the effect of dissolved oxygen in order to obtain a multiphase, time-dependent pitting corrosion degradation model incorporating the effect of dissolved oxygen concentrations [74]. Furthermore, Melchers et al. [74, 88] gave consideration to how the previous observations could be used to represent the effect of water velocity on the previously proposed models. They stated that it is essential to investigate the influence of water velocity on early corrosion behaviour; only then could the corrosion rate be correlated with the dissolved oxygen in the early stages of corrosion. They thereby confirmed that the depth is not an independent factor in marine immersion corrosion of mild steel; however, dissolved oxygen, water temperature, and local water velocity were found to be the main influencing factors [74, 88].

Guedes at al. [157] studied the effects caused by different environmental factors on the pitting corrosion behaviour of steel plates totally immersed in salt water conditions. They proposed a corrosion wastage model based on a non-linear time-dependent function. This model accounts for the effect of various environmental factors including salinity, temperature, dissolved oxygen, pH, and flow velocity [157].

Melchers et al. [6] studied the statistical characteristics of pitting corrosion, represented by the extreme value distribution 'Gumbel'. Since then, considerable progress has been made in the rational description and mechanistic modelling of individual pit initiation and early pit growth. Regardless, the modelling for growth in pit depth tends to be largely empirical and laboratory observations are unlikely to be representative of field conditions. In particular, experiments cannot include the precise effect of bacterial activity in pitting corrosion [6, 74, 139]. They proposed the phenomenological model for pit growth and extreme value of pit depth using 7 years of field data. From this analysis, they stated that only those pits that initiate immediately upon exposure, and then grow as stable pits, can become extreme depth pits. Distributions of all pit depths indicate the probability of occurrences of maximum pit depth for short and long marine immersion conditions. A Gumble distribution is commonly adopted as extreme valve distributions because it provides for less conservative probability estimates [6, 74, 139].

Melchers et al. [5] studied the variability of maximum pit depth of mild steel specimens subjected to marine immersion. Here the authors considered the effect of anaerobic conditions

for immersion pitting in mild steel. The data was calibrated and maximum pit depth was shown to be a function of sea water temperature [5, 139]. When considering the multiphase phenomenological model, it was found that pitting was most severe when widespread anaerobic conditions were established at the corroding surface. It was acknowledged that the Gumbel distributions plot that was used previously for expressing pit depth variability was combined with a simple power function. However, they reported that the pit growth is a more complex function involving several stages such as pit initiation, metastable pit and stable pit [5, 6, 110].

Melchers et al. [139] then introduced super stable pit growth which initiates immediately after exposure and grows without significant metastable activity [139]. They reported that, as a result of super stable pit there is likely to be a high degree of dependency among the depths of extreme (deepest) pits. By this time, when the super stable pits are introduced the use of extreme value distributions (Gumbel distributions) started to become doubtful because it was now known that the statistical population of super stable pits are likely to be different from the remaining pits. Melchers et al. [139] recommended the use of normal distributions (modelling the probability of occurrences) to represent the extreme pit depth of super stable pitting. Using the structural reliability system theory, the distributions of the pit depth (for the deepest depth) can be expressed as:

$$F_{X_{\max}}(a) = P[X_{\max} < a] = P[all \text{ pits } x_i < a] \tag{2.4}$$

Where, event x_i is the pit depth represented as random variable; P[$x_i < a$] the probability of occurrences; and X is the random vector which hold all component x_i. From this analysis, Melchers et al. [139] identified that if the probability distributions for the deeper pits are normal, the probability distributions for the extreme pits should also be normal distributions. They further established that these probability distributions have more certainty than those estimated by conventional approaches such as Gumbel distributions [139].

Khan et al. [12] proposed statistical methods to improve the estimation of degradation rate. They indicated that combining the statistical methods with a reliability assessment would offer a potential for better use of inspection results, and for the prediction of the probability of future leaks in offshore pipes as well as remaining life assessment [12, 163]. In pitting corrosion, the average degradation rate does not represent the real status of material degradation due to the nature of pit initiation and to its usually difficult location. Hence, for pit corrosion modelling purposes, focus is given to establishing the relationship between the maximum pit depths in the given exposure. Khan et al. [12] recommended a use of extremes value statistics in pitting

corrosion to investigate extreme values and proposed linear, power law and logarithmic extreme value models [12, 163].

$$Linear\ \mathrm{mod}el: \quad x - x_0 = k(T - T_i) \tag{2.5}$$

$$Power\ \text{law model:} \quad x - x_0 = k(T - T_i)^n \tag{2.6}$$

$$Logarithmic\ law\ \mathrm{mod}el: \quad x - x_0 = k\log(T - T_i) \tag{2.7}$$

Where, x_0 is the threshold depth of degradation (pit depth) at initiation time T_i ; x is the measured depth at time T ; and k is the pitting corrosion rate. Depths exceeding x_0 would grow, whereas depths lower than the x_0 may fail to grow [12, 163]. Khan et al. [12] and Kowaka [163] provided a brief list of the applicable distribution types for localized degradation.

Melchers et al. [141] proposed an extreme value analysis for long term marine pitting corrosion of steel affected by corrosive agent sulphate reducing bacteria (SRB). They argued that the conventional use of Gumbel distributions is no longer appropriate for deriving extreme value statistics for maximum depth of pits in pitting corrosion [141]. They stated that conventional use of Gumble distribution does not consider either stable or metal stable pit growth.

SRB is the main corrosive agent for longer term pitting corrosion. Modelling of long term pitting corrosion is rather difficult because of the lack of sufficient data in one exposure location hence the use of Frechet extreme value distributions is appropriate as it combines the data from different exposure times [141]. Melchers et al. [141] proposed a statistical model for longer-term, maximum pit depth which considers the effect of anaerobic conditions.

$$x(t,T) = C[e(t,T)/\rho(t)]t \tag{2.8}$$

Where, $e(t,T)$ denotes the rate of supply of nutrients to the corroding surface; t is the time elapsed since the commencement of overall anaerobic activity; and T is the mean water temperature. Also, if $\rho(t)$ is the proportion of the surface covered by pits, then the rate of supply of nutrient per pit at any time t is proportional to $e(t,T)/\rho(t)$ [141].

Mohammad et al. [164] proposed a prediction model of pitting corrosion characteristics using Artificial Neural Networks (ANNs). They used a pre-corroded steel specimen and immersed it in corrosive ferric chloride solutions in different concentrations. It was found that the ANNs results agreed well with those obtained from laboratory tests. They further stated that, by

increasing the corrosive concentration with extended immersion duration, it resulted in an increase in pitting density and pitting depth [164].

Valor et al. [135] proposed Markov chain models for the stochastic modelling of pitting corrosion [27, 28, 135]. Two different models of pitting corrosion were proposed: 1) a continuous-time, nonhomogeneous linear growth Markov process was used to model external pitting corrosion in underground pipelines, and 2) the distribution of maximum pit depths in pitting experiments was modelled combining pit initiation and pit growth processes [135].

Velazquez et al. [9] proposed a methodology for probabilistic mathematical modelling of the pit initiation process and its depth-of-growth process. Two stochastic models were developed: 1) the Poisson process which was used to modal pit initiation, and 2) the Gamma process to model the pit depth-growth [9]. After obtaining the pit depth, the maximum pit depth was studied using Block Maxima (BM) and the Peak-Over-Threshold (POT) methods.

Velazquez et al. [9] described the pit initiation as Non-Homogenous Poisson Process (NHPP). According to NHPP, pit initiation time was assumed with intensity function $\lambda m(t)$, where λ is defined as the mean pit density per area unit and $m(t)$ can be an arbitrary function. Hence, the expected number of pits in given time t can be expressed as:

$$E(N(t)\big|\lambda \int_{s=0}^{t} m(s) = \lambda(mt) \tag{2.9}$$

The pit growth was modelled using the Gamma process which is a continuous-time stochastic process with independent gamma increments. The Gamma probability density function can be expressed by:

$$Ga(\cdot\big|k,\theta) = y^{k-1}\theta^{-k}\,\frac{\exp(-y/\theta)}{\Gamma(k)} \tag{3.0}$$

Where k is shape parameter which controls the rate of the jump; θ the inverse of the scale parameters which controls the jump sizes; $Ga(\cdot\big|k,\theta)$ is the Gamma probability density function; and $y>0$ and $\Gamma(k) = \int_{t=0}^{\infty} t^{k-1}\exp(-t)dt$ is the Gamma function.

Finally, Velazquez et al. [9] reported that the use of statistical simulations in the modelling pitting corrosion is significant as to be familiar with different pit characteristics such as pit

depth, pit density and rate of pitting. They ensure that the NHPP process can determine the evolution of the total number of pits and, likewise, the Gamma process for the pit growth [9]

2.9 Challenges

There are many studies conducted on the mechanism, field-testing and laboratory testing in the field of pitting corrosion; however, there is no development of detailed studies for failures in offshore structures due to pitting characteristics. One critical requirement is the investigation of how pitting characteristics, such as rate, depth, density and distance, can cause a structural failure. Previously, empirical and statistical degradation models were developed by either fitting field or laboratory data. However these models, even though useful for specific site or operating conditions, still carry high uncertainty. Currently, several aspects of current knowledge on pitting corrosion are deficient and require further investigation. Some of these challenges have been identified and listed below:

- Structural failures due to pitting characteristics such as pit depth, pit rate, pit density and interfacial distances between pits is not fully understood; better understanding of these characteristics is crucial.
- The process of pit propagation and the rate of pit growth are not fully understood.
- Precise prediction mechanism of long term anaerobic corrosion requires essential study in order to develop a failure model.
- The total depth of pit and its rate of growth are of concern in marine and offshore structures; the precise mechanics of pit growth mechanism needs to be developed.
- There is still uncertainty in the pit depth measurement; a precise pit depth measurement technique needs to be developed.
- There is no precise way to observe the depth of deepest pit without destroying the specimen; this needs to be resolved.
- Several factors that can affect pitting corrosion in marine environments have been established in this paper; however, the effect of these factors on pit growth is still not fully understood.
- Mathematical relationship for the factors that affect pitting rate such as surface wetting, humidity, oil in the water, suspended solids etc. is not yet understood.
- The influences of pH on pitting corrosion under dynamic conditions may also be studied and the role of metal defect on pit initiation needs further analysis.

- Another possible expansion is the study of the repassivation mechanisms, including super saturation of the solution, precipitation of the passivating phase and subsequent increase in the electrical resistance of the pore.
- In this paper, several conventional and recent methods for modelling of pitting corrosion are discussed to evaluate the rate of corrosion; however, there is a need to find an appropriate method of estimating the corrosion rate and how it develops with time.

Provided that all factors that can cause pitting corrosion are known - as based on the mechanism of corrosion and by using risk assessment methodologies - a probabilistic risk assessment can be applied to predict and evaluate future failure due to pitting corrosion.

2.10 Conclusion

Pitting corrosion is a complex but important problem that is at the root of many structural and system failures. It has been studied for many years however crucial phenomena remains unclear. The aim of this paper was to identify and evaluate the parameters that affect pitting corrosion in marine and offshore environments. This paper has reviewed and discussed the mechanisms and characteristics of pitting corrosion, several factors that affect its development, as well as identification methods and modelling techniques. Based on the literature reviewed it is clear that pitting corrosion is a stochastic, probabilistic phenomenon that requires interdisciplinary concepts that incorporate surface science, metallurgy/material science, hydrodynamics and chemistry. From this study, the following conclusions suggestive of recent knowledge on pitting corrosion can be summarized as:

- Pitting corrosion is considered as one of the most destructive forms of corrosion; pitting mechanism and the characteristics of pitting is summarized in this paper.
- It is generally acknowledged that there are three stages of pitting.
- Pit can be initiated in many different ways and the growth of pits can be attributed to different phenomena.
- The several factors that affect pitting corrosion and the rate of pitting have been investigated; the critical factors that have most effect on the pitting rate are temperature, pH, bacterial and flow velocity, however, this varies on marine zones such as atmospheric, splash, emersion etc.
- Various experimental investigations have shown that different effects may serve as stabilizing factors for localized corrosion and it depends on the stage of development of corrosion pit and environmental conditions.

- Pit depth has been acknowledged as a critical factor and is the key parameter to describe pitting rate.
- Some standard laboratory methods of determining the pitting corrosion rate, and the effect of different factors on rate of pit growth, are considered to be inaccurate.
- Although a standard exists for statistical analysis of laboratory corrosion data, no such standard exists for the analysis of inspection data relating to corrosion measurement.
- Short term pitting corrosion can be modelled from the experimental field data; however, this data cannot be relied on for modelling of long term pitting corrosion.
- In recent years, there have been different attempts made on probability modelling for general corrosion as a function of time; however, less is available for pitting corrosion under marine immersion conditions.
- The use of statistical simulations in pitting corrosion is valuable for determining pitting characteristics such as pit initiation and pit growth.
- The power law is commonly used to express pitting depth as a function of time. Some of the statistical distributions are: Poisson, Exponential, Normal, Log normal and Extreme value distributions.
- Extreme value analysis is considered most appropriate for the study of pitting corrosion; extrapolation from a small-inspected area to a large area is possible with this method.
- A Gumbel distribution is widely used for the application of extreme value statistics in corrosion engineering.
- The conventional use of the Gumbel distributions is no longer appropriate to derive the extreme value statistics for maximum depth of pits in pitting corrosion. It is suggested that, for longer-term pitting corrosion, the use of Frechet extreme value distributions is more appropriate.
- Field test is suggested for generating long-term data. This would allow for the collection of relevant environmental data and would develop further understanding of degradation mechanisms and pitting corrosion rates.

2.11 Acknowledgements

Authors thankfully acknowledge support provided by National Centre for Maritime Engineering and Hydrodynamic (NCMEH) and Australian Maritime College (AMC).

3 Risk-based Maintenance (RBM) of an Offshore Process Facility using Bayesian Network

Abstract

Process plant and equipment may not remain safe and reliable if they are not maintained well. The main objective of any maintenance strategy is to increase equipment's life while maintaining the safety and reliability of the process systems. Risk-based maintenance (RBM) methodology provides a tool for maintenance planning and decision making to reduce the failure probability of equipment and the consequences of failure. It also assists to identifying the critical equipment based on the pre-selected acceptable level of risk. This article discusses a novel methodology for the design of an optimum maintenance programme integrating a dynamic RBM based reliability approach and a risk assessment strategy. In this study, Bayesian Network (BN) is employed to develop a new dynamic RBM methodology for the design of an optimum maintenance programme for offshore production facility. The application of this methodology has high degree of prediction capability which increases the reliability of the equipment and also optimizes the cost of maintenance. The developed methodology is applied to a case study involving an offshore oil and gas production facility. A sensitivity analysis is also conducted to study the critical equipment based on the risk levels. Based on the sensitivity analysis corrosion is found to be a predominant causes of components failure.

Keywords: Reliability, Risk-based maintenance, Probability, Bayesian network, Separator, offshore production

3.1 Introduction

Plant safety in the process industry is directly aligned to the reliability of its operation. Higher reliability of the process plant can be achieved through a robust inspection and maintenance programme. The main objective of the maintenance process is to make the use of the knowledge of failures and accidents to achieve the highest possible safety with the lowest possible cost. Over the past few decades, maintenance strategies progress from the primitive breakdown maintenance to more sophisticated strategies like condition monitoring and reliability cantered maintenance [165-167]. Risk based maintenance (RBM) methodology provides a tool for maintenance planning and decision making to reduce the equipment's failure probability and most importantly the consequences of failure [168]. To develop an appropriate maintenance strategy, it is necessary to estimate the impact of maintenance on assets and determine the relationships between likelihood of the undesirable events and the possible consequences. The most effective tool to estimate the likelihood of hazard and associated consequences is probabilistic risk assessment [169]. Several researchers [165-167, 170-176] demonstrate the application of the risk-based maintenance strategy. In the beginning of the twentieth century, the American Society of Mechanical Engineers (ASME) focused on performance criteria to improve safety and reduce the frequency of failure [171]. Later, the importance of risk was recognized as an important measure of systems safety. Hegemeijer et al. [175] developed a methodology for risk-based inspection for pressurized systems. The methodology was based on the risk assessment by evaluating the consequences and the likelihood of the equipment failure [167, 175]. Henry et al. [176] developed a risk ranked inspection procedure that is used in one of the Exxon's chemical plants to prioritize repairs that have been identified during equipment inspection. Dey et al. [174] presented a risk-based model for the inspection and maintenance of a petroleum pipeline, this tool reduces the amount of time spent on inspection. The author used Analytic Hierarchy Process (AHP) which is a multiple attribute decision-making technique to identify the factors that influence the failures for their risk-based model [174]. Khan et al. [177] developed a comprehensive methodology for risk-based inspection and maintenance. Their methodology integrated a quantitative risk assessment and evaluation method with one of the reliability analysis technique called fault tree analysis (FTA) [177]. This methodology was applied to different case study of ethylene oxide production facility. In their study a reverse fault tree (FT) was used to determine the optimal maintenance interval [165]. Recently, Khan et al. [165-167, 171, 178, 179] reported the significance of applying a risk based maintenances strategy in process industries.

Most of the aforementioned researchers have used the FTA to determine the likely failure scenarios and their associated probabilities. The well-known FTA and event tree (ET) approach is widely applied to identify the likelihood and consequences of accident scenarios in which following an accident initiation, a number of safety barriers must fail before severe consequences arise [180]. In the past few years, the FT/ET approach has gained widespread acceptance as being a mature methodology for analysing accident scenarios. However, these integrated techniques are implemented under specific conditions and have limited applications [181]. Although a static fault tree has been extensively used in risk analysis, these conventional integrated techniques are not suitable for the large and complex systems. Similar findings were reported in previous research [178, 182]. Khakzad et al.[182] reported that the application fault tree is not the most appropriate technique for large systems. Khakzad et at.[182] emphasized that fault tree fails to capture dependent failures and common causes failures [182]. The application of the Bayesian Network (BN) is another approach in conducting quantitative risk assessment. The BN analysis is becoming a popular probabilistic inference technique for reasoning under uncertainty. The BN analysis models multi-state variables, common causes of failure and conditional dependencies. Some of the priorities of using BN in comparison with the conventional methods such as FT and ET analysis are its ability to model complex systems, reducing parameteric uncertainty by having new evidences, and being able to apply user-friendly and compact graphical approach [171, 183, 184]. Further, BN makes it possible to perform probability updating and sequential learning [181, 182, 185, 186].

Offshore oil and gas process facilities has accounted for the highest rate of critical incidents compared to other domains in the petroleum industry. It involve hazardous chemicals (highly flammable and toxic) at extreme conditions such as temperature and pressure [165, 171]. The transient, intersecting, continuous and complex characters of offshore production facilities determine the variety of risks. In addition, the associated risk is extremely difficult to control [182, 187]. The purpose of the offshore production platform is to operate the wells, and to separate the fluid produced from the wells into oil, gas, condensate and water [171]. The availability of complex system, such as the oil and gas production platform is directly associated with the reliability of different components (units) and their maintenance policy. Therefore, an appropriate risk-based maintenance strategy is necessary to better define an appropriate maintenance policy, which can increase the reliability of the equipment and lead to a safe and fault free operations.

A dynamic RBM methodology using BN is proposed in this study to tackle safety of the complex process systems. This methodology can produce consistent and precise maintenance/inspection interval incorporating the conditional dependencies of sub-components which are possibly missed during the application of conventional methods. In this paper a BN model is develop to define failure scenarios and to calculate the probability of the failure. Furthermore, the BN is used to compare the risk against known acceptable criteria and finally to determine the appropriate maintenance interval for the equipment. A novel dynamic risk-based methodology for the maintenance/inspection scheduling is developed in this study and applied to the maintenance of an offshore production platform as a case study.

3.2 Risk Assessment

Out of the two main phases of RBM, risk assessment is the critical and foremost important phase, as the maintenance decisions are made based on assessed risk. Risk assessment is a technique for identifying, characterizing, quantifying, and evaluating the loss caused by an event [165, 171]. It starts with the identification of major potential hazards that each failure scenarios may lead to. For a particular failure scenario, the risk assessment can be performed qualitatively or quantitatively (Figure 3-1). Quantitative risk assessment is performed by the estimation of frequency of failures and its consequences [168]. This study is limited to the risk analysis using a quantitative approach. In the second phase consequence analysis is carried out.

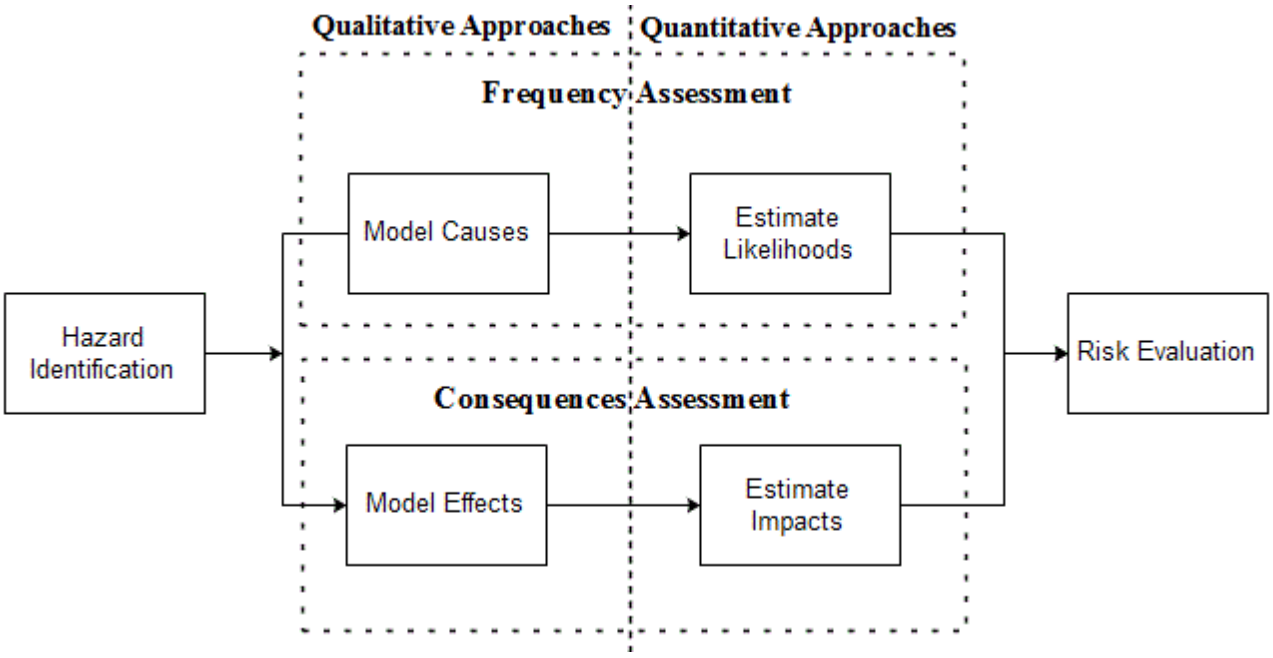

Figure 3-1. The risk assessment process [168, 171]

As demonstrated in Figure 3-1, risk assessment involves hazard identification, estimating their likelihood (number of events/time interval) and estimating the consequences (impact/event). The combination of these estimations represents the risk associated with the evaluated activity [168]. Risk assessment approach integrates reliability and consequences analysis at the various stages of the analysis, and attempted to answer the questions such as; i) what can go wrong?, ii) How can it go wrong?, iii) How likely is its occurrences?, and iv) What would be the consequences? [165, 167, 168, 171].

3.2.1 Bayesian network

The BN is a graphical structure for representing the probabilistic relationship among a large number of random variables and performing probabilistic interface with those variables [173, 186, 187]. BN model connects causes (independent variables) and consequences (dependent variables) as a nodes through direct arrows pointing the causes to consequences [188]. Each node in BN depicts an uncertain variable and demonstrates the causal relationship between two variables. It allows estimating likelihood of rare failures events of complex systems in an efficient way. BN also assists to update the prediction when new information is available through monitoring and inspection [173]. A conditional probability table (CPT) provides the probabilities of each state of the variable considering each combination of parent states. A common BN structure is illustrated in Figure 3-2, in which the RN represents the root nodes (primary events), the IN represents intermediate nodes and the PN represent the pivot node (top event). Similarly C signifies the possible consequences which are connected to the level of risk as the final result.

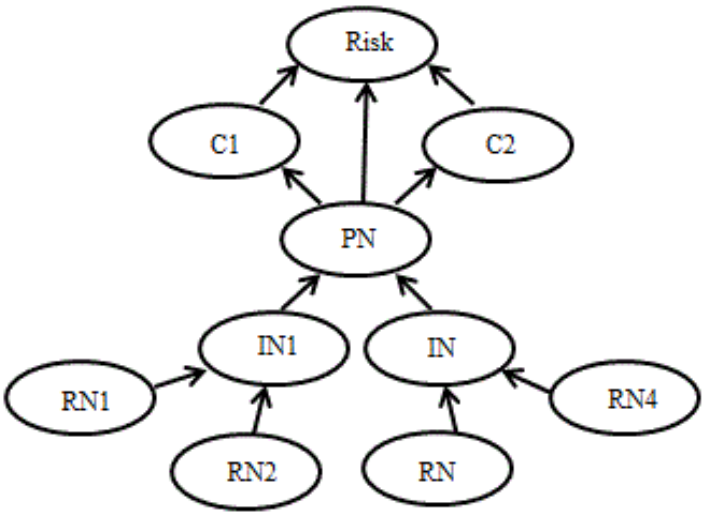

Figure 3-2. Structures of BN model (The arrow in the network represent the relationship between the nodes)

In BN, "probability inference of an event is conditional on the observed evidence". BN not only can implement forward or predictive analysis; it can also perform backward or diagnosis analysis. Considering the conditional dependencies of variables, BN represents the joint probability distribution P (U) of variables $U = \{A_1 \ldots\ldots A_n\}$ as;

$$P(U) = \prod_{i=1}^{n} P(A_1 \left| Pa(A_i) \right.) \tag{1}$$

Where $Pa(A_i)$ is the parent set of A_i in the BN, and $P(U)$ reflects the properties of the BN. It takes advantage of Baye's theorem to update the prior occurrence (or failure) given that the observation of another set of variables evidence E. The posterior probability distribution of a particular variable can be computed using different classes of inference algorithms, such as the junction tree or variable elimination, based on Baye's theorem (Equation 2) [178, 181, 182].

$$P(U \left| E \right.) = \frac{P(U,E)}{P(E)} = \frac{P(U,E)}{\sum_U P(U,E)} \tag{2}$$

3.3 The proposed dynamic risk-based maintenance methodology

Risk-based maintenance methodology provided a tool for maintenance planning and decision-making to reduce the failure probability of equipment and the relevant consequences [167]. The resulting maintenance programme maximized the reliability of the equipment and reduces the cost of total maintenance of process facilities. The concept of risk-based maintenance proposed in this study to achieve tolerable risk criteria. The developed risk-based methodology

includes several different steps as illustrated in Figure 3-3. To achieve the purpose of the RBM strategy in offshore production platform is the production system components were divided into major systems and subsystems. The components of each subsystem are identified and each system is analysed one at a time, until the whole plant has been investigated. Data required to analyse the potential failure scenarios for each system are collected. There are different ways that the data can be collected, the most common approach is based on the historical accidents and through the expert judgements. The failure data for the basic events used in this study were adopted from OREDA [189] and Lee et al. [189, 190].

The proposed RBM methodology starts by identify undesired event for a selected unit. In the first step, an undesired event is defined to develop a failure scenario. The undesired event is resolved into its immediate causes and the resolution of event is continued until the basic causes are identified. The failure scenario provides a description of a series of sub-events which leads to a final failure event. It may contain a single event or a combination of sequential events. The developed scenario does not determine that an accident will indeed occur, however, there is a reasonable probability for an accident to occur. Khan et al. [165, 171, 177] describes a failure scenario as neither a specific situation nor specific event, but a description of a typical situation that covers a set of possible events of situation. It is also a basis of risk study which tells us what may happen so that we can devise ways and means of preventing or minimizing the possibility of its occurrences [165, 171, 177]. The failure scenarios are generated based on the operational characteristics of the system, physical conditions under which operation occurs, geometry of the system and safety arrangements. Considering the failure scenarios and all relevant failure causes, a BN is developed. The probabilistic failure analysis approach using BN is used to identify major potential hazards (top events) that each failure scenario may lead to [166, 167]. The likelihood estimation is performed using BN by considering the failure scenarios and all relevant failure causes.

Subsequently (in the second step), the consequence analysis is considered to assess the potential consequences if a failure scenario does occur. The aim of the consequence analysis is to quantify the potential consequences of the credible failure scenario. Khan et al. [171] reported consequences in terms of damage radii (the radius of the area in which the damage would readily occur), damage to property, and toxic effects [171]. The calculated damage radii is later used to assess human health loss, environmental and production loss (in terms of dollars). Four major categories can be considered in the consequence assessment; human health loss, economic loss, environmental loss and system performance loss. This allows one to

distinguish between prioritization performed on each category. The assessment of consequences involves a wide variety of mathematical models. For example, source models are used to predict the rate of release of hazardous materials, the degree of flashing, and the rate of evaporation. Different mathematical models to quantify the consequences category is well described in Khan et al. [171]. In Figure 3-2, the pivot node (top event failure) in the developed BN is connected to each consequence node, takes into account the effect of the occurrence of the final failures on the individual consequence.

In the third step, the risk level is estimated by the BN considering the failure probabilities and the relevant consequences. The level of risk calculated reflects the total risk for the system. The computed risk is evaluated against the acceptance criteria. In this study three different states; low, medium and high are considered for the risk node. At this stage, the risk is estimated and assessed.

In the fourth step, an acceptable risk criteria is determined using BN to make a decision whether the estimated risk for each failure scenario is acceptable or not. This steps of RBM is aimed to evaluate the earlier computed risk through the novel methodology developed in Figure 3-3. At this stage, the acceptance criteria needs to be set up for the risk computed in earlier steps. Acceptance criteria of risk may be different from one organization to another and depends on the type of systems. Some of the commonly used risk acceptance criteria are ALARP (as low as reasonably possible), Dutch acceptance criteria and USEPA acceptance Criteria [165]. In this study, an open-ended methodology is adopted for risk acceptance criteria, which depend on the scope of the study, the criticality of the system, and the policy or strategy of the offshore production societies. Risk estimated in third step is compared with these acceptance criteria. Whenever the estimated risk exceeds the acceptable criteria, a further analysis is required to reduce the risk using risk-management plan perceiving that the acceptable risk value can be altered for different organizations and systems.

In the final step, the subsystems that failed to meet the acceptable risk criteria are studied to schedule a better maintenance plan that will reduce the risk. To schedule a better maintenance plan, the backward inference on the BN is employed. Considering the minimum potential risk (low), the backward analysis is carried out to determine the required value of the probability of failures for the root nodes. Consequently, after considering the revised probability for failures, the optimal maintenance time for the component is estimated. At this stage, the maintenance plan is developed according to optimal maintenance times.

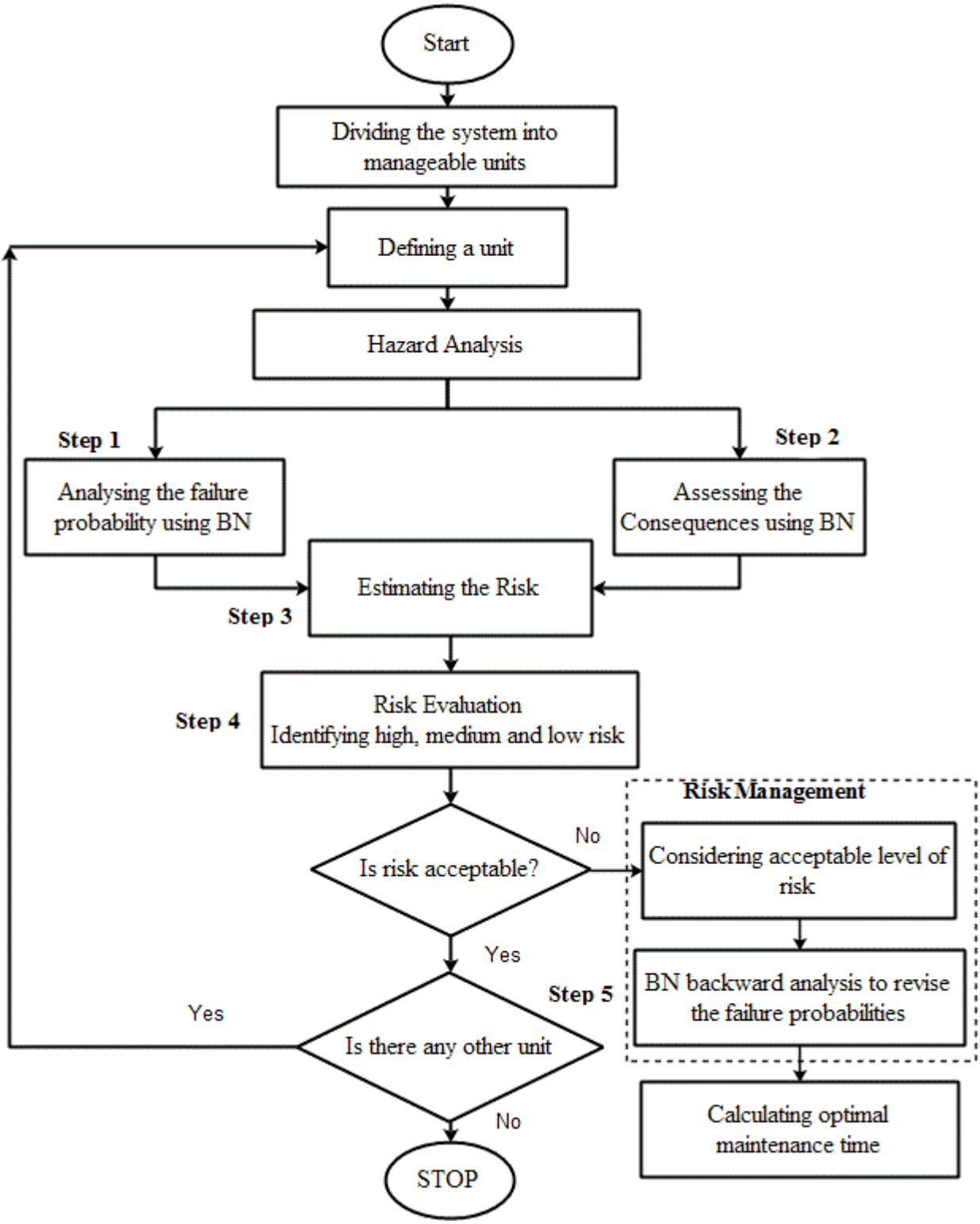

Figure 3-3. The proposed risk-based maintenance methodology for an offshore processing facility

3.4 Application of RBM methodology for an Offshore process facility: A case study

The developed RBM methodology is applied to design a maintenance plan for an offshore process facility on the platform. On the offshore production platform, the failure of a separator is a critical siltation with regard to well control. The separator in the offshore production platform is used to separate the fluid produced from the well into oil, gas condensate, gas and water. During this operation, hitting an unexpected high-pressure zone can lead to a well-control problem due to the increased influx of formations fluids which can exceed the limits of the separator. It is crucial to monitor the performance of the separator in the offshore platform. In the case of lower differential pressure between the wellbore and formation, the separator equipment at the surface must be able to handle the influx of formation fluids.

In the offshore production facilities, there are several functional subsystems and their system performance will which according to their operational characteristics and the reliability of the equipment's. In this study the most credible failure scenario is investigated for a release of crude oil from separation section causing fire and explosion. The failure probability of the primary causes for the proposed scenario is obtained from available literature Khan et al. [171] and from offshore reliability data (OREDA) [189]. The primary causes leading to release of crude oil from separation section causing fire and explosion are identified. There are 10 basic events, which contribute to the accident scenario. These events with their failure probability are listed in Table 3-1. As illustrated in Figure 3-4, the probability of the top event i.e. releases of crude oil from separation section causing fire and explosion is calculated using BN with the aid of computer software Netica. The frequency of occurrences of the undesired event when all initiating events occur is estimated as 5.17E-04 per year.

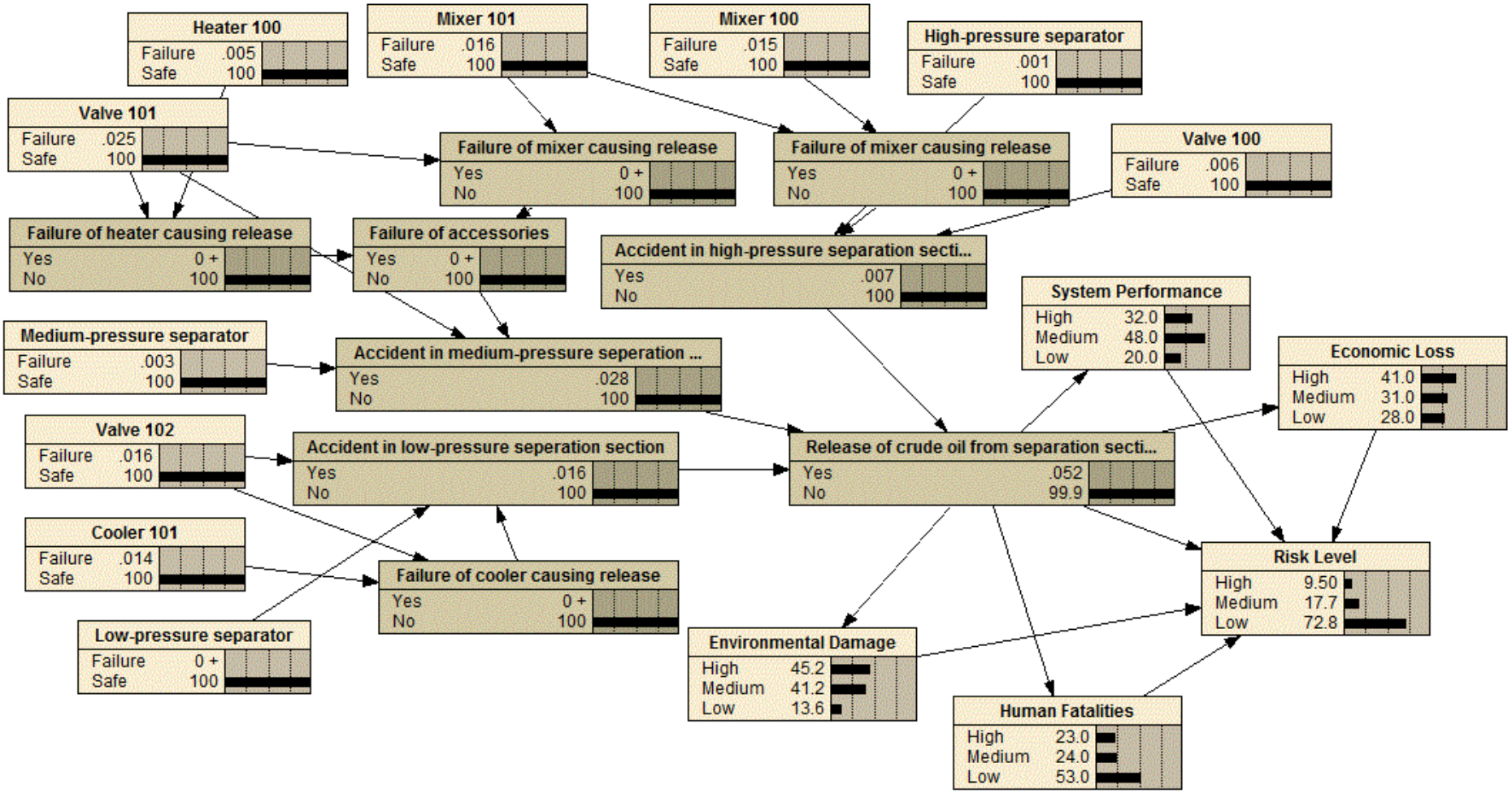

Figure 3-4. Developed BN to calculate risk level for scenario release of crude oil from separation section causing fire and explosion

Table 3-1. Components of the failure scenario and their probabilities

Index	Unit Name	Failure Probability	Risk Factors ($/h)
1	High-pressure separator	1.5000E-05	9.73E+4
2	Valve 100	5.7000E-05	
3	Mixer 100	1.5000E-04	
4	Medium-pressure separator	3.3000E-05	51.28
5	Valve 101	2.5000E-04	
6	Mixer 101	1.5700E-04	
7	Heater 100	4.6000E-05	
8	Low-pressure separator	6.3500E-06	1.45E+4
9	Valve 102	1.5600E-04	
10	Cooler 101	7.1000E-05	

The frequency of the top event is combined to quantify the risk factors. The risk factors for each main section are calculated by adopting the general input data for consequence analysis and specific data for separation from Khan et al. [171]. It is evident from the Table 3-1 that the separation section has the maximum risk factor of 973.4E+2 $/h, and the medium compression section has the lowest risk factor of 51.3 $/h. The acceptable risk criteria for the present problem is considered as 1.0 $/h; any value higher than this is unacceptable. To minimize the probability of failure to reduce the level of risk as low as possible, the maintenance plan is considered for all components and sub-components.

As illustrated in Figure 3-4, the failure of any of the main section such as accident in the high-pressure section, accident in the medium-pressure section and accident in the low-pressure section may individually lead to the release of crude oil from separation section causing fire and explosion. A BN is developed for the envisaged failure scenarios of different sections and a final unit. Three different states; low, medium and high risks are considered in this study. Considering the minimum potential risk (low), the backward analysis is carried out to determine the required value of the probability of failures for the root nodes. Considering the current condition for each of the units and their failure probabilities, the risk values are calculated and given in Table 3-2.

Table 3-2. The current and assigned risk values

State	Probability	Set evidence
High	0.0949	0
Medium	0.1774	0

Low	0.7275	100%

Whenever the risk value is higher than the acceptable level, the probability of failure for different units should be decreased. This is done by assigning 100% probability to low risk state as an evidence and then performing BN backward analysis to re-calculate the failure probabilities. After considering the updated probabilities and the particular failure function (distribution), the time intervals between the consecutive maintenance tasks are calculated, as demonstrated in Table 3-3.

Table 3-3. Result of risk estimation, revised probability and optimal maintenance schedule

Index	Unit Name	Failure Probability	Revised failure probability	Annual probability of failure	Optimal time (t) (days)
1	High-pressure separator	1.5000E-05	1.0269E-06	0.0090	25
2	Valve 100	5.7000E-05	3.9020E-06	0.0342	25
3	Mixer 100	1.5000E-04	1.4998E-04	0.7352	369
4	Medium-pressure separator	3.3000E-05	2.2591E-06	0.0196	25
5	Valve 101	2.5000E-04	1.7114E-05	0.1358	24
6	Mixer 101	1.5700E-04	1.5698E-04	0.7472	365
7	Heater 100	4.6000E-05	4.6000E-05	0.3368	372
8	Low-pressure separator	6.3500E-06	4.3470E-07	0.0039	25
9	Valve 102	1.5600E-04	1.0679E-05	0.0893	25
10	Cooler 101	7.1000E-05	1.4198E-04	0.7117	730

To calculate the annual probability of the failure of each unit the function demonstrated in Equation 1 is implemented.

$$Annual\ probability\ of\ failure = (1 - e^{\lambda t}) \quad (1)$$

Where, λ is the earlier failure probability of the components and t is time in hour (8760h). The maintenance interval (T) required to achieve the target probability was calculated using Equation 2.

$$T = \frac{-\ln[1-P]}{\lambda} \quad (2)$$

Where, *P* is the annual probability of failure for the revised components with low risk level.

Further, as illustrated in Table 3-3, the individual maintenance interval is different for each subsystems/equipment because this depends on the operational performance and the reliability of the each equipment. The minimum length of the maintenance interval for the valves is assigned as 24 days. Similarly, the maintenance interval for Cooler 101 is assigned as 730 days i.e. around once in every two years. Furthermore, the maintenance plan for the Mixer 100/101 and Heater 100 is assign to be 368 days i.e. once every year. Although the some of the equipment may be over maintained using this method, the acceptable value of risk and reducing the downtime necessary for maintenance justify the value of the developed methodology. The methodology developed in this study provides a dynamic tool to schedule maintenance according to the existing condition of different units. This methodology will help to lower the failure risk to meet the acceptable criteria by continuous monitoring the new evidences on failure probabilities of individual subsystem/equipment in a unit, and re-evaluating the failure and possible consequences using new evidences.

The sensitivity analysis is performed to investigate the most influencing factors as well as their contributions for the above-mentioned accident. This is conducted by assigning a zero probability to the individual factors influencing the release of crude oil from separation section causing fire and explosion. The BN model calculated the percentage contributions by comparing each case with the base case when all factors are active.

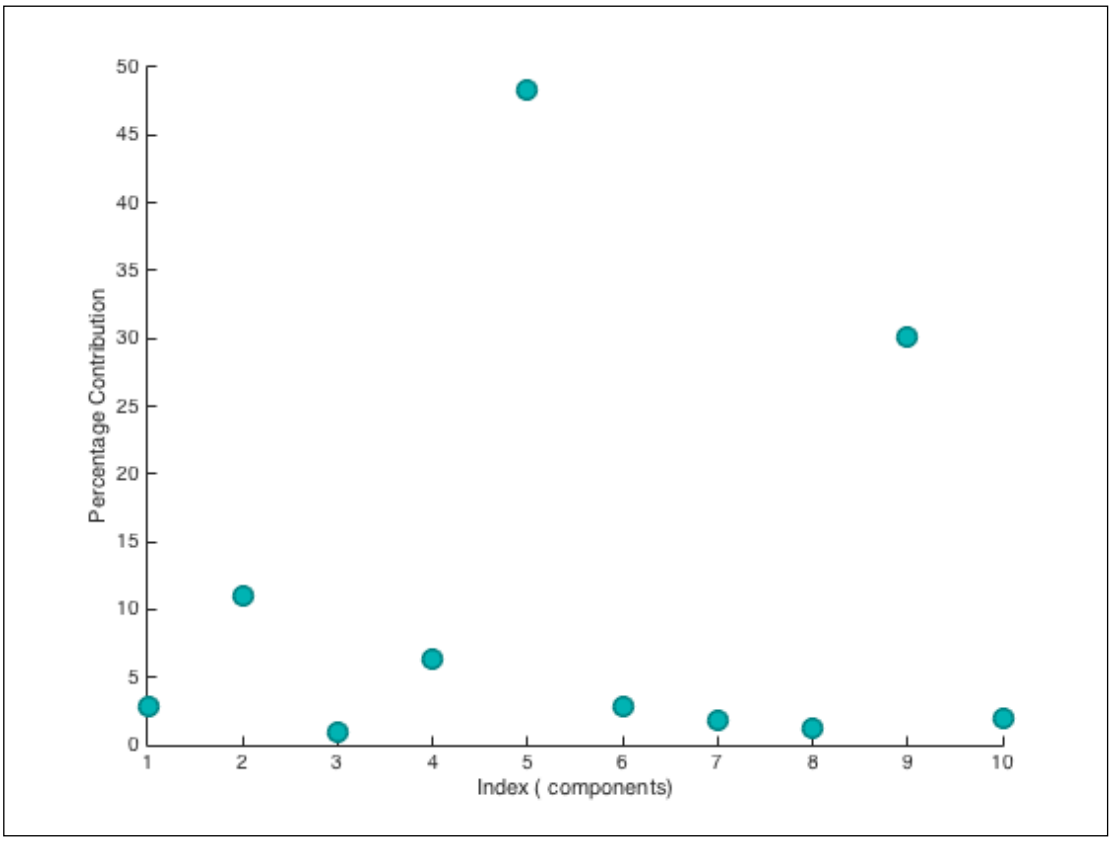

Figure 3-5. Contribution of the components to the offshore oil and gas production accident

Figure 3-5 demonstrates the entire root events with the highest importance measure calculated for a separator system in the offshore production facility, which could lead to the undesirable event. Figure 3-5 clearly demonstrated that Valve 101 and Valve 102 are most critical components with the highest contribution to the failure events. To prevent the leakage from the separator each well is equipped with these valves which regulates the rate of flow. These valves are fitted to the well head and before the production manifold, which separates the crude oil from sediments, solid, gas and condensates to allow the crude to be pumped in the pipeline or shipped through tankers. Considering the sensitivity analysis it is clear that these elements required more attention; hence the maintenance interval estimated for these elements is remarkably acceptable.

3.5 Conclusion

In this paper, a novel methodology for a risk-based maintenance strategy using BN is developed. This methodology is crucial to reduce the risk of failures and optimize the cost of maintenance including the cost of failure. The BN based RBM methodology is more dominant than previously developed conventional methodology. Furthermore it has a higher prediction capabilities to develop suitable maintenance plan for the safe and fault free operation of the facility. The paper illustrates the applicability of the proposed methodology to an offshore process facility. The failure analysis of different subsystems/equipment and their associated consequence are considered in a single network. Application of the developed methodology for the maintenance scheduling of an offshore oil and gas production platform demonstrated that preventive maintenance time can be altered for each components in the system. This maintenance planning minimizes the risk of equipment failures in this unit to an acceptable level. This methodology provides useful information on; 1) the causes of failures for different units; 2) the probable consequences on different subsystem failures in a unit; 3) the risk of a unit failure; and 4) the frequency of required maintenance to retain the acceptable level of risk for offshore production facility. The risk-based approach minimizes the consequences (related to safety, economics, and environment) of a system outage/failure. This will in turn result in a better asset and capital utilization. A risk-based maintenance plan can be used to improve the existing maintenance policies through optimal decision procedures in different phases of the life cycle of a system.

3.6 Acknowledgements

Authors thankfully acknowledge support provided by National Centre for Maritime Engineering and Hydrodynamic (NCMEH) and Australian Maritime College (AMC).

Chapter 4 has been removed for copyright or proprietary reasons.

It has been published as: Bhandari, J., Khan, F., Abbassi, R., Garaniya, V., Ojeda, R. 2017. Pitting degradation modelling of ocean steel structures using Bayesian network, Journal of offshore mechanics and Arctic engineering, 139(5), 2-11. doi:10.1115/1.4036832.

5 Accelerated Pitting Corrosion Test of 304 Stainless Steel using ASTM G48; Experimental Investigation and Concomitant Challenges

Abstract

Marine and offshore structures constructed with stainless steel are regarded as having high corrosion resistance due to their superior self-passivating properties. However, they are equally susceptible to environmental degradation, especially due to pitting corrosion in highly corrosive marine environments. Pitting immersion tests performed on 304 austenitic stainless steel specimens using ASTM G48 presented significant challenges. Some of the issues encountered during these tests include unspecified experimental factors that control the pitting process such as pH, specimen size limitations, materials' properties, and the variation on the quality of the test solution. To overcome these challenges, the effect of surface finishes and aeration of the test solution on the corrosion behavior of 304 stainless steel specimens in 6% ferric chloride were examined and compared. The result shows that an aerated solution has much lower concentrations of pits compared to quiescent solutions. Controlled aeration eliminates unwanted crevice corrosion background noise. Subsequently, to suit larger specimens, the ASTM G48 was modified. This study presents the modified ASTM G48 procedure. A series of pitting corrosion tests on stainless steel specimen with different thickness were conducted and data were statistically evaluated. The generalized extreme value distribution, such as Weibull, provides adequate statistical descriptions of the pit depth and pit diameter distributions. The modified ASTM G48 offered advantages in the extraction and interpretation of the data for pit characteristics in the accelerated pitting corrosion test simulating actual marine environment.

Keywords: Pitting, ASTM G48, Large Specimens, Stainless steel, Weibull distributions

5.1 Introduction

Stainless steel is employed in many industrial and architectural applications due to its high corrosion resistance [218]. Stainless steel has a high resistance to corrosion due to the presence of about 18% of Cr which forms a shining, thin passive film that protects the structure from the external corrosive environment. By increasing chromium and nickel contents, this type of steel becomes increasingly resistant to pitting corrosion. However, higher concentrations of these alloying elements result in lower carbon solubility and carbide segregation. Unfortunately, the Achilles heel of these films is a propensity to catastrophic local breakdown [219]. Heat treatments, whether intentional or accidental, may provoke carbide precipitation at grain boundaries, which often causes steel to become susceptible to pitting corrosion [220].

Pitting corrosion is one of the most widespread and insidious forms of localized corrosion of passive metals and it commonly occurs in a range of aggressive environments [195, 221]. This type of corrosion is generally confined to a small area of the metal surface and it can cause the structure to fail by perforation or by generating stress corrosion cracks [222]. Moreover, pits are nucleated on a microscopic scale and are always covered by corrosion products. Thus, pitting is one of the more destructive and undetectable forms of corrosion in metals. Pitting corrosion is commonly observed in austenitic steel exposed to aqueous media containing chloride ions. The most commonly aggressive ion is the chloride anion found in many natural and industrial environments including seawater. Moreover, Pitting corrosion has always been considered as one of the major operational problems in power plants and process facilities [209, 223, 224]. Murata, Benaquisto and Storey [225] summaries the recent corrosion related incidents in the process industry.

Field performance testing in a relevant environment is the most reliable form of evaluating pitting resistance of steel but it can take many years to produce useful performance data. Therefore, laboratory tests, which simulate natural exposure in an accelerated manner consistent to the field performance, are required to produce data in months rather than years [226]. A wide range of accelerated corrosion test techniques are available either as standards or company specific instructions [227, 228]. Their acceptance criteria vary. Some of the described methods leave certain details to be

decided by the test laboratory, and these details may have a decisive influence on the results.

The main objective of accelerated corrosion testing is to simulate the field environment under laboratory conditions and therefore, the controlling factors for accelerated corrosion test are similar to those in the field tests. In recent years, there has been a development in corrosion testing from qualitative to more quantitative methods. Additionally, the prerequisites for corrosion testing in product qualification are changing [191] . Quantitative methods for characterization of corrosivity have been introduced to make it possible for a better translation of laboratory test results into in-service performance [229-231].

The ASTM G48 standard is widely applied for pre-qualification of corrosion resistant alloys, welds and weld overlay within the oil and gas industry [232]. This test also has the advantage of directly demonstrating the desired end result i.e. an improved resistance to chloride-induced crevice corrosion [233]. ASTM G48 testing in ferric chloride solution allows a quick assessment of pitting corrosion resistance of stainless steel. Although ferric chloride solution is regarded as a very aggressive test solution, there are similarities between this solution and the real environment in which a corrosion pit may develop during service in seawater [234]. Several researchers [81, 227, 232, 233, 235-246] have used ASTM G48 for their experimental studies of pitting corrosion.

However, ASTM G48 standard does not provide the specific inspection and testing regimes necessary to ensure pitting corrosion resistance for specific stainless steel (such as 304 specimens), suitable for seawater service. Corbett [239] reported problems in utilizing ASTM G48 to evaluate high-alloy stainless steels. His study addressed some specific challenges including ferric chloride solution preparation, duration of test, and required test temperature. However, the author failed to discuss the problems that may be encountered during the testing of larger specimens as well as their optimal orientation within the test solution. Furthermore, the study failed to provide any explanation as to the differential oxygen level and stagnation of the solution.

The present work employs the ASTM G48-11 [234] standard to evaluate the extent of pitting corrosion damage on dog-bone shaped 304 stainless steel specimens. During the experimental procedure, several challenges came to light including the limited

information available on experimental factors and response variables such as the pH, chemical properties of the ferric chloride and its proper concentration, orientation of the specimens, and time of exposure, all of which control the pitting process. Empirical knowledge, gained through experimentation, is presented in this paper to address these challenges. Further, an attempt has been made to unravel the possible solutions by modifying the ASTM G48 test standard.

5.2 Experimental Details

5.2.1 Materials and Methods

For these experiments, test specimens were cut from UNS 304 stainless steel plate with the standard plate using a numerically controlled water-jet cutter. The chemical composition of UNS304 SS, used in this study, is given in Table 5-1. Figure 5-1 illustrates the typical 230 mm long and 60 mm wide dog-bone shaped specimen, with a gauge length and width of 90 mm and 20 mm respectively. Mechanical grinding, polishing and buffing of stainless steel were also typically used to produce attractive mirror finishes. In this experiment, wet grinding with emery paper was used to polish all specimens. The specimens were thoroughly degreased well with acetone and rinsed with ethanol and then immediately placed in desiccators to avoid contact with the atmospheric environment. Each specimen was weighed to within 0.001gm before and after the test.

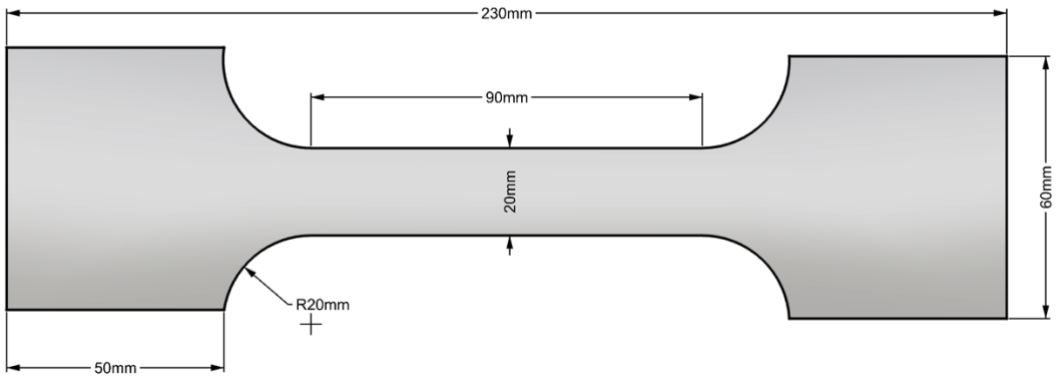

Figure 5-1. Schematic diagram of the stainless steel test specimen

Table 5-1. Chemical composition of UNS 31600 grade 304 SS used for the experiments

Alloy		C%	Mn%	Si%	P%	S%	Cr%	Mo%	Ni%	N%

304	Min.	-	-	-	-	-	17.5	-	8.0	-
	Max.	0.07	2.0	0.75	0.045	0.030	19.5	2.470	10.5	0.1

Pitting tests were conducted at 22°C for 72 hours in the ferric chloride solution according to the procedure outlined in ASTM G48-48. As outlined in ASTMG48, a stock solution of 6% ferric chloride (Fecl3.6H2O, Merck-supply) was prepared by dissolving 100gm of Fecl3.6H2O in 900mL of deionized water. This solution serves as a particularly aggressive chloride environment and is often used to assess the susceptibility of alloys to this type of corrosion. The acidic solution, high chloride concentration (3.9 %) and its strongly oxidizing nature makes this solution quite aggressive to accelerated pitting corrosion tests for stainless steel. The pH of the media is fixed by the test solution as the minimum ratio of the solution volume and specimen area 5 ml/cm^2 specified in ASTM G48-A. Hence, there is no control on pH variation. The pH of the test solution was measured before and after the test using OHAUS ST20 pH and Temp, 0.01 pH.

The solution was poured into the polypropylene tray and kept in a water bath until a temperature of 22 ±2 ºC was reached. At this point, the specimens were immersed in the solution. Figure 5-2 illustrates the immersed specimens in the ferric chloride solution bath. As illustrated in Figure 5-2, two different orientations were investigated to examine the consistency of the pitting corrosion. Three specimens were tested (triplicated) for each orientation to compare the results. After the recommended test period of 72 hours, the specimens were rinsed with water and a nylon brush was used for removing corrosion products. They were then dipped in acetone and left to dry at room temperature. The weight losses of the specimens were recorded and as discussed in the next section the specimens were examined under an optical microscope.

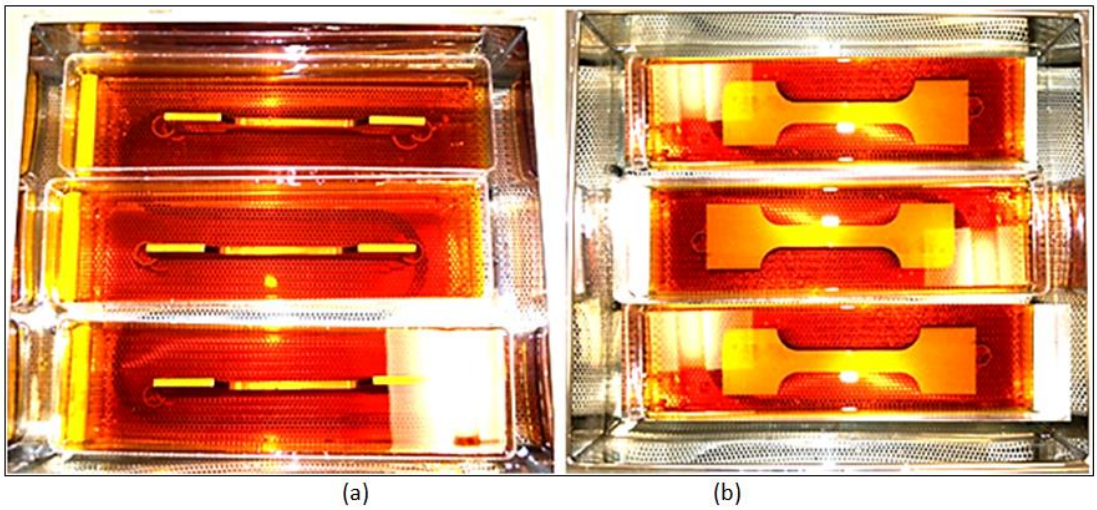

Figure 5-2. ASTM G48 experimental procedure, specimens immersed in ferric chloride solution, a) vertical orientation on edges, b) flat surface orientations

5.2.2 Microscopic Image Processing

A Metallurgical Microscope (ME300TZB-2L-14M) was employed to measure the depth and diameter of the pits in each specimen. The diameter of the pit was determined from photographs by measuring the area of pitting mouth with the calibrated microscopic software (Am scope MU series). The pit depths were measured by applying fine focus techniques. The distance required shifting the optical objectives between the focal points on the top surface of the specimen and on the bottom of the pitting, and was recorded by digital dial-gauge. The pitting morphology in each specimen was observed on a scanning electron microscope (SEM) and optical surface profiler. The SEM images were obtained by using a model (FEI MLA650, CLS-UTAS) at 10 kV accelerating voltage. The chemical composition of the stainless steel surface after the immersion test were also evaluated using energy-dispersive X-ray spectroscopy (EDX). Energy Dispersive X-ray (EDX) analyzer is attached with the SEM for acquiring the EDX analysis.

5.2.3 Physical Characterization of Pit

An optical surface profiler measurement of a pit formed on the surface of 304 stainless steel specimens is illustrated in Figure 5-3. Each single pit formed was observed to have either a circular or an elliptical shape with the depth of a pit equal or greater than

0.025mm. The size of a pit was characterised by its depth and its radius, which was measured at the pit aperture. The pit radius was obtained from SEM observation of the top view. To validate the pit depth measured by a metallurgical microscope, 3D optical surface profiler measurement was performed using differential focusing techniques as shown in Figure 5-3.

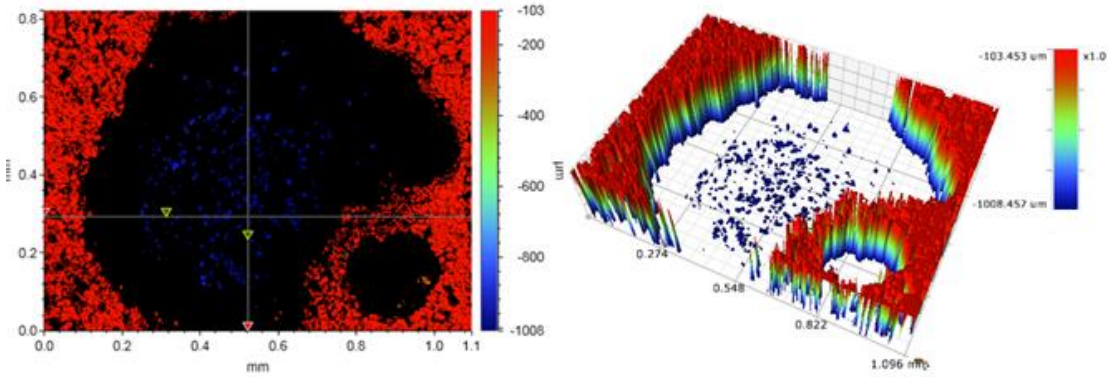

Figure 5-3. Optical surface profiler image of a pit formed on the surface of the specimen

As demonstrated in Figures 5-4 and 5-5 the presence of excessive crevice corrosion on the top surface of the test piece was not expected. It is expected that the top section was nearer the air-solution interface and was therefore theoretically subjected to a higher concentration of oxygen. The observed pits were examined through visual inspection, under the optimal microscope and using SEM. As illustrated in Figures 5-4 and 5-5, the size of the pits were unexpectedly larger in diameter and depth. Excessive pitting and crevice corrosion was also observed on the edges of the specimens. Subsequently, to eliminate the unwanted corrosion noise that appears using ASTM G48, it is essential to conduct further test and analysis. It is equally crucial to provide recommendations to perhaps modify standard test procedure whilst testing larger specimens.

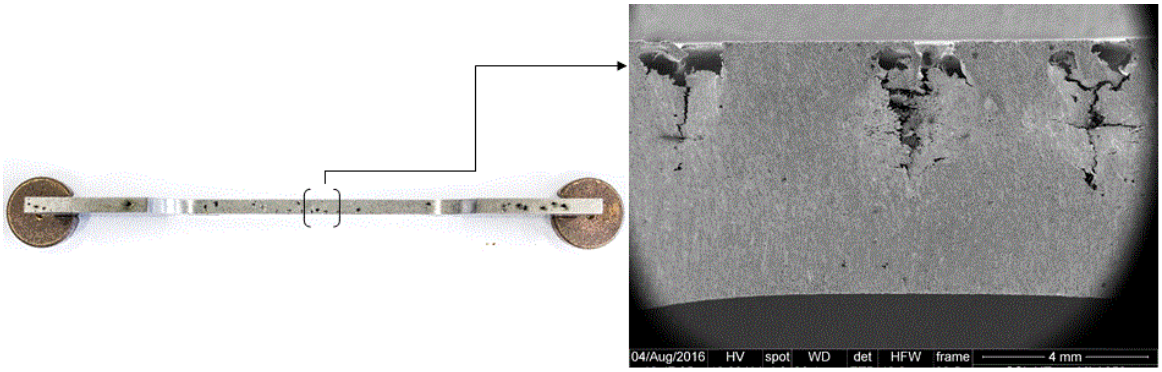

Figure 5-4. The edge of tested specimens with excessive pitting and crevice corrosion (left) and the SEM morphologies of pit formed (right)

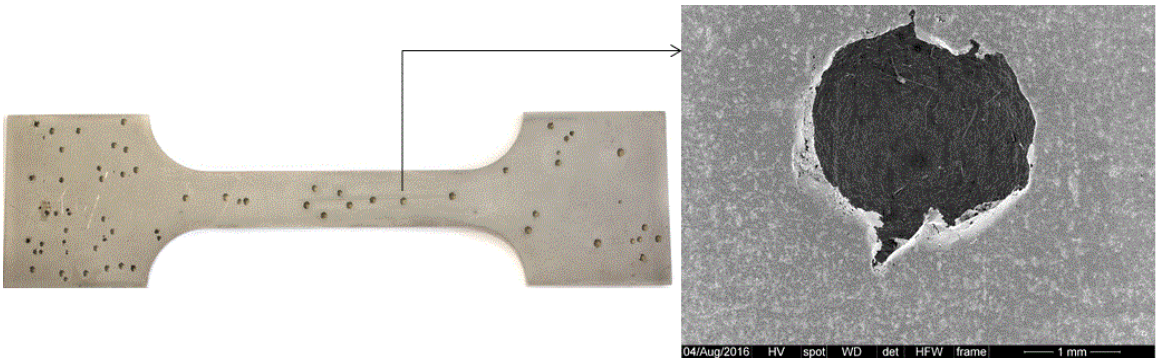

Figure 5-5. A tested specimen with pits on the top surface (left) and SEM morphology of the pit (right)

5.3 Overview of Identified Challenges

The critical parameters that are known to cause localized corrosion of stainless steels in accelerated testing are low pH level, variation in oxygen level, elevated temperature, surface finish and exposure period. ASTM G48 provides no or little guidelines nor precision to these parameters. Previous work reported in the open literature [232, 233, 239, 244, 247, 248], used a different values for these factors to achieve the desired results. Using insights gained through experimentation, the present section reviews these factors and discusses the drawbacks and reliability of using ASTM G48 as an accelerated laboratory procedure for pitting corrosion.

5.3.1 Specimen Orientation

The use of ASTM G48 standard for larger specimens (refer Figure 5-1) has highlighted some unanticipated problems. The presence of excessive amounts of gross random background ‘corrosion noise’ masked the normal pitting corrosion at non-equipotential

sites on the surface. The corrosion noise is qualitatively and quantitatively unpredictable and prevents any assessment of the parameters such as pitting density and pitting depth.

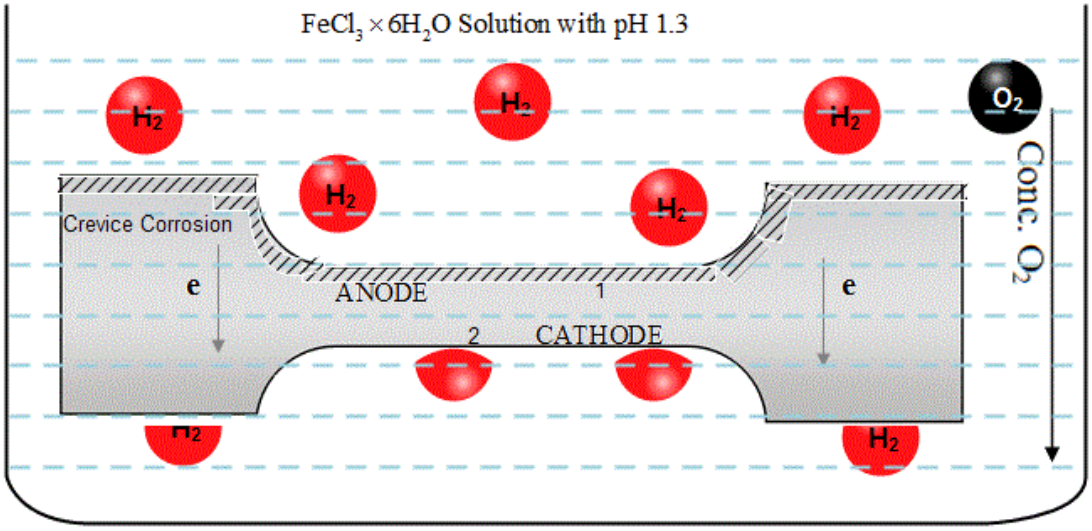

Figure 5-6. Location of the test piece in the solution and chemical reaction

As shown in Figure 5-6, excessive crevice corrosion on the top sections of the test pieces was observed. In order to eliminate this level of corrosion interference, the following mechanism was postulated to occur. Figure 5-6 also illustrates the location of the test piece in the ferric chloride solution. The onset of corrosion is slow in the beginning and then speeds up towards the end of the 72 hour immersion period.

Upon immersion of the specimen into a stagnant solution, hydrogen gas was produced from the acid present in the corroding solution with a pH of about 1.3. After immersion, bubbles of hydrogen formed slowly and rose unimpeded from the top surface directly into the solution. Bubbles of hydrogen formed at the lower sections escaped more slowly due to surface tension between the gas/liquid interface and the metal surface. As the region of liquid just above the test piece becomes more saturated with hydrogen, oxygen levels decrease slowly by displacement with hydrogen in comparison with oxygen at the lower levels. As the localised oxygen concentration gradient becomes more established over time, the conditions become more favourable for the start of crevice corrosion. This will occur on the top surface of the specimen where the oxygen concentration is lowermost. Thus, over time, the top of the specimen becomes anodic, and consequently, the bottom section will be cathodically protected. In all tests, severe crevice corrosion has been observed on the top sections, while corrosion at the bottom

section was almost absent. To eliminate this challenge associated with orientation of the test specimen and the stagnation of test solution, the ASTM G48 is modified and the detail is presented in section 4.

5.3.2 Oxygen Concentration Differential

In an accelerated laboratory test, rate of oxidation is faster and the addition of a catalyst may form pit more quickly [240]. In this study, the major problem using ASTM G48 appeared to be the absence of discussion or acknowledgement of varying oxygen levels surrounding the test piece in the quiescent solution. It was assumed that this would lead to severe crevice corrosion due to differential aeration. This corrosion was most prevalent on the top section of the test piece and on the machined edges. The underside of the test piece was almost completely free from corrosion as a result of cathodic protection. The excessive corrosion on edges was thought to be exacerbated by cold working during the machining operation when the test piece was cut from a larger sheet of metal. This study proposed a method of maintaining the consistent oxygen level by aerating the solution.

5.3.3 pH

Although pH is the key factor which controls the pitting process [195, 249], ASTM G48 does not suggest the precise pH measurements for the ferric chloride solution. The literature shows that pH of the as-made ferric chloride solution appears to vary in different laboratory tests. Many experiments [101, 102] were carried out to understand the effect of pH on pitting corrosion in marine environments and simulated under laboratory conditions. Malik, Ahmad, Andijani and Al-Fouzan [76] performed electrochemical tests on metal and found that corrosion rate increases with increasing acidity of the solution. Melchers [23] reported that the highly acidic conditions (i.e. low pH) are associated for pit to be propagated. Mathiesen, Alle and Andersen [232] used ASTM G48-A for their experimental studies and recommend the pH of ferric chloride solution to be between 1-2. In this study, the pH of ferric-chloride solution was measured at 1.2±0.1 throughout the experiment. This was achieved by dissolving 100gm of anhydrous ferric chloride in 900ml of distilled water at 22±2 ºC. Hence, it is important to ensure that the pH value of the test solution is consistent for the better accuracy of the results.

5.3.4 Surface Condition

The state of the metal surface is known to affect pitting susceptibility [17, 29]. The more homogeneous the surface, both chemically and physically, the higher the potential for pitting. Consequently, the numbers of pits is expected to be lower, and metal resistance to pitting will increase [17, 22, 58]. Surface roughness is caused by local 'weak' points in the protective oxide film where a critical Cl^- concentration is present, or by homogeneities resulting from surface preparation. Either situation can increase the number of active sites for pit nucleation [17]. The roughness of a material's surface depends on the surface preparation. This preparation is conducted to ensure proper adhesion of the coating. The coating is used to protect the materials from the environment by making a smoother surface and thereby reducing the possibility of localized corrosion occurring [41]. The surface roughness offers advantages to change the characteristic of sites for pit initiation [17, 41, 54].

Figure 5-7 shows the SEM image of the pit formed at the surface of an unpolished specimen. It is noted that the initiation of pitting corrosion is usually related to defects or inclusions on the surfaces. These micro defects were observed on the surface of the specimen prior to the immersion test which was observed under an optical microscope. Similarly, Figure 5-7 also illustrates the chemical composition at the mouth of the pit using SEM and EDX. The EDX analysis indicated the presence of a mixture of Fe-Cr-O-Ni-S. It was also observed that Fe is the main chemical component to produce a pit where there is a mechanical defect. The result was agreeable with the studies conducted by Wang, Cheng and Li [250].

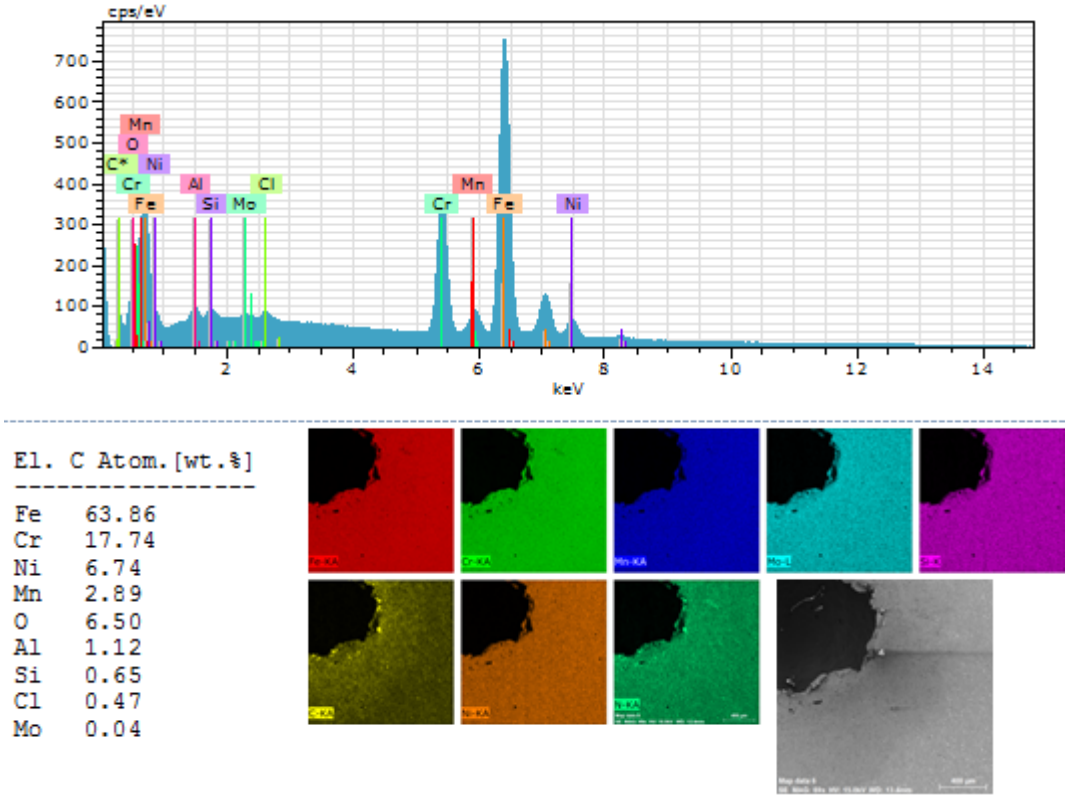

Figure 5-7. SEM image of the pit near the surface defect area with the chemical and material composition

ASTM G48 provides very little information on the surface preparation of the specimens. Rough surfaces can induce stress in the surface layer, which may cause their metallurgical properties to deteriorate and make them less suitable for corrosive environments. In addition; this metal surface involves microscopic scratches, strains, metal debris and embedded abrasives. This study found that it crucial to consider the surface finish up to mirror finish for a specimen to avoid unwanted corrosion noise using ASTMG48. Further analysis on surface preparation and associated results are discussed in the modified ASTM-G48 sections.

5.3.5 Temperature

Temperature is one of the critical factors in pitting corrosion because it greatly influences the corrosion behavior of steels. Many materials do not pit at a temperature below a certain value which may be extremely high and reoccurring [195, 196] . Melchers [80] stated that the reaction process for corrosion speeds up with higher temperatures after the initial phase, and that this suggests that corrosion rate increases with increase in the temperature. The ASTM G48 standard suggests an immersion test

to be carried out at a fixed temperature of 22ºC or 50ºC. However, these temperatures are not designed as per the temperature criterion for materials acceptance.

Several researchers have applied ASTM G48 with different temperatures to conduct the pitting corrosion resistant test for stainless steel and the results presented were all somewhat inconsistent. Bakrachevska [245] conducted the ferric chloride test for the stainless steel pipe at 30ºC and 40ºC to investigate the resistance to pitting of materials at different temperatures. The author reported the weight loss per unit area and claimed with the temperature of 22ºC, there was no observation of visual pits on the specimens. Maurer [233] reported that for mill acceptance, G48 was modified to require testing at a temperature of 35 ºC, although ASTM G48 suggested using 50ºC as well. They also claimed that 40ºC is an acceptable temperature for ASTMG48 in order for the specimen to avoid crevice corrosion. Mathiesen, Alle and Andersen [232] adopted ASTM G48 to test corrosion of overlay welds in different grades of stainless steel and used the testing temperature of 35ºC and 40ºC. They reported that Critical Pitting Temperature (CPT) technique can be used as an alternative ASTM G48 in doubtful cases. They recommended that more work needs to be done to establish suitable acceptance temperature using ASTM G48 standard. Based on the experimental work conducted in this study, a suitable test temperature for larger stainless steel specimens is suggested and is presented in section 4.

5.3.6 Exposure Period

The ASTM G48 suggests a test time of 72 hours, while a number of researchers [132, 241, 244, 251-253] successfully used from 24 hrs, 48hrs, and 196hrs to 30 days to achieve desired results. Corbett [239] recommended that a standard test time of 48 hours be adopted for pitting corrosion resistance of stainless steel. Similarly, Byrne [243] suggested ASTM G48 test at 50ºC for 24 hours with acceptance criteria of no pitting and maximum weight loss of $4g/m^2$.

In this study, a time dependent immersion test was conducted for the specimen up to 72 hours. This test was conducted at the temperature of 22ºC to quantify specimen immersion time for creating the desired characteristic corrosion pit morphology. The specimen was removed after every 24 hours during the immersion test and pit characteristics data were recorded. It was concluded that the pits were initiated and fully developed within 48 hours of immersion test using ASTM G48 test procedure at 22 ºC.

Hence, an immersion time of 48 hours was selected based on the above observations to produce the desired pitted morphology onto the specimen. This recommendation agrees with Corbett [239] recommendation.

5.4 Application of Modified ASTM G48- A Method for Larger Test Piece

Based on the aforementioned challenges, ASTM G48 was modified in order to provide precise evidence on the controlling factors and to suit large specimens. To eliminate excessive corrosion noise at the edges of the specimen, aeration of the solution and the surface preparation of a specimen were initiated. It is expected that the aeration of the ferric chloride solution will maintain the motion of the solution to the specimen.

The resistance of so-called "acid-resisting" metals to acid corrosion is largely due to the fact that they do not replace hydrogen with acids [254]. In the pitting process, the dissolved oxygen should be as active in producing pits as an acid used in accelerated testing. In order to obtain the similar concentration of the dissolved oxygen through the stagnant solution aeration is introduced. As demonstrated in Figure 5-8, the air bubbles were introduced in the ferric chloride solution. The edge of the specimen was polished by wet grinding, using emery paper of 400 to 600 grit number. Subsequently, the specimen was treated to a mirror finish by a buffing process. The specimen was immersed in the ferric chloride solution for 48 hours at 22 ºC. The pH of the ferric chloride solution was recorded constantly as between 1.2-1.3 throughout the test.

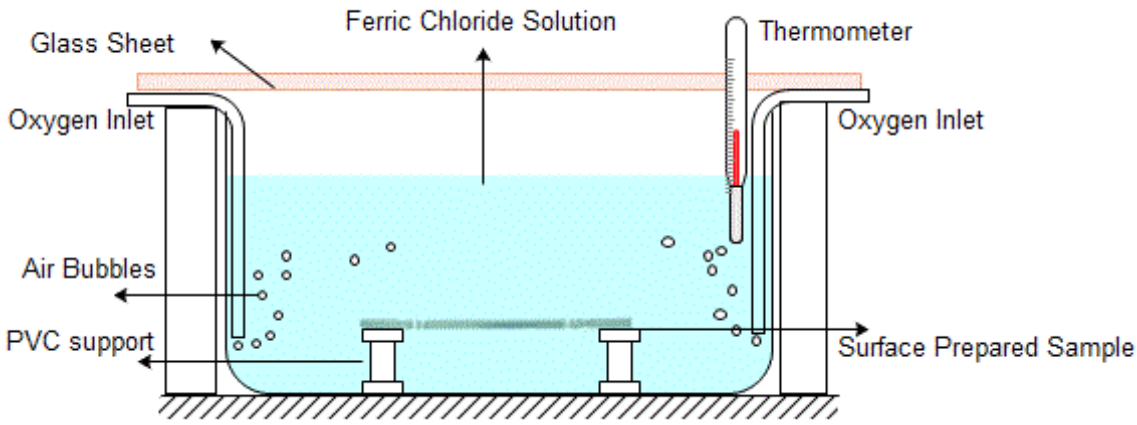

Figure 5-8. Experimental setup for pitting Test, a modified ASTM G48 approach

5.4.1 Result and Discussion

To investigate systematic errors caused by the abovementioned factors using ASTM G48, accelerated laboratory tests were conducted by modifying the experimental set-up. Figure 5-9 shows the pit formed on the surface of the specimen after aerating the solution and considering the surface finish for the specimen. The pit distributions patterned for specimens using existing and revised ASTMG48 standard was also analyzed and the corresponding SEM images were obtained. It is observed that aeration provides more realistic pit by avoiding unwanted effect of stagnation. Aerated solution is observed to have a higher corrosion potential compared to de-aerated solutions. This results is in good agreement with the results reported by Mameng, Bergquist and Johansson [255].

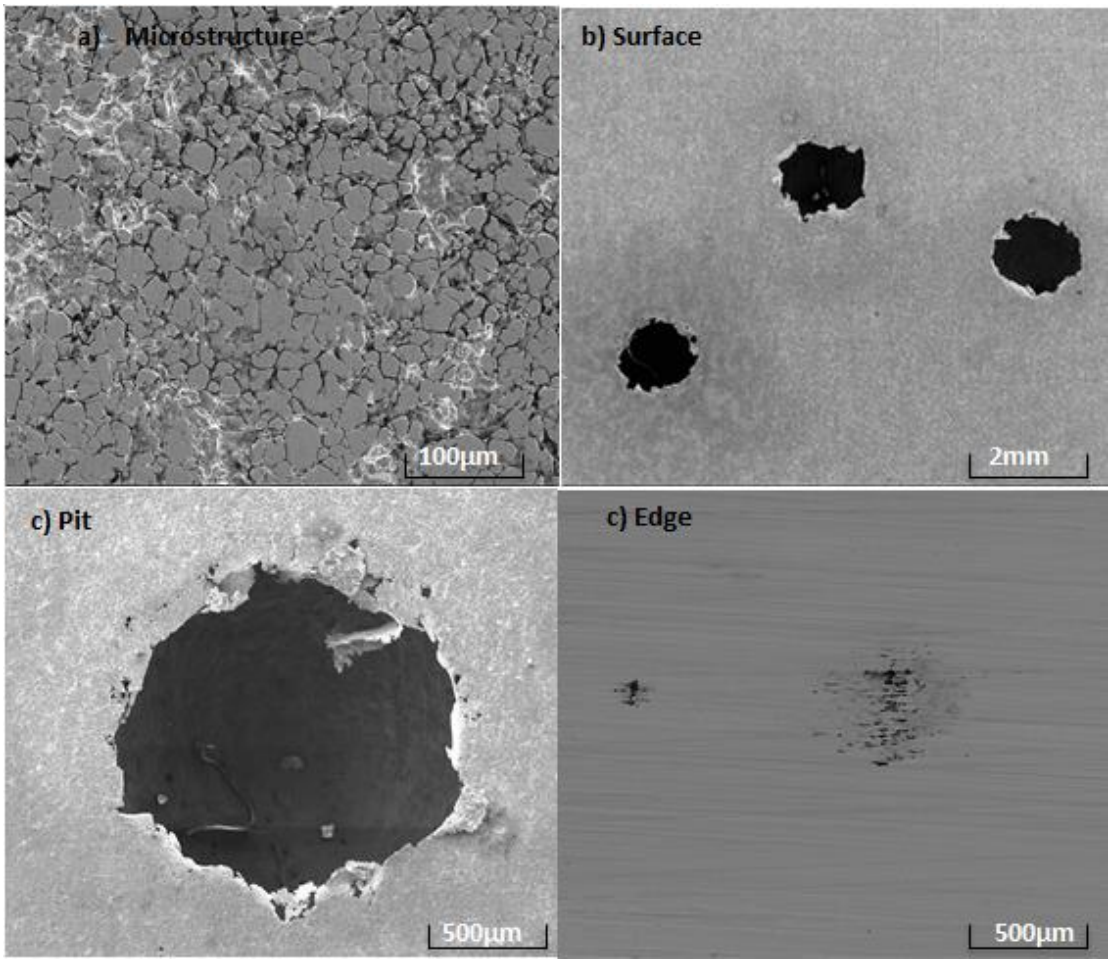

Figure 5-9. SEM image of pit morphology and pit distributions at the surface and edge of the tested specimen after modifying test standard

Figure 5-10 shows the comparison of the corrosion depth versus diameter for the tested specimen using existing ASTMG48 standard and with modified approach. It is clear from the surface plot that the size of the pits using existing standard is significantly larger compared to the modified standard. The pit depth data achieved from modified standard agrees with the findings reported by Woldemedhin and Kelly [256] where they predicted the maximum pit size on stainless steels under atmospheric conditions. Through the modified approach, the pits observed after the immersion test were approximately hemispherical shapes. The largest pits were observed to be large in diameter but quite shallow. The comparable result were reported in the previous studies [102, 257]. In the modified approach, the specimens were placed in the mid-section of the water bath with the PVC supports on both sides. This provided the minimum contact between the supports and the tested specimens. Remarkably there were no significant attacks at the crevice formed by the PVC support points.

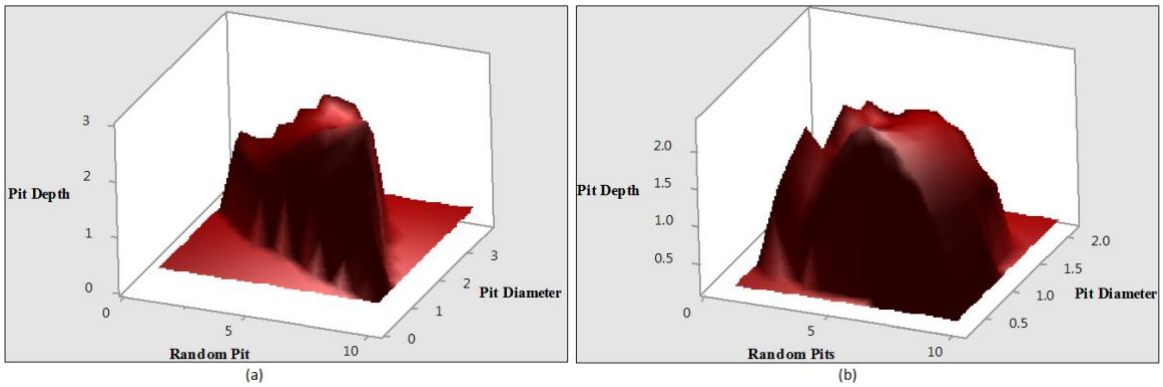

Figure 5-10. Comparison of the pit depth and diameter for a) test result using ASTM G48 standard and b) Test result using modified ASTM G48 Standard

Figure 5-11. The edge of the tested specimens after aerating the solution and considering surface finish of the test piece

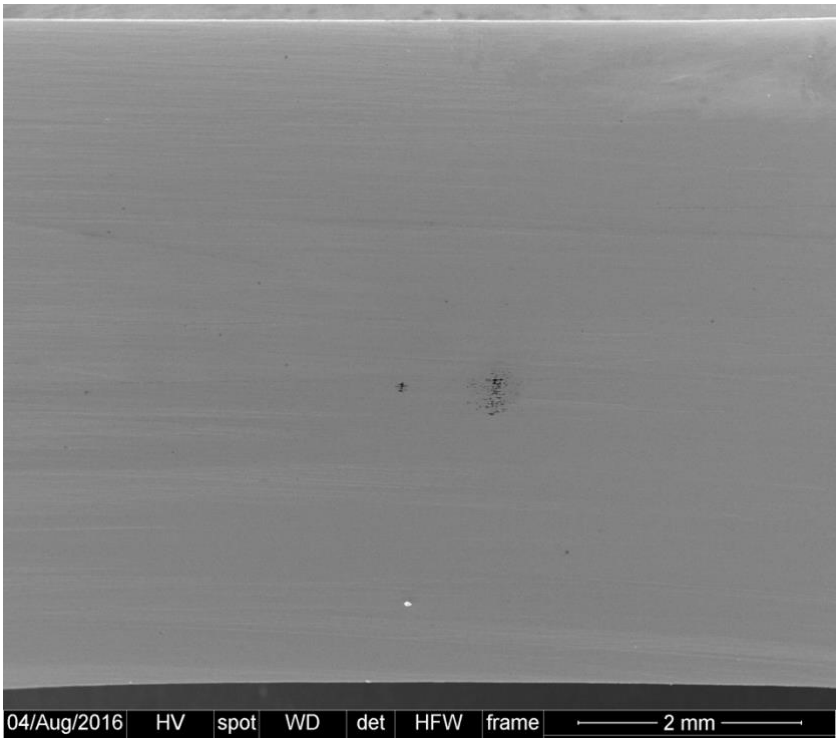

Figure 5-12. SEM image for pitted edge of the tested specimen after modifying test standard

It is necessary to compare the edge effect of tested specimens in order to confirm the effect of surface finish on the pitting corrosion. Figure 5-11 shows that the edges of the specimens were locally attacked by pitting corrosion during the immersion tests. However, density of unwanted crevices and pitting corrosion has been significantly reduced after the surface treatment. The specimens were also examined using a SEM as illustrated in Figure 5-12. A remarkable change in appearance can be observed when comparing the surface both with and without surface treatment (refer Figure 5-12). It is understood that the surface treatment removes the MnS inclusions successfully without dissolution of the substrate. It is also anticipated that rough surface creates the capillary effect in close crevices and this fact changes kinetics of the pitting corrosion. The rough surfaces of a metal also exhibit lower pitting potentials as by increasing the roughness, less-open pit sites are maintained during the early stages of growth as metastable pits. Therefore, there is more restricted diffusion of metal cations during propagation which can then result in the transition from metastable to stable pit growth. Comparable conclusions were also reported by Zatkalíková, Bukovina, Škorík and Petreková [92] for AISI 304 stainless steel. Hence, the ASTM G48 standard had better specify the importance of surface finish to eliminate the unwanted corrosion noise. Accordingly,

this study recommends mirror finish for the area on a specimen which should be protected from corrosion noise.

5.5 Statistical analysis of Pitting Data Observed on Modified standard

Based on the modified ASTM-G48-A, series of pitting corrosion test with eight different specimen thicknesses were considered: 0.9, 1.6, 2, 2.5, 3, 4, 5, 6 mm. subsequently, the entire pit depths and pit diameters data set for each specimen were recorded in a total of 24 (triplicated) immersed specimens. During the statistical analysis, individual pits which penetrated the thin specimen were assumed to have the depth equivalent to specimen thickness. During the measurements, the insignificant pits near the specimen edges (refer Figure 5-12) were discarded. The probability distribution was fitted to the specimens resulting in maximum data sets using the maximum likelihood estimator (MLE). The goodness of fit test was applied to determine how well a particular distribution fits the observed data.

5.5.1 Pit Depth & Diameter Distributions

The total number of measurable $0.05 \leq$ 6 mm pits observed in the set of specimens for eight different thicknesses was recorded at around 890-1200. Histogram and the probability distribution function that best fits the pitting corrosion depth data are illustrated in Figure 5-13. As shown in Figure 5-13, generalized extreme value distribution (type III), i.e. Weibull distributions best fits the pit depth data.

$$F(t) = 1 - \exp(-((t-\gamma)/\eta)^m) \quad (1)$$

Eqn. 1 represents the Weibull distributions where γ, η and m are the location, scale and shape parameters, respectively. Most of the published work [28, 137, 141, 258, 259] reported that pitting corrosion followed generalized extreme value (GEV) distribution. Khalifa, Khan and Haddara [259] applied the extreme value method to predict the maximum localized corrosion of process components with a specified precision.

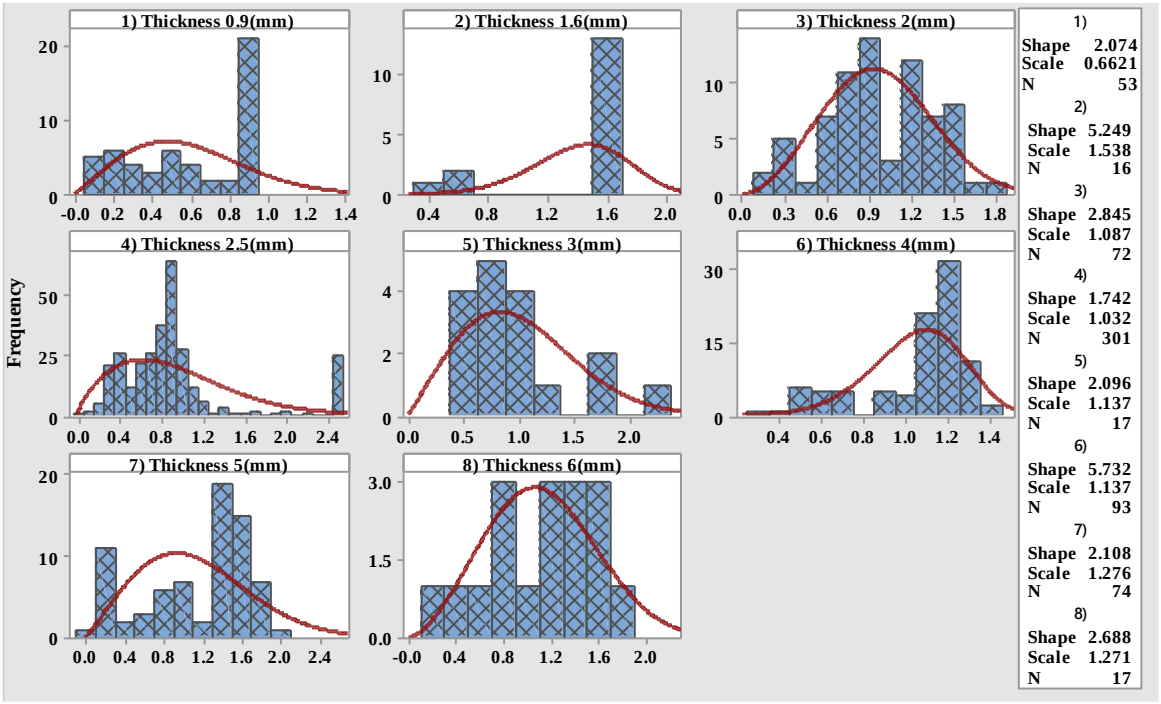

Figure 5-13. GEV (Weibull) distribution fitted to the experimental pit depth histogram for distinctive thickness of stainless steel specimen investigated.

Figure 5-14 a) shows the comparison of two common distributions employed to estimate the probability density functions that best fitted the pit depth data. Normality test was also conducted using Anderson-Darling test considering normal distributions. Based on this analysis it is clear that the data does not follow normal distributions. Instead the pit depth data shows the best fit distribution using Weibull. As shown in Figure 5-14 the p-value is less than or equal to the significence level, hence the decision is to reject the null hypothesis and conclude that the pit depth data do not follow normal distribution. Also it is visually clear from the the normality test that the data points do not follow the fitted distribution line and the data are skewed from a curved line.

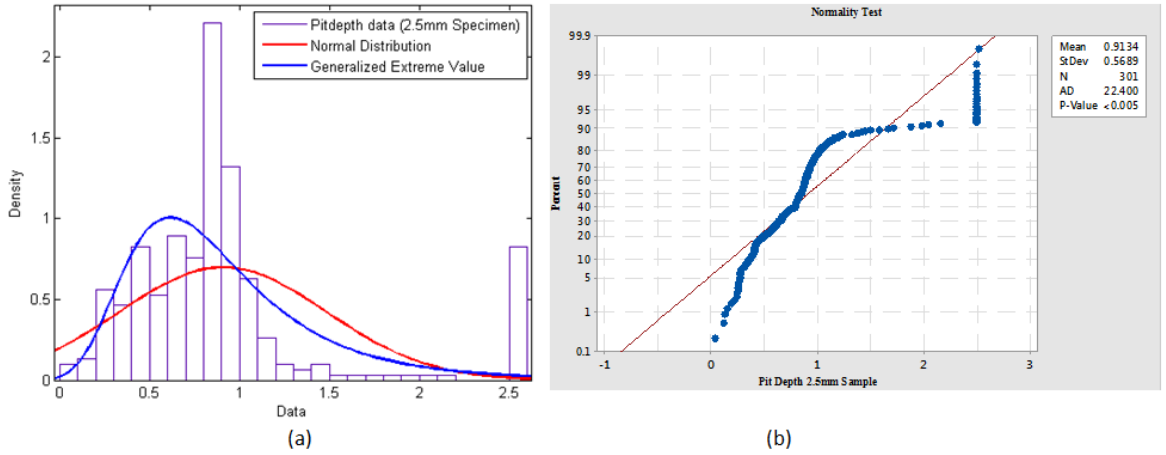

Figure 5-14. Probability density function comparison of the pit depth data (a), Normality test (b).

In the histogram, (refer Figure 5-13) the shallow pits are those which after nucleation repassivate, or those that also repassivate after reaching a metastable state after immersion in the ferric chloride solution for 48 hrs. The high peak in the histogram used for specimen 0.9mm and in 1.6mm thickness, indicates the pit penetrating the entire thickness of the specimen. The maximum pit depth for the specimen that is fully penetrated is assumed to be equal to the specimen thickness. Caleyo, Velázquez, Valor and Hallen [260] also reported that the Weibull and Gumbel distributions are the most likely distributions to fit the pitting depth and rate for relatively short exposure.

Similarly, the pit diameter was recorded for each pit observed during the microscopic examinations. Figure 5-15 shows the Anderson-Darling approach to identify the distribution that best fits the pit diameter data. It is found that the Weibull distribution provides a best fit for the pit diameter data as well. Figure 5-15 shows that the data points are in good agreement with the fitted distribution line in Weibull distributions. The histogram shown in Figure 5-16 seems to completely ignore the bell-shape and is symmetric about the means, which indicates that the pit diameter data does not to follow normal distributions. It can be noticed in Figure 5-16 that the shape parameter changes in the "bell curve" with respect to specimen thickness. In fact, the skewness values for each distribution change in each thickness. The reason for such a difference in shape parameters for each thickness might be the existence between growing pits located very close to each other. Similar conclusions were made by [9, 28, 260].

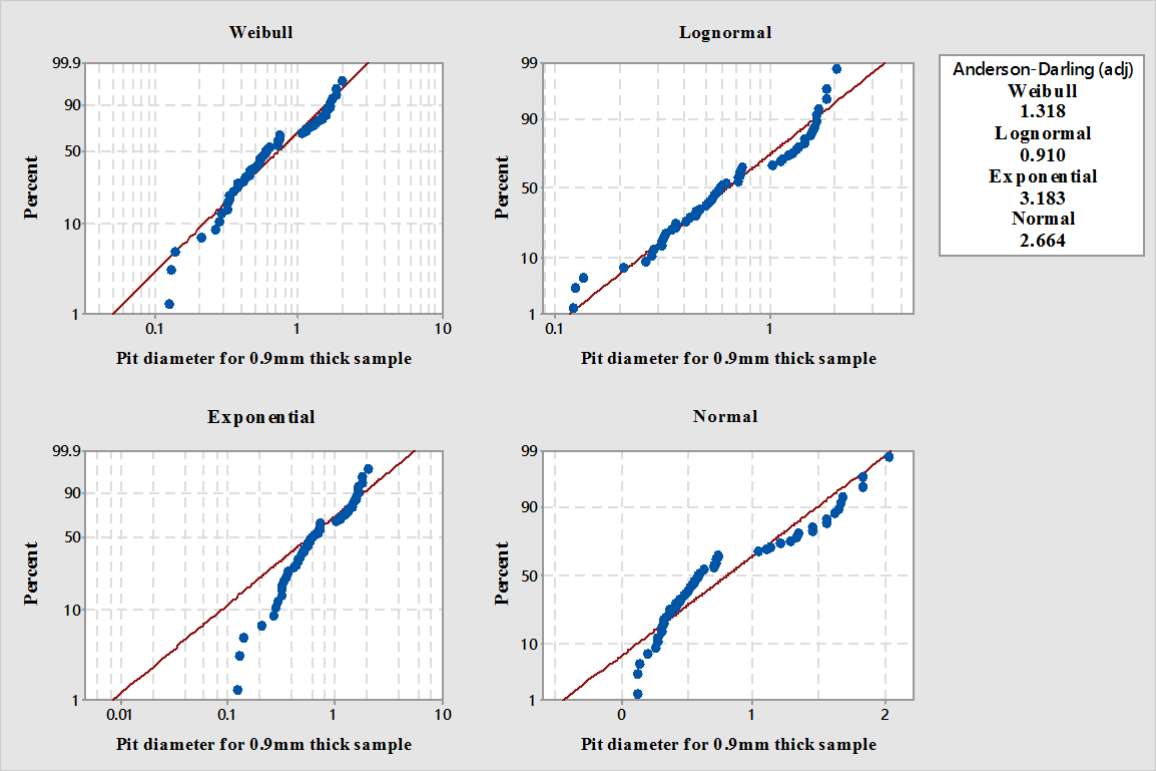

Figure 5-15. A specimen probability plot based on Anderson-Darling approach to identify the best fit distributions for the pit diameter data

In Figure 5-16, it can be seen that some of the pit diameters are relatively large especially in the thicker specimens. This could be due to the aggressiveness of the ferric chloride solutions and the amount of inclusion and defect present in the specimen. The above analysis indicates that for the specimens studied, the statistical distribution for the observed depth and diameter of pits does not necessarily have to be of the Gumbel or Fréchet type as these distributions most commonly use extreme value distribution for pitting [138, 141, 258, 260, 261]. It is agreed that for the short-term immersion of the specimens, the Weibull is the most appropriate distributions for the observed pit depth and diameter data. It is also equally important to note that this present analysis has quite varied pitting data for 304 stainless steel immersed in the ferric chloride solution for 48 hrs. at the temperature of 22±2 ºC. The pitting data for the same specimen in the actual marine immersion environment can be different and hence distinctive and complex statistical analysis may be required.

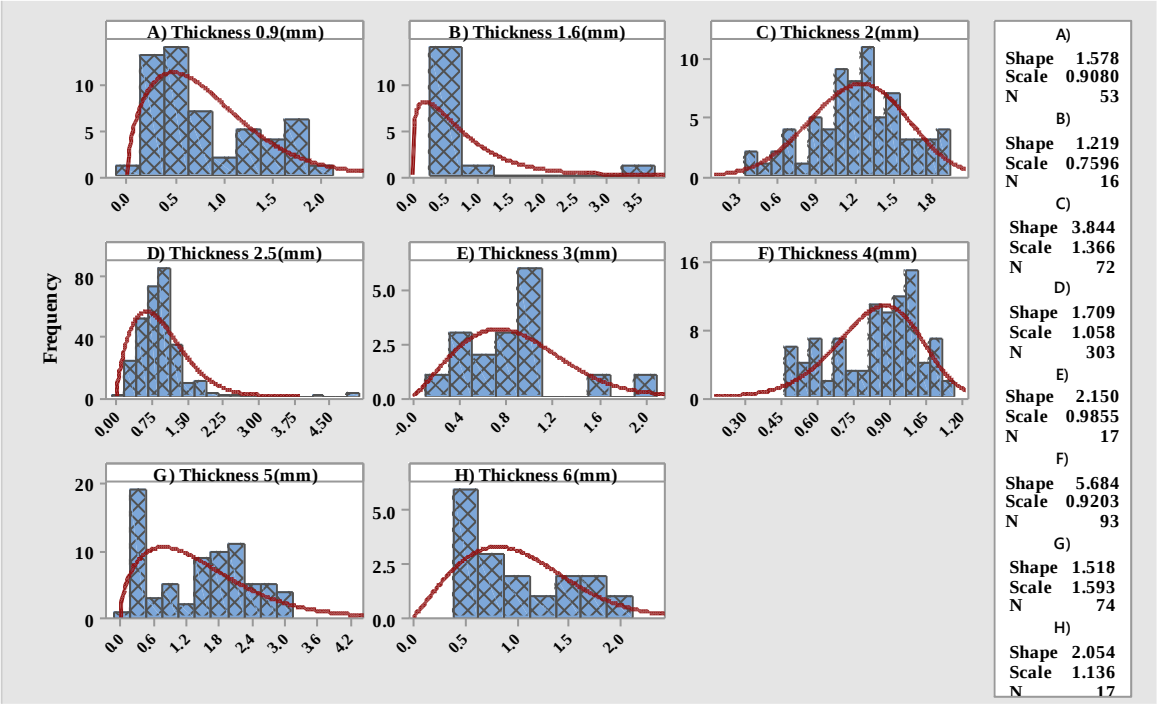

Figure 5-16. Histogram of the measured pit diameter for different thickness specimens and the fitted Weibull distributions

5.6 Conclusion & Recommendations

Pitting corrosion is a complex but important problem that is at the root of many structural and system failures. Hence, precise and realistic laboratory testing techniques are crucial to simulate real-world environments. In this study, the application of ASTM G48-A for a pitting corrosion resistance test for the larger specimens was found to be challenging. The presence of excessive amounts of gross random background 'corrosion noise' has masked the normal pitting corrosion at non-equipotential sites on the surface. To eliminate the unanticipated problems during the ASTM G48 test, the standard is revised and a modified approach has been presented in this study. The result obtained from the modified test was validated with previous studies conducted under controlled laboratory conditions for 304 stainless steel. Validation of the pit size was accomplished by comparing the predicted pit size with the pit size obtained from previous studies. It has been shown that generalized extreme value distribution (Weibull) is found to provide best fit for both pit depth and pit diameter distributions observed from the short-term immersion test. From this study, the following recommendations were suggested for conducting pitting corrosion resistance tests using the ASTM G48 standard;

- Aerating the solution to avoid differential aeration. Aeration is preferred over stirring, since a solution saturated with oxygen will be more consistent in terms of oxygen content and thus subject to fewer variations than a stirred solution. It is hoped that this procedure will eliminate all unwanted bulk corrosion resulting from different concentrations of air in the solution during the 48 hour immersion period;
- Surface finish is an important procedure to eliminate the unwanted corrosion noise as a result of surface stresses caused by machining. It is recommended to consider the surface finish up to a mirror finish in the area which is more vulnerable to unwanted corrosion attack;
- Furthermore, the presence of excessive surface roughness presented a series of sharp stress risers that would form anodes which in turn would initiate severe corrosion mask.
- It is recommended that the test temperature should be maintained at 22 ±2ºC;
- The pH value of ferric-chloride solution to be maintained as consistent throughout the test to achieve realistic results;
- Regular monitoring of the oxygen levels will aid in identifying the oxygen depletion around the surface of the specimen;
- To verify the result obtained from the test, electrochemical investigation such as potentiodynamic and potentiostatic polarization and zero resistance ammeter (ZRA) were suggested. This helps to measure and validate the corresponding corrosion rate;
- A dye penetrant examination should be included, in combination with microscopy, in order to locate and identify pits on the exposed coupon.

5.7 Acknowledgement

Authors thankfully acknowledge the support provided by the National Centre for Maritime Engineering and Hydrodynamic (NCMEH) and the Australian Maritime College (AMC). The grant, received from the University of Tasmania (2016) under the Research Enhancement Grants Scheme (REGS), is highly appreciated.

6 *Experimental and Numerical Strength Assessment of Steel Specimen subjected to Pitting Corrosion*

Abstract

This paper presents an experimental and numerical investigation into the ultimate tensile strength of the stainless steel specimen with varying thickness subjected to different level of pitting corrosion deterioration. The surface of 24 of 304L stainless steel dog bone specimens was subjected to accelerated pitting corrosion using a modified version of the ASTM G48-48 process. The pitting corrosion damage was established using microscopic image processing. Uni-axial tensile strength tests were performed on both corroded and un-corroded stainless steel specimens of different thicknesses to study the ultimate strength reduction based on the severity of pitting corrosion. Non-linear finite element analysis simulations of the pitted and undamaged specimens were performed to predict changes to the ultimate strength due to pitting. A comparison of the numerical experimental results suggests very good agreement between the two. It was observed that the reduction of ultimate strength due to pitting is influenced by the degree of pitting, depth of pit, pit location and thickness of the specimen.

Keywords: Stainless steel, Pitting corrosion, Tensile test, Numerical Study, Degree of Pitting

6.1 Introduction

Aging steel structures may be subjected to strength and stiffness changes beyond their baseline condition for design. These changes may impair the safety and serviceability of the structure and should be considered as part of the process by which a structure is evaluated for continue future service [262]. Marine steel structures such as ships, offshore platforms, pipelines and underwater storage and shore facilities operate in an aggressive environment which make them prone to suffer various types of damage as they age [263]. Over the structure's lifetimes, the result of the interactions between metallic structures of ships and offshore platforms with the maritime environment, corrosion occurs. Corrosion may be considered as the undesirable deterioration of such structures in reacting with their surrounding environment [264-266]. Corrosion can lead to structural material degradation, this material degradation results in loss of mechanical properties of the structure such as strength, ductility and impact strength. Material degradation also leads to loss of material and, at times, to ultimate failure [4, 267]. Hence the assessment of the ultimate strength of corroded structures is crucial, since realistic safety margins for a structural system cannot be determined unless the ultimate strength is precisely estimated [268].

There has been significant development of experimental and computer-based simulation techniques for studying and accurately predicting the ultimate strength of the complex structures under pitting corrosion; especially for steel structures [263, 268-284] . Most of these studies have been carried out on simulated pitting corrosion patterns by varying Degree of Pitting (DOP), pit depth, pit shape, pit size, pit distribution and location. Paik, Lee and Ko [273] studied the ultimate strength characteristics of plate element with pit corrosion wastage under axial compressive loading used for offshore and marine structures. They performed a series of collapse tests on box-type plated structures plate with pit corrosion is performed in by a varying the amount of pit corrosion damage. They also carried out series of ANSYS non-linear Finite Element Analyses (FEA) for steel plate elements under axial compressive loads with varying the degree of pit corrosion intensity and plate geometric properties. The plate with pit corrosion was modelled to be simply supported along all edges keeping

them strength. Later they compared both experimental and numerical methods to validate the strength capacity of the plate element under pitting corrosion.

Dunbar, Pegg, Taheri and Jiang [270] investigated the effect of localized corrosion on initial buckling, ultimate collapse and post-ultimate responses for stiffened plates using FEA. For their numerical analysis they use steel with Young's modulus of 207 GPa with no strain hardening, poisson's ratio of 0.3, a density of 7.85 mg/m^3 and a yield stress of 350Mpa. The axially loaded finite element model was composed of 1296 quadrilateral shell element with six degree of freedom at each node. Nakai, Matsushita, Yamamoto and Arai [285] studied the effect of pitting corrosion on local strength of hold frames of bulk carriers using a series of experimental tensile tests series of buckling tests and later elasto-plastic analysis using Finite Element simulations. To evaluate the effect of pitting corrosion, a series of tensile tests and compression tests were conducted with actual corroded members and artificially pitted members following the investigation of actual pitting corrosion on hold frames of 14-years old bulk carrier. They studied the effect of pit location on ultimate strength of steel plate and claim that the ultimate strength gets smaller as the location of pits gets closer to the centre of the web plate.

Abdel-Ghany, Saad-Eldeen and Leheta [19] studied the effect of pitting corrosion on the strength capacity of steel offshore structure. They identified that the offshore structure's capacity depends on the cross-sectional dimensional of the structural members. Decreased in the materials thickness due to pitting corrosion is very critical in regards to structural integrity. Similarly, Teixeira and Soares [280] presents a study of the collapse strength of corroded plates with random spatial distributions of corroded thickness. They proposed the alternative way to simulate the uniform reduction of the plate thickness due to corrosion, or a localized area of reduced thickness. Teixeira and Soares [280] consider the spatial distributions as the alternative to represent reduction in plate thickness due to corrosion and it can be well describe by a stochastic simulation of random fields. Huang, Zhang, Liu and Zhang [277] studied the effect of pitting corrosion on the ultimate strength characteristics of the hull plate. Attempt has been made to develop a formula for assessing the ultimate strength of hull plate with pitting corrosion damage under biaxial in-plane compressive loading. They claim that, previous research was only focused on developing the formula for assessing the

ultimate strength of plate with pitting corrosion damage when plate is subjected to uniaxial in-plane compression. However, they assumed that there is no corrosion on the plate edges for the corroded plate and the ultimate strength is the average stress on the plate edge.

Silva, Garbatov and Soares [276] studied the effect of non-linear randomly distributed non-uniform corrosion on the ultimate strength of unstiffened rectangular plate subjected to axial compressive loading. A series of 570 plate surface geometries where generated by Monte Carlo simulation for different degree of corrosion, location, and age and FE analysis was conducted. They claim that the plate with the initial imperfections can be precisely analysed with the finer mesh size and lead to the good quality result. Sultana, Wang, Sobey, Wharton and Shenoi [286] presents a study that concentrates on a comparison between steel plate and stiffened panel subjected to localised corrosion. They used finite element analysis (FEA) method to investigate the effect of random corrosion on the compressive strength capacity of marine structures. Using the FEA they determine the reduction in the ultimate strength capacity of the stiffened panels over time and the effect of corrosion severity, aspect ratio and slenderness ratio was also investigated.

Garbatov, Soares, Parunov and Kodvanj [283] performed tensile strength tests on small-scale corroded specimens, so as to derive their mechanical properties. The specimens were cut out of a box girder that was initially corroded in real seawater conditions. As a result of the tensile tests, the mechanical properties of the specimens were determined, namely modulus of elasticity, yield stress, tensile strength, resilience, fracture toughness and total uniform elongation, demonstrating that those material parameters are influenced by the severity of corrosion degradation. Most recently, Rahmdel, Kim, Kim and Park [287] introduced a novel stepwise method to predict ultimate strength reduction in offshore structures under pitting corrosion. Interestingly they proposed six steps in attempt to finding the relationship between the ultimate strength reduction (USR) with pit depth and the relationship between ultimate strength reduction and the age of the structures. The main objective of the present paper is to study the effect of specimen thickness for strength assessment of the pitted plates under uniaxial tension. In order to achieve this goal, the paper presents the experimental and numerical study of the specimens with varying thickness, which were firstly corroded

and then tested under uniaxial tensile load. The surface of 24 corroded specimens with differing pit characteristics was analysed to investigate the strength reduction due to pit physiognomies. The numerical study is validated with the experimental result.

6.2 Experimental Methodology

In order to establish the effect of thickness in the ultimate strength of the pitted specimens subjected to uniaxial tension a series of destructive tensile test were conducted. Eight different specimen thicknesses were considered: 0.9, 1.6, 2, 2.5, 3, 4, 5 and 6 mm. Dog-bone shaped tensile test specimens were cut from UNS 304L stainless steel plates using a numerically controlled water-jet cutter. Figure 6-1 illustrates the typical 230 mm long and 60 mm wide dog-bone shaped specimen, with a gauge length and width of 90 mm and 20 mm respectively. The cross-sectional area for the specimen was selected based on the Australian Standard, AS 1391-2007 Metallic materials—tensile testing at ambient temperature [288].

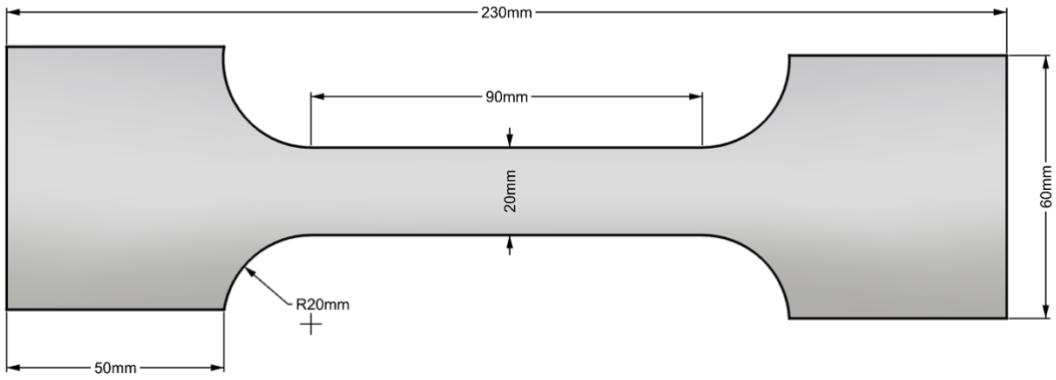

Figure 6-1. Schematic diagram of the stainless steel test specimen (not to scale).

The chemical composition of UNS304L stainless steel adopted in this study, is reported by Bhandari et al. (2017) which is summarized in Table 6-1.

Table 6-1. Chemical composition and mechanical properties of 304L used for the experiments [193, 289]

Alloy		C%	Mn%	Si%	P%	S%	Cr%	Mo%	Ni%	N%
	Min.	-	-	-	-	-	17.5	-	8.0	-

304	Max.	0.07	2.0	0.75	0.045	0.030	19.5	2.470	10.5	0.1

An accelerated pitting corrosion procedure, immersion in a ferric chloride solution as outlined in ASTM G48-48, was utilized to obtain the desire level of pitting corrosion degradation of the specimens within an acceptable time frame. A stock solution of 6% ferric chloride (Fecl3.6H2O, Merck-supply) was prepared by dissolving 100gm of Fecl3.6H2O in 900mL of deionized water. The specimens were immersed in this solution at 22ºC for 72 hours. It was found that although the ASTM G48-48 process is often used to assess the susceptibility of alloys to pitting corrosion, its application to 304 austenitic stainless steel specimens presented significant challenges for the larger samples (Lau et al. 2017). Hence, a modified ASTM G48 procedure specifically tailored to accelerated corrosion of larger 304 stainless steel specimens was successfully developed and reported [193].

6.3 Experimental Results

Figure 6-2 shows the pitted surface of 5mm thick specimen as observed by Scanning Electron Microscope (SEM) after the accelerated corrosion procedure. The depth and diameter of all pits located along the gauge length of the corroded specimen were recorded using microscopic image processing as detailed by [193]. Pits located in the grip section of the specimens were ignored as it was assumed that they would not to affect the failure behaviour of the specimen.

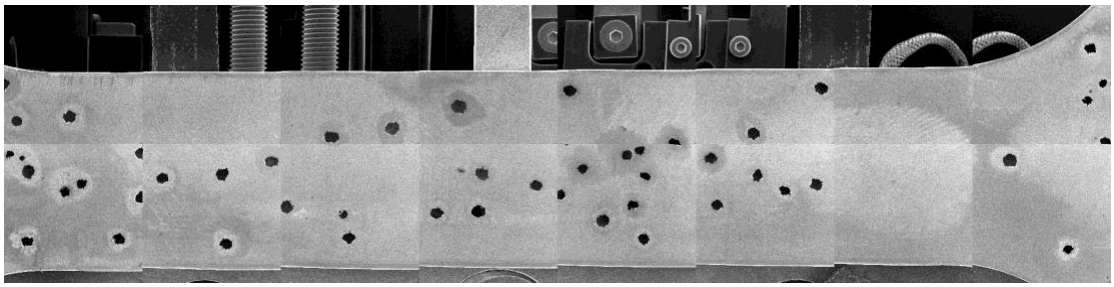

Figure 6-2. Pitting Corrosion Degradation of a 5mm thick specimen observed using SEM

The minimum, maximum, mean values and standard deviation for pit depth and pit diameter measured for each thickness are given in Table 6-2. It is considered that the

corrosion data from all specimens follow the same time dependency for a mean value and standard deviation.

The Degree of pitting intensity (DOP%) is introduced to denote the extent of pitting corrosion in each specimen. DOP% is defined as the percentage of the corroded surface area with respect to the original plate surface area, namely

$$DOP\% = \frac{1}{ab}\sum_{i=1}^{n} A_{Pi} \times 100\% \quad (1)$$

Where n is number of pits, A_{Pi} is the surface area of the ith pit, a and b are length and width of the specimen, respectively. An experimental database including the characteristics of all cases and their corresponding results is shown in Table 6-2. Table 6-2 presents the pitting corrosion data for specimen with various thicknesses which was triplicated to monitor consistency within experimental results. In addition, the DOP %, Ultimate tensile strength in MPa(UTS), Elongation results are summarised in Table 6-2.

Table 6-2. Specimen details and quantitative measure of level of pit corrosion of specimen

Group			***Pit Depth***					***Pit Diameter***				
Specimen Designation	Thickness (mm)	DOP%	Min(mm)	Max(mm)	Mean (mm)	St. Dev(mm)	Min (mm)	Max(mm)	Mean (mm)	UTS(MPa)	% Elongation	St. Dev(mm)
A1C	*0.9*	1.18	0.01	Penetrate	0.61	0.31	0.21	2.04	0.81	354	13	0.58
A2C	*0.9*	2.30	0.25	Penetrate	0.90	0.17	0.25	1.99	1.10	328	13	0.54
A3C	*0.9*	2.14	0.25	Penetrate	0.90	0.22	0.41	1.77	1.33	411	8	0.45
C1C	*1.6*	0.20	0.27	Penetrate	1.40	0.42	0.27	3.63	0.69	360	14	0.81
C2C	*1.6*	4.07	0.29	Penetrate	1.60	0.58	0.29	1.88	0.42	457	18	0.61
C3C	*1.6*	1.32	Penetrate	Penetrate	1.60	0.00	0.49	3.96	3.65	390	13	0.44
D1C	*2*	1.53	1.48	Penetrate	1.53	0.19	1.31	2.34	1.62	346	9	0.26
D2C	*2*	6.02	0.32	Penetrate	1.52	0.43	0.42	2.81	1.60	431	19	0.65
E1C	*2.5*	5.73	0.23	Penetrate	0.89	0.55	0.23	1.90	0.97	487	25	0.42
E2C	*2.5*	3.87	0.32	Penetrate	1.41	0.64	0.40	2.73	1.47	509	22	0.76
E3C	*2.5*	10.61	0.23	Penetrate	0.71	0.66	0.19	1.55	0.75	459	21	0.30
F1C	*3*	0.03	0.61	1.30	1.01	0.56	0.42	0.70	0.56	550	25	0.20
F2C	*3*	0.31	0.43	1.10	0.80	0.22	0.28	2.06	0.46	559	27	0.68
F3C	*3*	3.20	0.25	1.67	1.56	0.50	0.45	4.25	2.56	487	13	1.27
G1C	*4*	6.35	0.25	1.65	1.46	0.35	0.33	2.74	2.05	577	35	0.55
G2C	*4*	4.22	0.51	1.44	1.27	0.23	0.52	1.40	1.13	605	44	0.20
G3C	*4*	3.80	0.28	1.77	1.35	0.23	0.57	1.85	1.21	595	40	0.27
H1C	*5*	0.95	0.03	1.75	1.49	0.63	0.22	3.00	0.79	595	35	1.32
H2C	*5*	0.88	0.55	1.90	0.97	0.48	0.27	2.76	0.62	561	33	0.92
H3C	*5*	1.58	0.28	1.49	1.44	0.39	0.60	2.30	1.95	572	36	0.52
I1C	*6*	0.66	0.33	1.96	1.71	0.66	0.58	2.22	1.14	582	35	0.78
I2C	*6*	0.34	0.25	1.65	1.28	0.47	0.53	1.64	0.73	598	46	0.35

I3C	*6*	0.54	0.66	1.50	1.29	0.44	1.37	2.35	1.89	588	40	0.49

As shown in Figure 6-3 Tensile test were conducted on a JIS B 7721 Universal test machine at University of Tasmania. The specimens were gripped in threaded connectors, aligned using pins and clevises, and loaded by crosshead displacement at a rate of 0.5mm/minute. Force-displacement output was continuously recorded to each specimen until failures. Strain gauges were not applied as pits act as local stress/strain raisers causing inaccurate readings. For unpitted specimen extensometer were used to record the stress and strain. Eighteen specimens (triplicated) with different thickness and different corrosion degradation levels are used to determine the effects of pitting corrosion degradation on the mechanical properties. A single undamaged specimen for each thickness was tested to establish a control baseline. The average reported intact specimen has a minimum ultimate tensile strength of 515 MPa and the minimum yield strength of 205 MPa with a total uniform elongation is >40% with the Young's modulus of 193-200GPa [289]. It is assumed that if the specimens are intact, without corrosion, the failure will occur along the neck of the specimens and the yield strength will be around 250~275 MPa and the Young modulus is 190~200 GPa .

Figure 6-3. Experimental tensile test layout and ruptured pitted specimen

The load shortening curve were presented in the subsequent section. There was a problem of slippage at the jaws of tensile test machine at the test. The problem was

solved using a Toe compensation technique as outline in [290]. In a typical load shortening curve, there is a toe region, which does not represent a property of the material. It is an artifact caused by a take-up of slack, and alignment or seating of the specimen. In order to obtain correct values of such parameters as modulus, strain, and yield point, this artifact must be compensated for to give the corrected zero point on the strain or extension axis.

6.4 Numerical Methodology

The numerical investigation was performed using the Finite Element method [291] applied through the general purposed finite element package ANSYS Mechanical relese16. The analyses included both material and geometrical nonlinearities and were conducted using ANSYS 17 in windows 7 64-bit operating system. High Performance Computing (HPC) was utilized with Shared-Memory Parallel (SMP) with 4 processors. The ANSYS parametric design language (APDL) was used to generate, solve and post-process the models. This particular modelling approach was chosen to allow for fast modification to the size and distribution of the pits on the corroded specimens without redrawing and meshing the model manually.

The next step in establishing the FEA model was to assign boundary and load conditions. Typical tensile testing involves a fixed support at one end of the tensile test specimen and a force at the other. The analytic model of the undamaged sample with the boundary conditions simulated to uniaxial tensile test is shown in Figure 6-4. As shown in Figure 6-4, the test specimen is assigned to obtain the given property onto the numerical model. The test specimens were provided with its loads, using fixed end condition on one side and displacement was applied at the other end. The displacement, which acted on the opposite face to the fixed support, was stepped in increments. As shown in Figure 4 the force and the displacement were applied on the upper and bottom surface of the specimen end edge. Which is a practical representation of uniaxial tensile test. Finally, selections on output were made which would dictate which data was recorded throughout the FEA. Since we had provided the input force, the main information we were interested in was the force on the gauge length section of the specimen. To find this, deformation probes were placed along a line on either end of the narrow section.

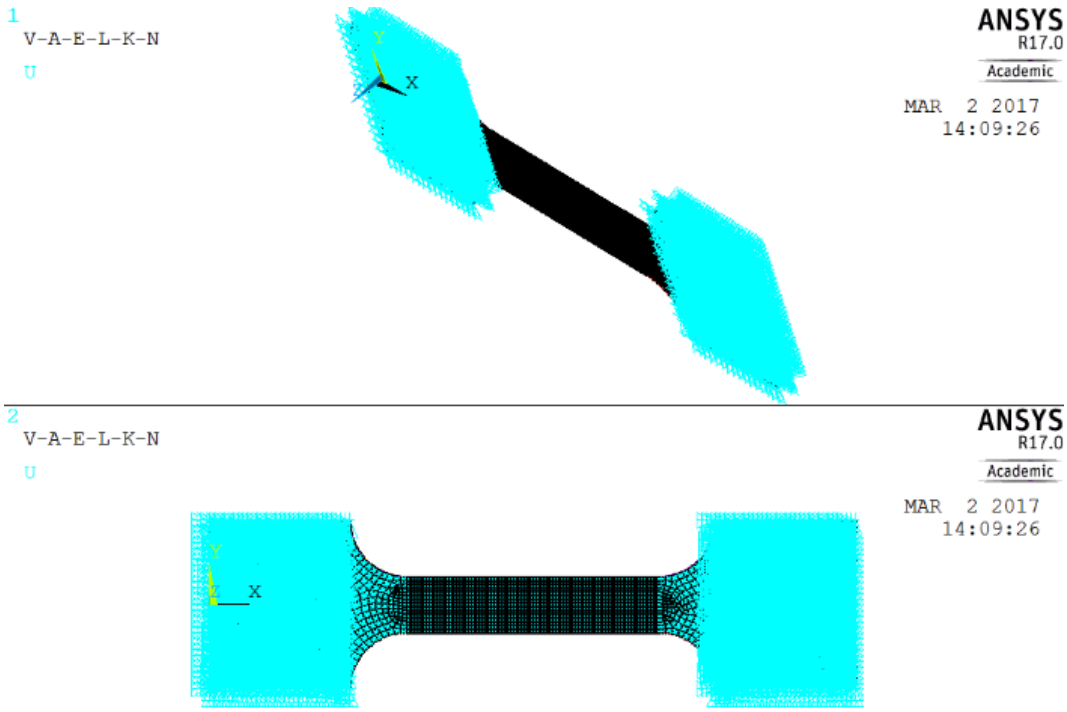

Figure 6-4. Development of intact model and boundary condition to replicate uniaxial tensile test of specimen

In order to correctly represent the ultimate strength behaviour of the corroded and uncorroded specimens it is necessary to select an appropriate constitutive model of 304 stainless steel. A constitutive model represents the mathematical relationship between stress and strain; For ultimate strength finite element simulations of ductile materials the constitutive model must be able to represent the material non-linearities that occur once the yield point is reached. Several non-linear constitutive models are available in ANSYS.

Nonlinear material behaviour is entered into Ansys by means of entering stress and strain points into a table in the pre-processing stage of modelling. Ansys 15 will accept up to 20 stress-strain points, though it is common practice to use simplified material models to reduce computation time. Un-simplified material models are referred to as 'multi-nonlinear,' while there are three commonly used simplified models. The simplest of these being 'elastic perfectly plastic,' requiring only the material's young's modulus

and a single data point corresponding to the material yield strength. This model assumes perfectly plastic behaviour past the yield point. A 'Bi-linear' material model also consider linear elastic behaviour until the yield point, but it includes strain hardening past yield define using a tangent modulus E_T normally defined as E/200. In this investigation, and in order to obtain a better representation of the non-linear material behaviour, a Multilinear Isotropic (MISO) model was chosen. A MISO model can accept up to 20 stress-strain points, though it is common practice to use simplified material models to reduce computation time. The stress strain data for 304L at room temperature was adopted from a report published by the Idaho National Laboratory [271, 292, 293]. The data for Young's modulus, yield strength, ultimate tensile strength and Poisson's ratio as seen in Table 6-3 were included.

Table 6-3. Assigned mechanical properties of 304 stainless steel [292]

Modulus of Elasticity, E (GPa)	200
Yield Strength, $\sigma_{Yield}[MPa]$	270
Ultimate Tensile Strength, σ_{UTS} $[MPa]$	515
Poisson Ratio, v	0.3

Figure 6-5 shows the True stress strain data adopted from [293]. They have conducted a series of quasi-static tensile test for 304L and 316L stainless steel at different temperature to develop a continuous engineering stress-strain curve with larger strain region.

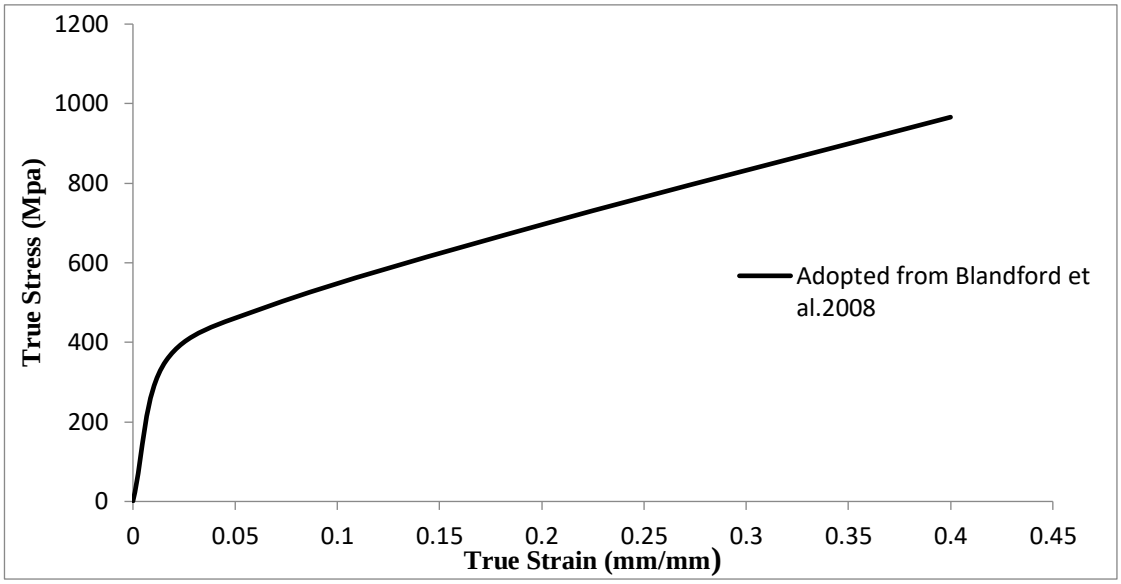

Figure 6-5. True stress strain measurements of 304 Stainless steel adopted from the Idaho National Laboratory [293].

Blandford, Morton, Snow and Rahl [292], [293] reported that, at room temperature (RT), the yield strength of the 304L test specimens varied from 260 to 305 Mpa and the ultimate strength varied from 659 to 670 Mpa. Similarly, the engineering total strain, or engineering strain at fracture, varied from 71% to 82% and measured reduction in area was quite high (ranging from 76% to 89%). They conclude that this variation shows good ductility qualities over the temperature range. Several published articles on numerical modelling of 304L [271, 293-296] have adopted [292, 293] stress strain data in their numerical studies.

Meshing plays a vital role in discretization technique; therefore the quality and type of meshing was chosen based on the precision of the result and to achieve solution faster. To improve the mesh quality around the pits each pit site is made up of 8 volumes which are individually map meshed using rotational volume sweeping. As shown in Figure 6-6 a region of refined mesh circulating the pits outer circumference was also map meshed to further refine the model. The remaining centre area of the tensile specimen was free meshed and served as a transition region to the base of fillets, which were again, mapped meshed using volume sweeping.

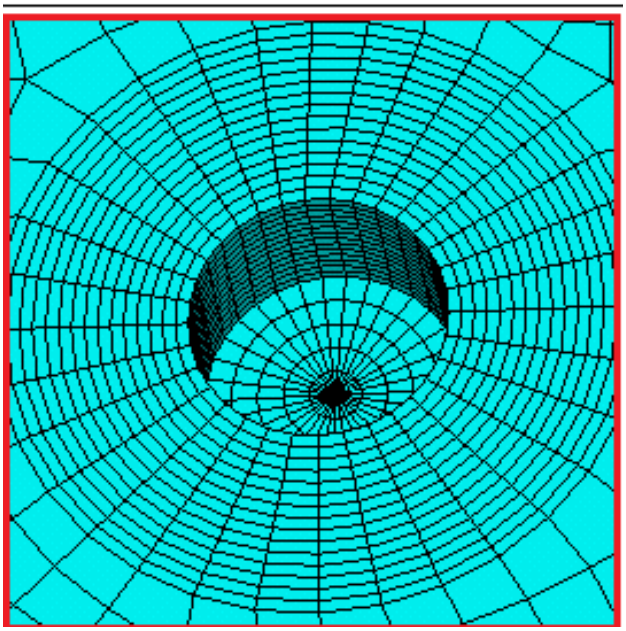

Figure 6-6. Refined mesh around the cylindrical pit side.

Three elements of the ANSYS library, namely SOLID185, SOLID 186 and SOLSH190, were found suitable to model the non-linear problem in hand, making it necessary to conduct a series of tests to ascertain which element type gave the most accurate result. SOLID185 is linear element with three translational degrees of freedom at each of its 8 nodes, whilst SOLID 186 is a high-order 20 node element with also three translational degrees of freedom per node. SOLSH190 is used for simulating shell structures with a wide range of thickness (from thin to moderately thick) and possesses a continuum solid element topology and features eight-node connectivity with three degrees of freedom at each node: translations in the nodal x, y, and z directions.

An undamaged 6mm thick sample in uniaxial tension was simulated to compare the performance of the aforementioned elements. The numerical force displacement plot was compared to experimental load displacement curve. As illustrated in Figure 6-7, minimal difference was observed using the three elements. SOLSH190 was discarded as the element is not capable of accurately modelling the topology of the pits. According to ANSYS [297], due to its mid side nodes, SOLID186 can better represent irregular shapes and was therefore selected over SOLID185.

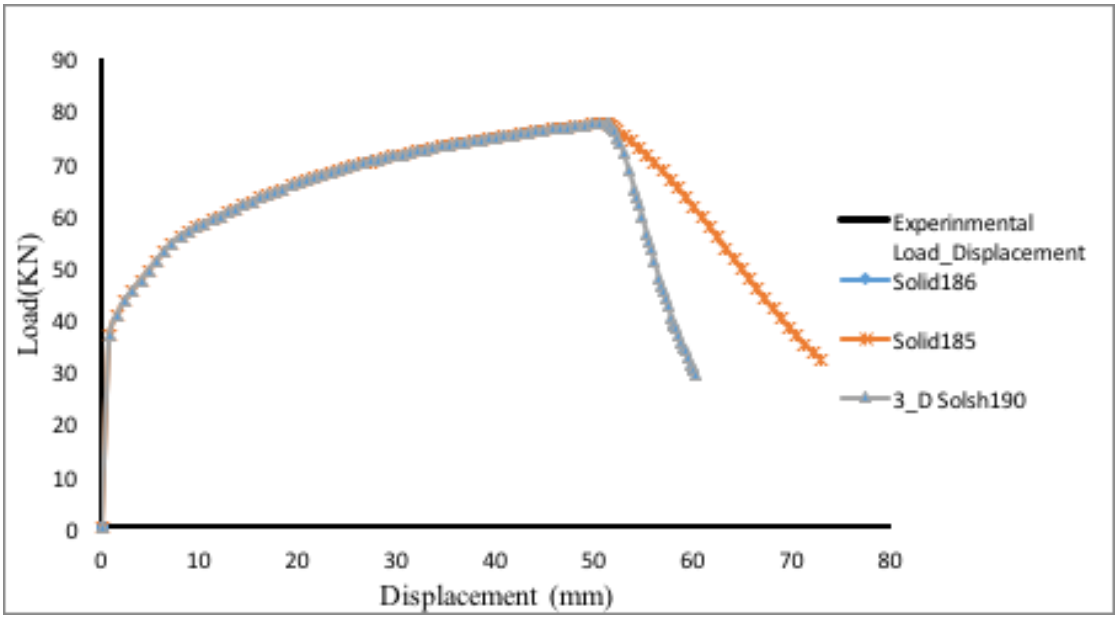

Figure 6-7. Comparisons of experimental and FE simulated load-displacement curves for 6mm undamaged specimen using different element types.

The crucial steps in the numerical simulation process involved defining the most appropriate pit topology idealization in order to enable an accurate representation of the average physical flaw. Based on the microscopic examination, most of the pits were observed to be of cylindrical shape. Figure 6-8 represents the pit characteristics examined using scanning electron microscopy (SEM). Modelling of a pit as a cylinder has advantages in its simplicity. We do expect, however, the shape of a pit to vary from that depicted in Figure 6-8 all the way to a more conical pit or semi-spherical shape, depending on material, grain morphology and corrosion conditions. The simple cylindrical representation is valuable, and represents an average pit shape in stainless steel specimen so the cylindrical pit was used for the modelling purposes.

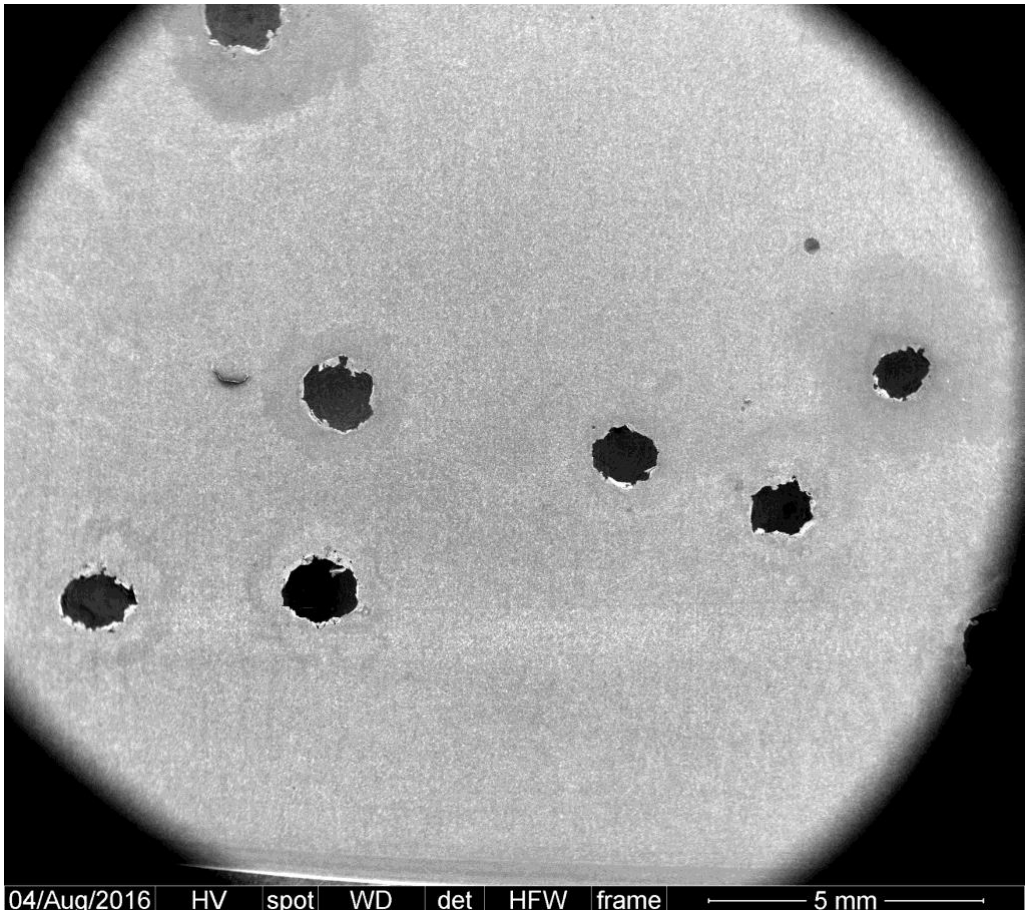

Figure 6-8. SEM image of pit morphology and pit distributions at the surface of the tested specimen

The pitted specimen was modelled using APDL script considering number of pits, individual pit depth, radius and location to be modified by simply changing the numbers in an array. The pits were generated by revolving separately generated areas, once the pits were all created, the rest of the solid model was created by means of extruding areas, before all the volumes were glued. This technique meant the sample was pre-divided up into several regions which later allowed the use of map meshing and also helped with mesh refinement. Figure 6-9 illustrates the duplication of Figure 6-8 considering the pit dimension and its location along the specimen. The mesh refinement must satisfy the need for a fine mesh to give an accurate stress distribution in a reasonable analysis time. The optimal solution is to use a finer mesh in areas of high stress: in the cylindrical hole of the pitting corrosion and in the supports regions as illustrated in Figure 6-9.

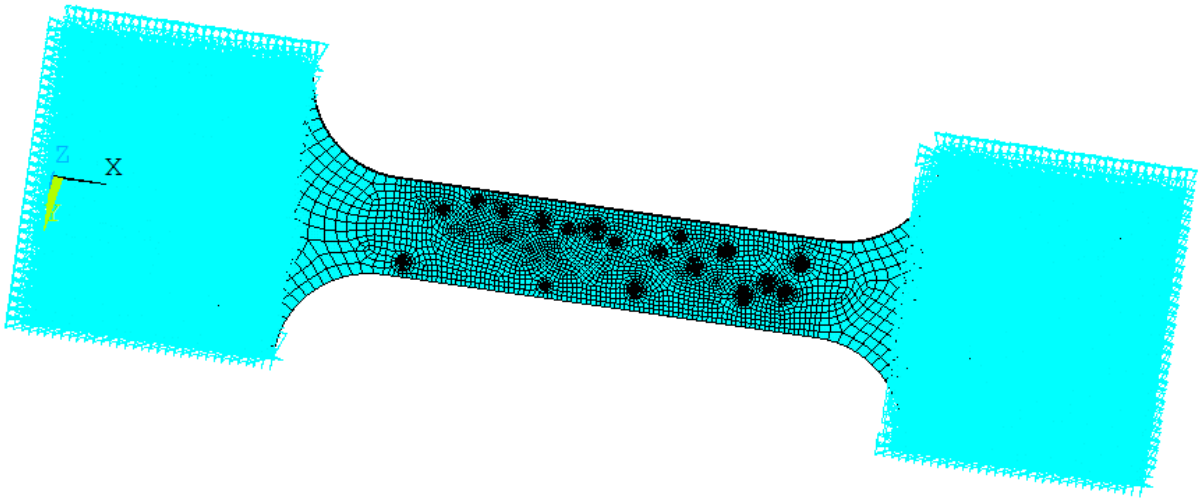

Figure 6-9. Numerical modelling of the corroded specimen with cylindrical pit

To improve the mesh quality around the pits each pit site is made up of 8 volumes which are individually map meshed using rotational volume sweeping. A region of refined mesh circulating the pits outer circumference was also map meshed to further refine the model. The remaining centre area of the tensile specimen was free meshed and served as a transition region to the base of fillets, which were again, mapped meshed using volume sweeping.

A convergence study was performed to select the most appropriate mesh density of the base specimen. Figure 6-10 shows the meshed tensile specimen with $0.5mm^3$ elements in the centre and transition regions as well as the refined mesh around the pit site will provide satisfactory result in the optimal simulation time.

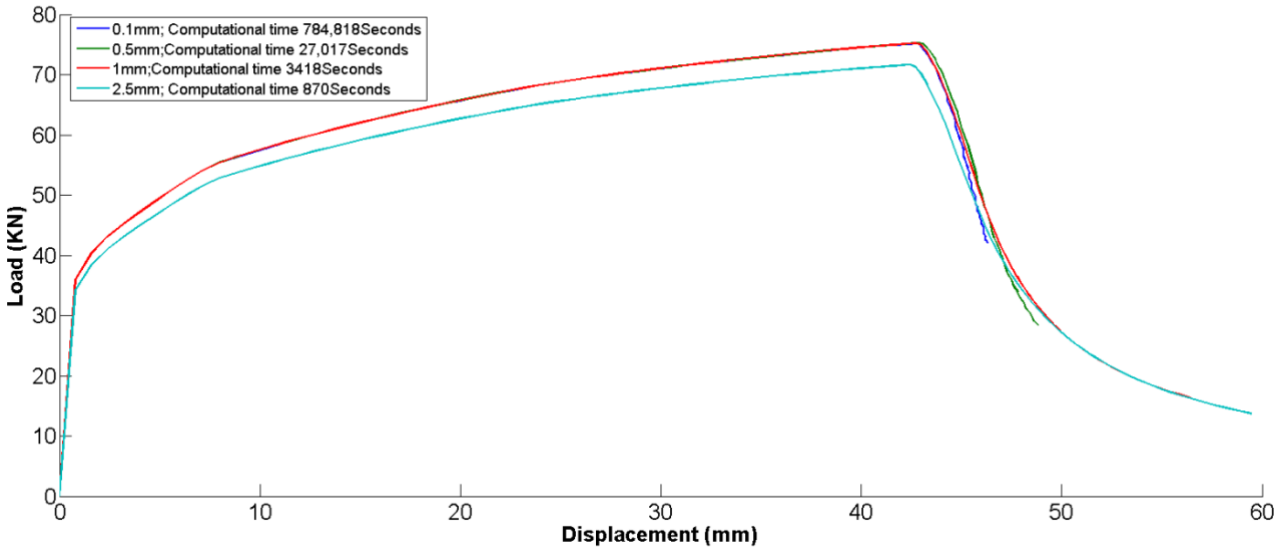

Figure 6-10. Results from convergence study obtained based on the simulation time

6.5 Numerical result and Discussion

In total 24 tests were conducted on corroded specimen which was made of 3 sample from each thickness. The result presented below shows comparison of each thickness with corroded and uncorroded specimen. A comparison of the experimental and numerical load-displacement relationships for the validation models is given in Figure 6-11-Figure 6-18. Figure 11-Figure 18 shows the resulting load-displacement curve for undamaged specimen and corrosion pitted specimen for thicknesses of: 6mm, 5mm, 4mm, 3mm, 2.5mm, 2mm, 1.6mm and 0.9mm respectively. It can be simply realised that the FEM results are in relatively good agreement with the test results. As expected the results show that in all cases the ultimate strength of the pitted specimens is lower than that of the undamaged specimens. The observed behaviour are be attributed to the localized stress effects generated around the pits which lead to early failure of the material. Such localized failure manifests in the early and gradual decrease in the stiffness of the pitted material, as shown in Figure 6-11-Figure 6-18. A decrease in total elongation of the pitted compared to undamaged specimens is also evident. Since the corrosion attack was selective and limited to the surface only, the apparent loss for elongation at fracture is attributed to the same effect of localized stress at the pits, rather than degradation of ductility in the bulk section of the specimen.

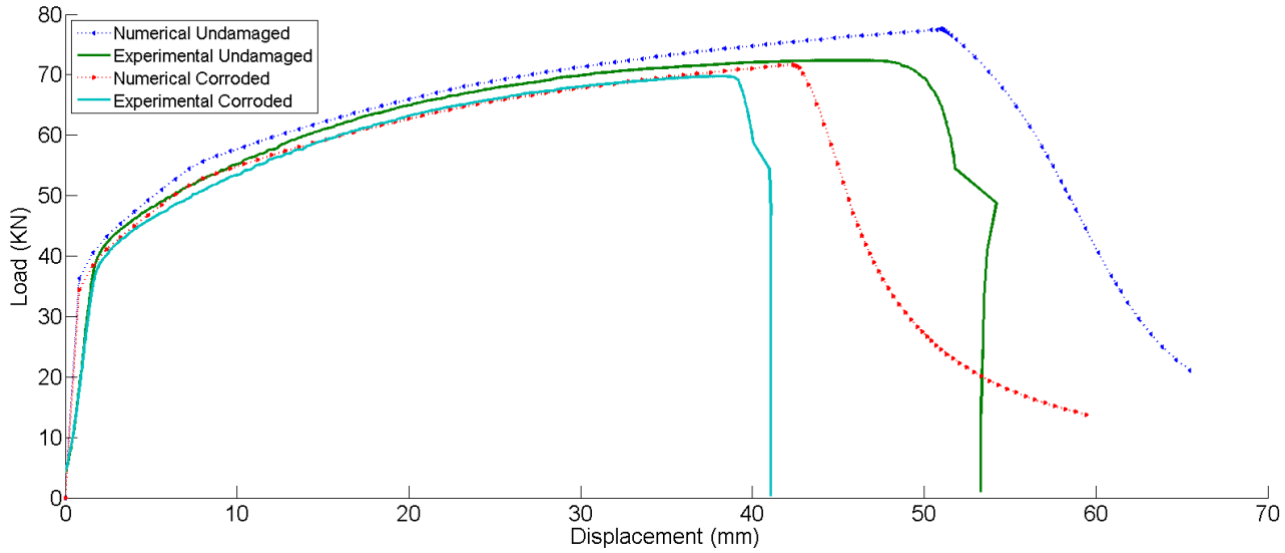

Figure 6-11. Comparisons of experimental and numerical of load-displacement relationships for 6mm (I1C) thick specimen

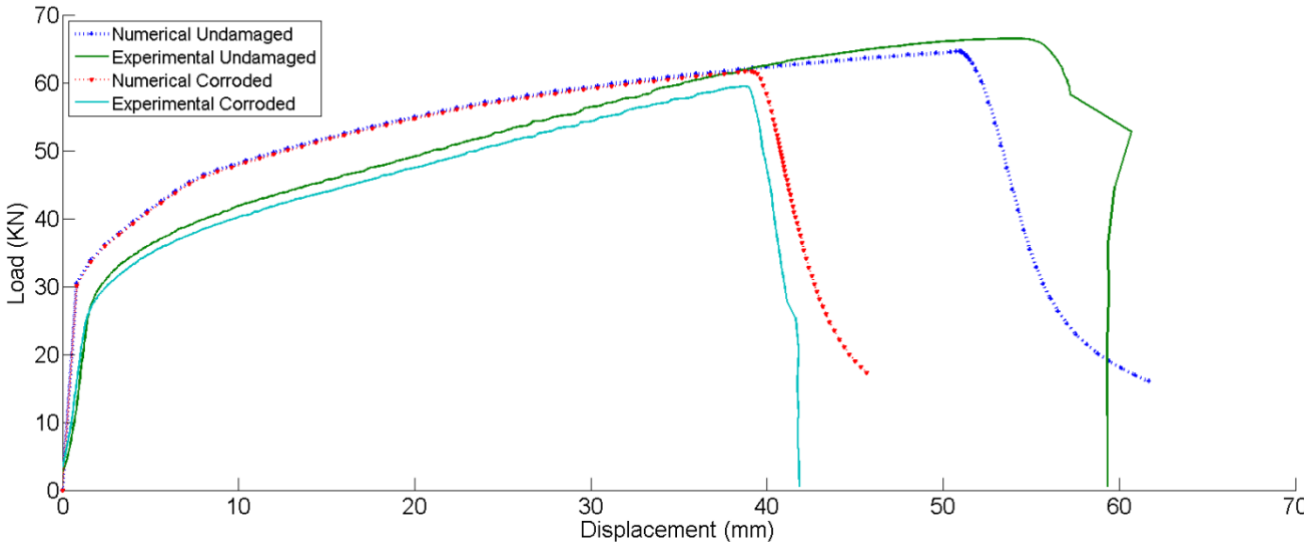

Figure 6-12. Comparisons of experimental and numerical of load-displacement relationships for 5mm (H1C) thick specimen

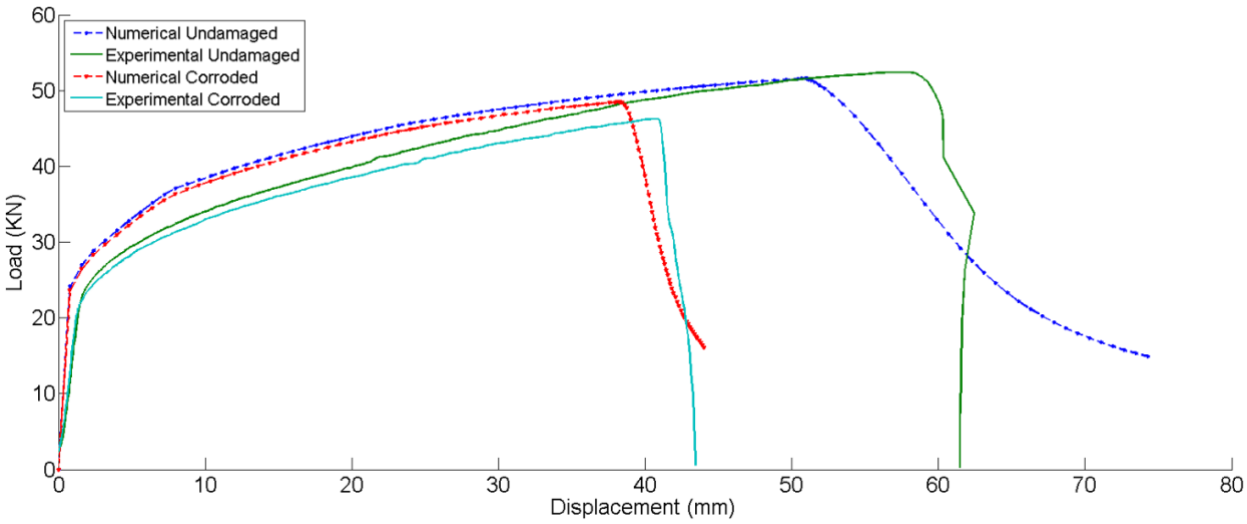

Figure 6-13. Comparisons of experimental and numerical of load-displacement relationships for 4mm (G1C) thick specimen

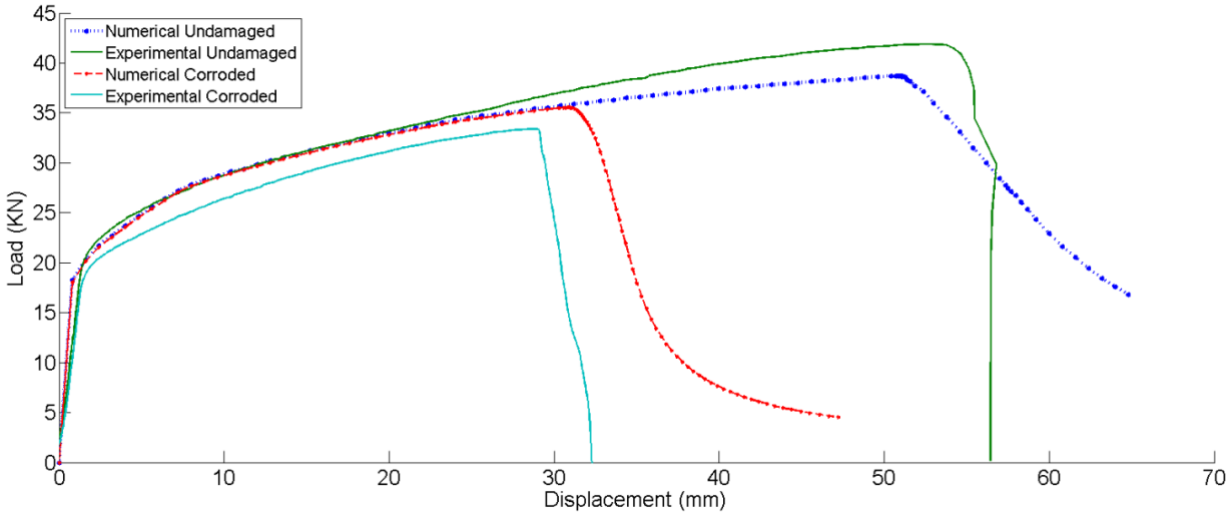

Figure 6-14. Comparisons of experimental and numerical of load-displacement relationships for 3mm (F2C) thick specimen

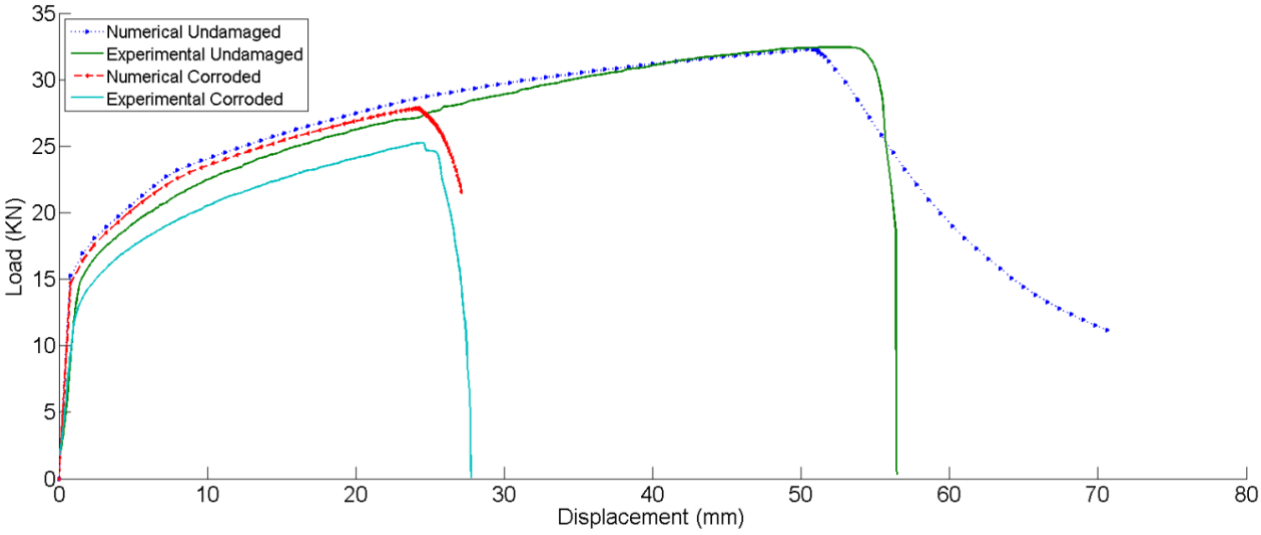

Figure 6-15. Comparisons of experimental and numerical of load-displacement relationships for 2.5mm (E2C) thick specimen

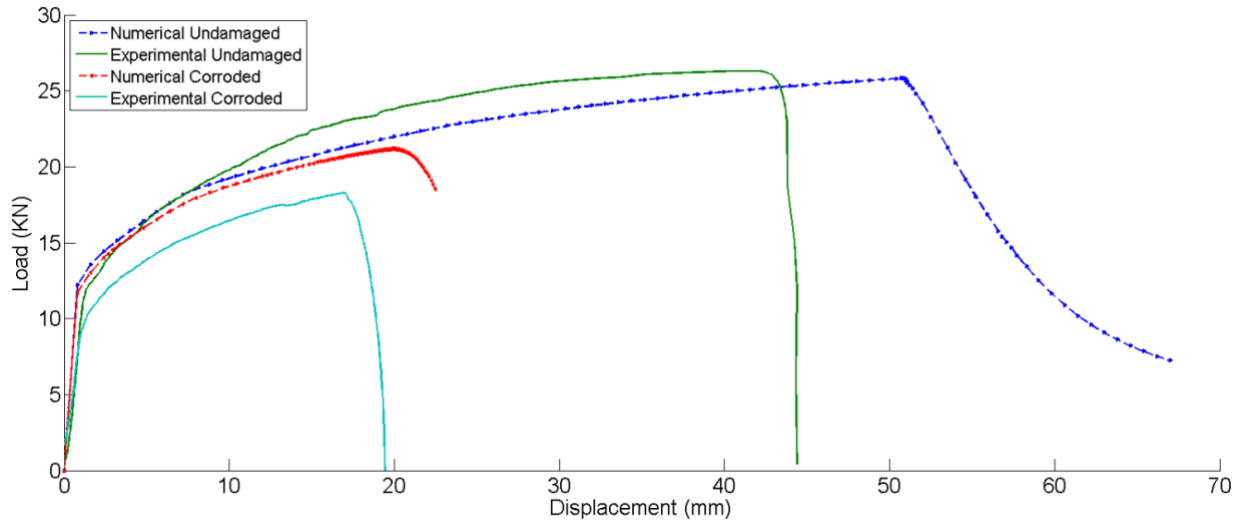

Figure 6-16. Comparisons of experimental and numerical of load-displacement relationships for 2mm (D1C) thick specimen

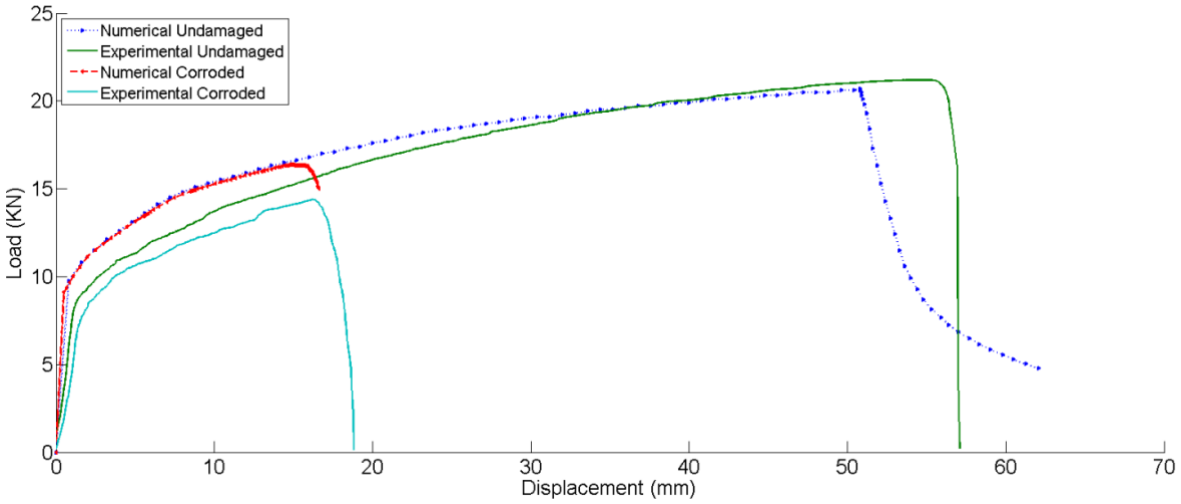

Figure 6-17. Comparisons of experimental and numerical of load-displacement relationships for 1.6mm (C2C) thick specimen

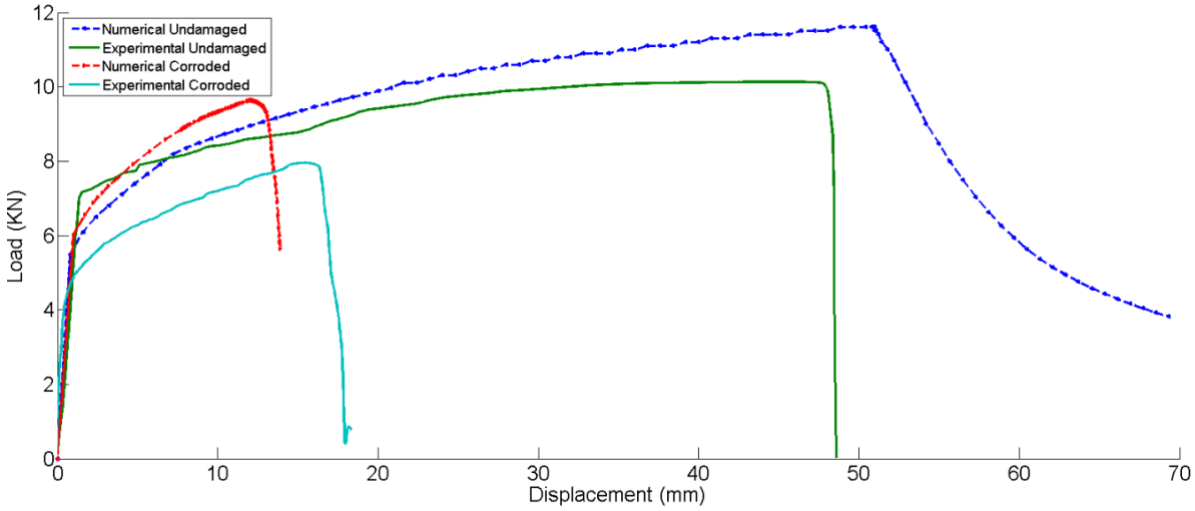

Figure 6-18. Comparisons of experimental and numerical of load-displacement relationships for 0.9mm (A1C) thick specimen

Figure 6-11-Figure 6-18 also compares the numerical results with the experimental result for both undamaged and pitted sample for each thickness. It is notable that numerical results show similar trends to the tested experimental results and capture non-linear load-displacement response of the specimens up to peak load. It indicates that the finite element analyses are capable of predicting the experimental behaviour of the specimens when these are subjected to a uniaxial tensile load.

Figure 6-19 shows the comparisons of the experimentally and numerically obtained ultimate strength values for all pitted samples. It is notable that the ultimate strength for pitted samples is over predicted using numerical analysis. This might be the effect of the pitting corrosion at the edges of the specimen which was not considered in numerical modelling. The unaccounted loss of specimen thickness due the accelerated corrosion process may have also contributed to over prediction of ultimate strength in numerical analysis.

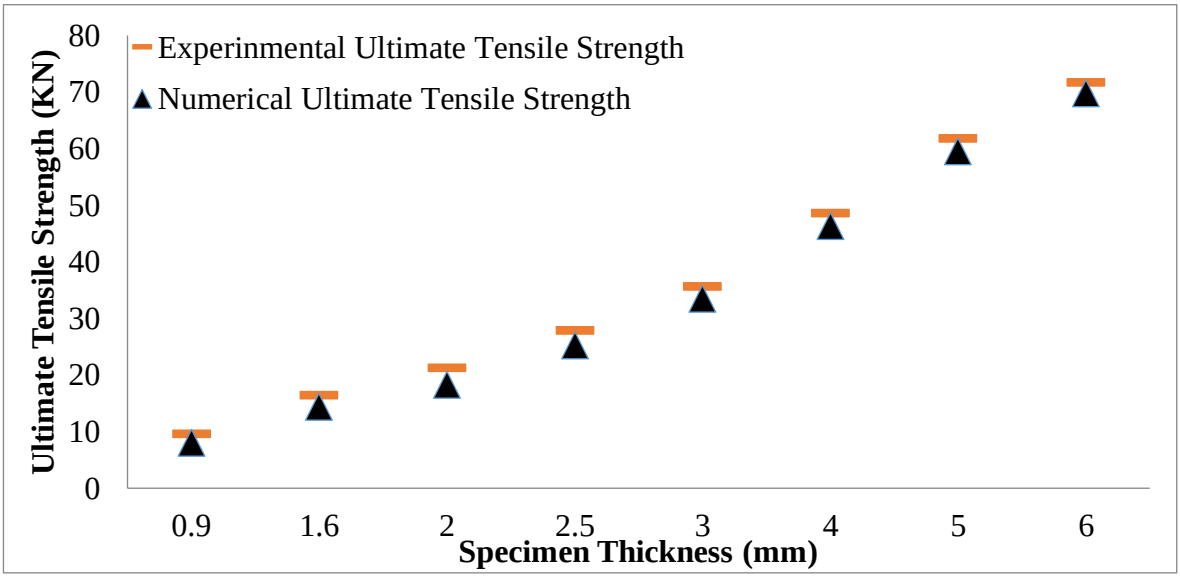

Figure 6-19. Comparison of ultimate tensile strength obtained experimentally and numerically for pitted specimen

Figure 6-20 shows the comparisons of percentage deviation on ultimate tensile strength obtained experimentally and numerically for pitted specimen. It can be appreciated that numerically obtained results for the thinner specimens present a higher deviation on ultimate strength predictions than the thicker ones. The 0.9mm thick specimen has the largest deviation (19.1%)whilst the 6mm thick specimen has only a 2.7% deviation from experimental results. This might be due to more pits on thinner sample and most of the pits were penetrated through the entire sample (refer Table 2). Unfortunately, the fully penetrated pits were not successfully modelled using FEA because of mesh limitation and volume sweeping. Hence, the fully penetrated pit in FE were considered as 10% less then specimen thickness.

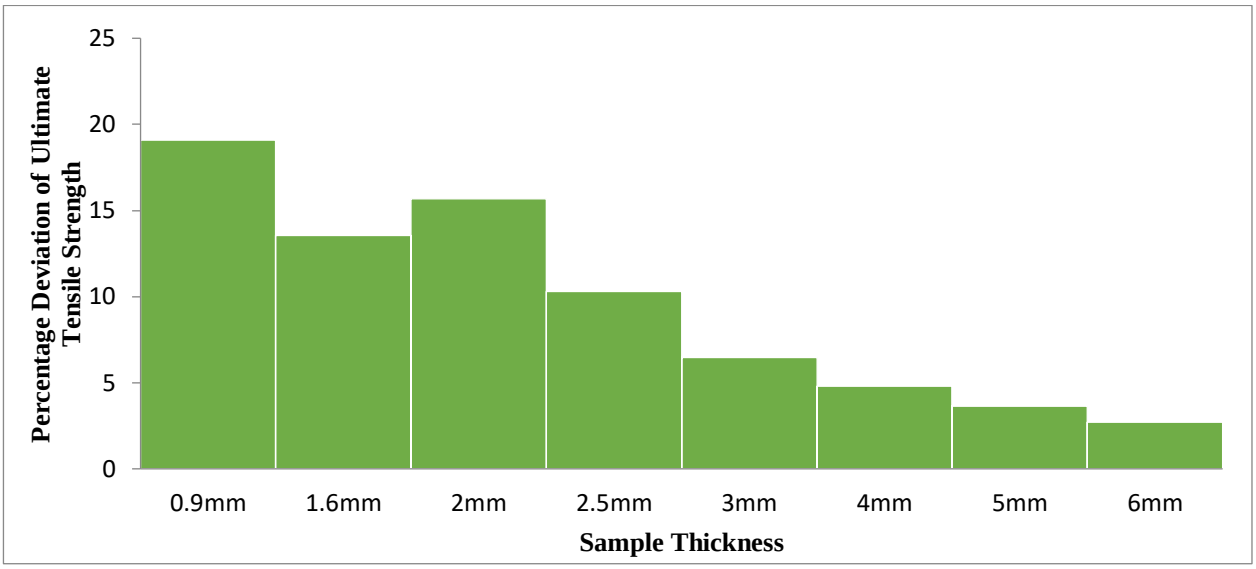

Figure 6-20. Comparisons of percentage deviation on ultimate tensile strength obtained experimentally and numerically for pitted specimen

Figure 6-21 shows stress distribution (von Misses) for pitted specimen. As illustrated in Figure 6-21 the lowest stress is always at edge of pit opening on the surface. The maximum stress is always found on the tip of deepest part of pit. It is shown that the maximum stress is on a deepest notch of the pit although the pit has other notches that could potentially act as stress raiser. These notches are also potential sites of accumulation of corrosive agent. Additionally, it can be seen from Figure 6-21 that the notches formed as a preferential site for the pit growth. This means the notches were anodic site. When loads can influence corrosion inside pit such as reported in [298], these pit shapes may influence the rate of corrosion on particular sites of pit and assist in forming deeper pits.

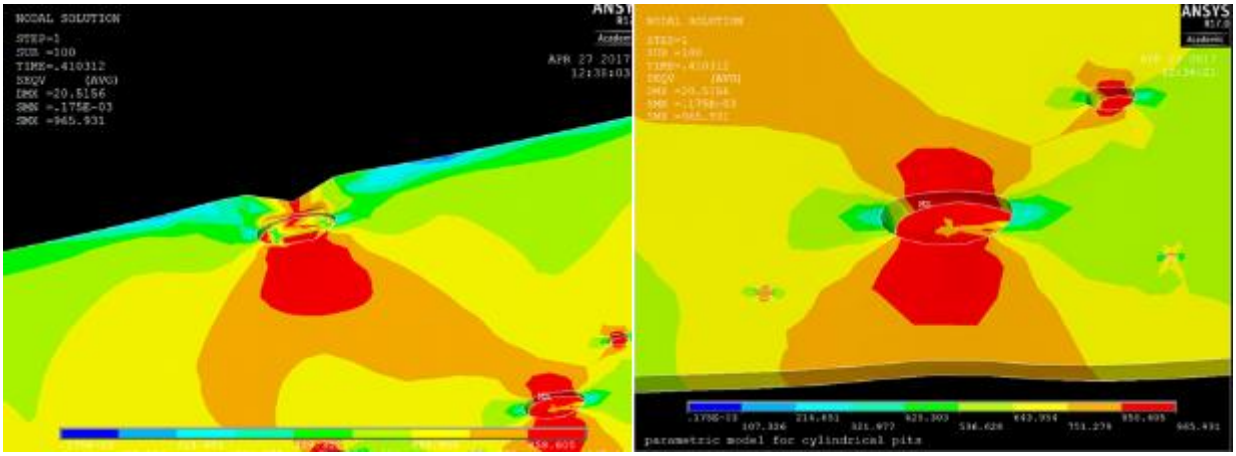

Figure 6-22. Location of minimum stress is always at pit opening

Figure 6-23 illustrates the comparison of ultimate tensile strength of the 6mm thick specimen with varying level of DOP 1%, 5% 10% and 25%. It is evident from Figure 6-23 that the specimen tensile strength is significantly decreased as the level of DOP increases. This trend was consistent throughout the specimen with different thickness. Similar findings were reported by [263, 272, 273, 275-278]. It can be concluded that the ultimate strength of a pitted specimen under uniaxial tensile load is governed by the DOP.

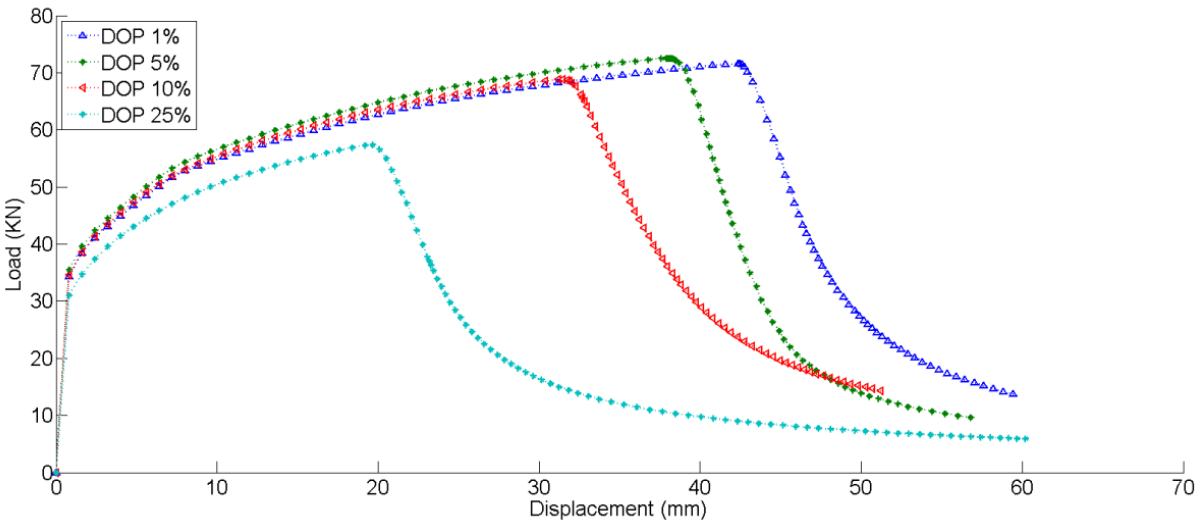

Figure 6-23. Load Vs Displacement for a 6mm thick steel specimen with varying level of DOP

Figure 6-24 shows deflected shapes of specimen with different pit corrosion intensities immediately after the ultimate strength is reached; (a) with DOP 0.66; (b) DOP 10.6%. It is interesting to note that the maximum deflection of a specimen with larger DOP is

small at the ultimate limit stress compared to that with smaller DOP. This is due to the fact that the larger localized plasticity develops earlier in the plate with greater pit corrosion intensity. The presence of pitting also meant that the cross section of the test volume was no longer uniform. This meant that there would be discrepancies in elongation across the specimen's depth. The deformation probe line provided something of a solution to this problem by considering the average deformation across the line.

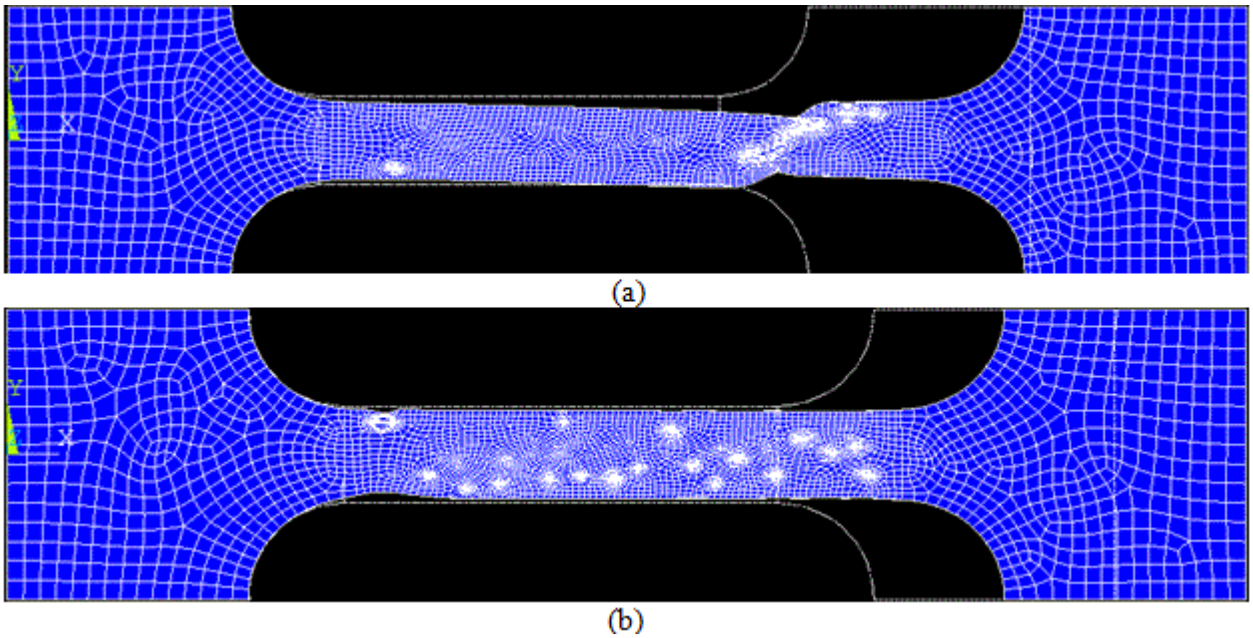

Figure 6-24. Deflected shapes of a pitted specimen under uniaxial tensile load; (a) DOP 0.66%; (b) DOP 10.6%

6.6 Conclusion

The work presented here determines the effect of pitting corrosion deterioration on steel specimens of different thickness subjected to tensile loading. Accelerated pitting corrosion tests were conducted for specimen with various thicknesses according to aa modified ASTM G48-48 procedure. Uniaxial tensile tests were performed on undamaged and pitted specimens, so as to derive their strength characteristics. A series of ANSYS large deflection finite element analyses for a pitted and undamaged specimen under uniaxial tensile load were carried out, varying the pit corrosion intensities and the specimen thickness. Some available tested models influenced by pitting corrosion are numerically simulated and validated with experimentally results. The results show good capability of the software to establish a framework for establishing the ultimate strength of the pitted specimen. It is evident that the ultimate

strength of a plate element can be significantly decreased due to pit corrosion. It was found that numerically obtained results for the thinner specimens present a higher deviation on ultimate strength predictions than the thicker ones. The ultimate strength of a specimen with pit corrosion and under tensile load is governed by the DOP (degree of pit corrosion intensity). In contrast, it has been realized that the ultimate strength of a pitted specimen is governed by the DOP and its thickness. However the strength assessment may influence as changes of materials properties and aging effect is considered. The results presented in this study shows that the numerical modelling for strength prediction for pitting structures is valuable techniques and will be very useful for damage tolerant design of steel plated structures with pit corrosion.

6.7 Acknowledgements

Authors thankfully acknowledge support provided by National Centre for Maritime Engineering and Hydrodynamic (NCMEH) and Australian Maritime College (AMC). The grant received from University of Tasmania (2016) under the Research Enhancement Grants Scheme (REGS) is highly appreciated.

7 Conclusions

Pitting corrosion is regarded as one of the predominant causes of structural failure and its effects on offshore structures are reported to be catastrophic. Hence, significant attention should be given to predicting the occurrence of pitting corrosion in offshore structures and the adequate measures which should be taken to prevent and control the consequences. This project aimed at improving the safety and reliability of offshore structures susceptible to pitting corrosion. The detailed conclusions from the present work are as follows:

1) From the wide and extensive literature review on offshore safety and from the historical offshore accidents it was surveyed that pitting corrosion is one of the prominent concerns in offshore sectors; hence it is important to consider it in research. It is anticipated that the output of this study will be beneficial to all parties concerned and is expected that it will contribute to knowledge enhancement in the academic world and industry.
2) There are many studies conducted on the pitting mechanism, field-testing and laboratory testing in the field of pitting corrosion; however, there is no development of detailed studies for failures in offshore structures due to pitting characteristics. One critical requirement is the investigation of how pitting characteristics, such as rate, depth, density and distance, can cause a structural failure. Previously, empirical and statistical degradation models were developed by either fitting field or laboratory data. However these models, even though useful for specific site or operating conditions, still carry high uncertainty.
3) A novel methodology for a risk-based maintenance strategy using BN is developed. This methodology is crucial to reduce the risk of failures and optimize the cost of maintenance including the cost of failure. Application of the developed methodology for the maintenance scheduling of an offshore oil and gas production platform demonstrated that preventive maintenance time can be altered for each components in the system.
4) Due to limited time and resources, the proposed work did not consider the pitting corrosion field test where the pitting process can be constantly measure until failure of the system. However, Laboratory-based pitting immersion tests

performed on 304 austenitic stainless steel specimens using ASTM G48 to study the pitting process and the effect of environmental factors which controls pitting process.

5) A Bayesian Network based methodology is proposed for predicting pitting corrosion depth of structural steel exposed to seawater in long-term anaerobic conditions. Emphasis is placed on modelling the pitting depth by combining the multi-phase phenomenological and empirical models. The proposed model is critically important for the management of older offshore structures as well as for the design of new infrastructure to ensure safety and serviceable long life.
6) Finally, series of ANSYS large deflection finite element analyses for a pitted and undamaged specimen under uniaxial tensile load were carried out, varying the pit corrosion intensities and the specimen thickness. Some available tested models influenced by pitting corrosion are numerically simulated and validated with experimentally results.
7) The further improvement of this work could be analysing effect of pitting corrosion on systems such as the structural elements of marine and offshore structures, Static process equipment and Rotating machinery.
8) The influence of mechanical loads on pit growth kinetics as well as a criterion of transformation of pit into fatigue crack is also considered as a further improvement of this work.

8 Appendices

Appendix A-Pitting Corrosion Depth Data Adopted from ASTM (Phull et al., 1997)

Ocean City (New jersey)			**Wrightsville beach (North Carolina)**			**Key west, Florida**		
Exposure Period (years)	***Corrosion rate (µm/year)***	***Corrosion loss (pit depth) (mm)***	***Exposure Period (years)***	***Corrosion rate (µm /year)***	***Corrosion loss (pit depth) (mm)***	***Exposure Period (years)***	***Corrosion rate (µm /year)***	***Corrosion loss (pit depth) (mm)***
0.5	192	0.36	**0.5**	161	0.31	**0.5**	136	0.16
0.5	213	0.33	**0.5**	165	0.5	**0.5**	146	0.36
1	209	1	**1**	123	0.68	**1**	107	0.81
1	322	1.31	**1**	213	1.28	**1**	119	0.39
3	100	1.57	**3**	87	2.44	**3**	124	2.17
3	107	1.87	**3**	214	4.44	**3**	84	1.19
5	92	2.24	**5**	68	1.39	**5**	84	1.23
5	100	1.46	**5**	224	4.11	**5**	75	1.40
Freeport Texas			**Port Huenema, California**			**Talara, Peru**		
Exposure Period (years)	***Corrosion rate (µm /year)***	***Corrosion loss (pit depth) (mm)***	***Exposure Period (years)***	***Corrosion rate (µm /year)***	***Corrosion loss (pit depth) (mm)***	***Exposure Period (years)***	***Corrosion rate (µm /year)***	***Corrosion loss (pit depth) (mm)***
0.5	120	0.27	**0.5**	550	0.95	**0.5**	196	0.48
0.5	105	0.37	**0.5**	245	0.44	**0.5**	180	0.35
1	105	0.53	**2**	113	0.8	**1**	147	0.73
1	91	2.58	**2**	121	0.83	**1**	137	0.84
3	99	2.77	**2.9**	125	3.5	**3**	129	3.4
3	137	6.07	**2.9**	173	1.88	**3**	126	2.52
5	135	6.07	**5**	207	2.12	**5**	131	2.98

5	86	2.59		**5**		**5**	136	2.59
KeAhole, Kona, Hawaii			**Innisfail, Queensland Australia**			**Sakata Harbour, Japan**		
Exposure Period (years)	***Corrosion rate (µm /year)***	***Corrosion loss (pit depth) (mm)***	***Exposure Period (years)***	***Corrosion rate (µm /year)***	***Corrosion loss (pit depth) (mm)***	***Exposure Period (years)***	***Corrosion rate (µm /year)***	***Corrosion loss (pit depth) (mm)***
0.5	240	0.84	**1**	207	3.63	**0.5**	86	0.18
0.5	235	0.44	**1**	233	2.23	**0.5**	89	0.27
1	165	0.73	**3**	174	1.62	**1**	168	0.22
1	536	6.07	**3**	185	1.59	**1**	171	0.27
3.2	204	2.11	**5**	162	2.2	**3.1**	68	1.32
3.2	79	1.27	**5**	146	1.59	**3.1**	62	1.21
5	56	1.09				**5**	94	1.98
5	97	1.41				**5**	68	2.61
Genoa, Italy			**Kyndby Isefjord, Denmark**			**Studsvik, Sewden**		
Exposure Period (years)	***Corrosion rate (µm /year)***	***Corrosion loss (pit depth) (mm)***	***Exposure Period (years)***	***Corrosion rate (µm /year)***	***Corrosion loss (pit depth) (mm)***	***Exposure Period (years)***	***Corrosion rate (µm /year)***	***Pit depth(mm)***
0.5	145	0.54	**0.5**	82	0.25	**0.5**	108	0.25
0.5	194	0.32	**0.5**	106	0.22	**0.5**	103	0.22
1	158	0.79	**1.5**	95	0.41	**1**	128	0.6
1	214	0.75	**1.5**	122	0.7	**1**	131	0.69
3	215	4.42	**3.1**	91	1.69	**3.2**	69	1
3	224	6.07	**3.1**	90	1.72	**3.2**	62	0.92
5	115	3.88	**5**	100	1	**5**	73	1.58
5	123	1.86	**5**	79	1.85	**5**	72	1.4
Bohus-Malmon, Sweden			**Isle of Wight, England**					
Exposure Period (years)	***Corrosion rate (µm /year)***	***Corrosion loss (pit depth) (mm))***	***Exposure Period (years)***	***Corrosion rate (µm /year)***	***Corrosion loss (pit depth) (mm)***			

0.5	103	0.18	**0.5**	226	0.36
0.5	95	0.21	**0.5**	156	0.31
1	86	0.35	**1**	148	0.44
1	94	0.43	**1**	355	1.06
3.1	99	2	**3.1**	84	1.07
3.1	119	1.83	**3.1**	104	1.42
5	101	1.88	**5**	87	1.19
5	79	2.25	**5**	79	1.58

9 Bibliography

[1] M. Schumacher, Seawater corrosion handbook, (1979).
[2] M.G. Stewart, A. Al-Harthy, Pitting corrosion and structural reliability of corroding RC structures: Experimental data and probabilistic analysis, *Reliability Engineering & System Safety*, **93** (2008) 373-382.
[3] W. Maureen, V.A.A. Lisa, V.W. Lorenzo, Corrosion-Related Accidents in Petroleum Refineries: Lessons learned from accidents in EU and OECD countries, Publications Office of the European Union, 2013.
[4] L.T. Popoola, A.S. Grema, G.K. Latinwo, B. Gutti, A.S. Balogun, Corrosion problems during oil and gas production and its mitigation, International Journal of Industrial Chemistry, 4 (2013) 35.
[5] R. Melchers, Pitting corrosion of mild steel in marine immersion environment-Part 2: Variability of maximum pit depth, *Corrosion*, **60** (2004) 937-944.
[6] R. Melchers, Statistical Characterization of pitting corrosion-part 1: data analysis, Corrosion, 61 (2005) 655-664.
[7] R. Melchers, Transient early and longer term influence of bacteria on marine corrosion of steel, Corrosion Engineering, Science and Technology, 45 (2010) 257-261.
[8] R. Melchers, R. Jeffrey, The critical involvement of anaerobic bacterial activity in modelling the corrosion behaviour of mild steel in marine environments, *Electrochimica Acta*, **54** (2008) 80-85.
[9] J. Velázquez, J. Van Der Weide, E. Hernández, H.H. Hernández, Statistical modelling of pitting corrosion: extrapolation of the maximum pit depth-growth, Int. J. Electrochem. Sci, 9 (2014) 4129-4143.
[10] R. Melchers, Corrosion wastage in aged structures, Condition assessment of aged structures, (2008).
[11] HSR;, Offshore hydrocarbon release statistics and analysis, in: H. HID statistics report 2002, Health and Safety Executive, UK, 2003. (Ed.), UK, 2002.
[12] F. Khan, R. Howard, Statistical approach to inspection planning and integrity assessment, Insight-Non-Destructive Testing and Condition Monitoring, 49 (2007) 26-36.
[13] H. Li, B. Brown, S. Nešić, Predicting Localized CO2 Corrosion in Carbon Steel Pipelines", Corrosion/2011, Paper, (2011).
[14] A.A.P. Sidharth, Effect of pitting corrosion on ultimate strength and buckling strength of plate-a review, Digest Journal of Nanomaterials and Biostructures, 4 (2009) 783-788.
[15] R. Melchers, Pitting corrosion of mild steel in marine immersion environment-Part 1: Maximum pit depth, Corrosion, 60 (2004) 824-836.
[16] M.G. Stewart, Mechanical behaviour of pitting corrosion of flexural and shear reinforcement and its effect on structural reliability of corroding RC beams, Structural safety, 31 (2009) 19-30.
[17] Z. Szklarska-Smialowska, *Pitting corrosion of metals*, National Association of Corrosion Engineers (NACE),1986, Houston, TX, 1986.
[18] G. Frankel, Pitting corrosion of metals a review of the critical factors, Journal of the Electrochemical Society, 145 (1998) 2186-2198.
[19] R. Abdel-Ghany, S. Saad-Eldeen, H. Leheta, The Effect of Pitting Corrosion on the Strength Capacity of Steel Offshore Structures, in: *ASME 2008 27th International*

Conference on Offshore Mechanics and Arctic Engineering, American Society of Mechanical Engineers, Estoril, Portugal, 2008, pp. 801-805.
[20] P.R. Roberge, Corrosion engineering: principles and practice, McGraw-Hill New York, 2008.
[21] N.T.S. Board, Columbia Gas Transmission Corporation Pipeline Rupture, in, 2014.
[22] T.H. Abood, The influence of various parameters on pitting corrosion of 316l and 202 stainless steel, in: *Department of Chemical Engineering of the University of Technology*, University of Technology(UOT), Iraq, Baghdad, 2008.
[23] R.E. Melchers, Pitting Corrosion in Marine Environments: A Review, Department of Civil Engineering and Surveying, University of Newcastle, 1994.
[24] R.E. Melchers, Experiments, science and intuition in the development of models for the corrosion of steel infrastructure| NOVA. The University of Newcastle's Digital Repository, (2009).
[25] S. Caines, F. Khan, J. Shirokoff, Analysis of pitting corrosion on steel under insulation in marine environments, *Journal of Loss Prevention in the Process Industries*, **26** (2013) 1466-1483.
[26] C.G. Soares, Y. Garbatov, A. Zayed, G. Wang, Influence of environmental factors on corrosion of ship structures in marine atmosphere, Corrosion science, 51 (2009) 2014-2026.
[27] A. Valor, F. Caleyo, L. Alfonso, D. Rivas, J. Hallen, Stochastic modeling of pitting corrosion: a new model for initiation and growth of multiple corrosion pits, Corrosion Science, 49 (2007) 559-579.
[28] A. Valor, F. Caleyo, D. Rivas, J. Hallen, Stochastic approach to pitting-corrosion-extreme modelling in low-carbon steel, Corrosion Science, 52 (2010) 910-915.
[29] I. Zamaletdinov, Pitting on passive metals, Protection of Metals, 43 (2007) 470-475.
[30] P.G.R. Zaya, Evaluation of Theiores for the Initial Stages of Pitting Corrosion, in: McMaster University, McMaster University, McMaster 1984.
[31] R. Roberge, Forms of Corrosion in Pictures, in: Welcome to Corrosion Doctors, Kingston Technical Software, Kingston, 2013.
[32] U. Evans, L. Bannister, S. Britton, The Velocity of Corrosion from the Electrochemical Standpoint, Proceedings of the Royal Society of London. Series A, 131 (1931) 355-375.
[33] V. Evans, The Corrosion And Oxidation Of Metals (Second Supplementary Volume), 1976.
[34] G. Thompson, R. Furneaux, G. Wood, J. Richardson, J. Goode, Nucleation and growth of porous anodic films on aluminium, (1978).
[35] R.E. Melchers, Corrosion uncertainty modelling for steel structures, Journal of Constructional Steel Research, 52 (1999) 3-19.
[36] G. Schiroky, A. Dam, A. Okeremi, C. Speed, Pitting and crevice corrosion of offshore stainless steel tubing, Oilonline, (2009).
[37] R.C. Alkire, K.P. Wong, The corrosion of single pits on stainless steel in acidic chloride solution, Corrosion science, 28 (1988) 411-421.
[38] J. Agar, T. Hoar, The influence of change of size in electrochemical systems, Discuss. Faraday Soc., 1 (1947) 158-162.
[39] R. Melchers, M. Ahammed, Nonlinear modelling of corrosion of steel in marine environments, Department of Civil Engineering and Surveying, University of Newcastle, NSW, Australia, 1994.

[40] H.-H. Strehblow, P. Marcus, Mechanisms of pitting corrosion, Corrosion mechanisms in theory and practice, (1995) 201-238.
[41] S.F. Wika, Pitting and Crevice Corrosion of Stainless Steel under Offshore Conditions, (2012).
[42] P. Pistorius, G. Burstein, Metastable pitting corrosion of stainless steel and the transition to stability, Philosophical Transactions of the Royal Society of London. Series A: Physical and Engineering Sciences, 341 (1992) 531-559.
[43] J. Galvele, Tafel's law in pitting corrosion and crevice corrosion susceptibility, Corrosion science, 47 (2005) 3053-3067.
[44] K.P. Wong, R.C. Alkire, Local chemistry and growth of single corrosion pits in aluminum, Journal of the Electrochemical Society, 137 (1990) 3010-3015.
[45] R. Angal, Principles and prevention of corrosion, Alpha Science International, 2010.
[46] G. Frankel, N. Sridhar, Understanding localized corrosion, *Materials Today*, **11** (2008) 38-44.
[47] R.J.R.E. Melchers, Corrosion tests of mild steel in temperature seawater, in: Research Report.217.12.2001, The university of Newcastle, Newcastle Australia, 2001.
[48] M. Nuñez, Prevention of metal corrosion: new research, Nova Publishers, 2007.
[49] S. Dallek, R. Foley, Mechanism of pit initiation on aluminum alloy type 7075, Journal of the Electrochemical Society, 123 (1976) 1775-1779.
[50] M.P. Ryan, Why Stainless steel corrodes, Nature 415, 6873 (202) 770-774.
[51] R. Melchers, Influence of seawater nutrient content on the early immersion corrosion of mild steel-Part 1: Empirical observations, Corrosion, 63 (2007) 318-329.
[52] R.E. Melchers, Probabilistic models for corrosion in structural reliability assessment—Part 2: models based on mechanics, Journal of Offshore Mechanics and Arctic Engineering, 125 (2003) 272-280.
[53] R.E. Melchers, Effect of small compositional changes on marine immersion corrosion of low alloy steels, *Corrosion science*, **46** (2004) 1669-1691.
[54] M.H. Moayed, N. Laycock, R. Newman, Dependence of the Critical Pitting Temperature on surface roughness, *Corrosion Science*, **45** (2003) 1203-1216.
[55] N. Greene, Predicting behavior of corrosion resistant alloys by potentiostatic polarization methods, Corrosion, 18 (1962) 136t-142t.
[56] S. Frangini, N. De Cristofaro, Analysis of the galvanostatic polarization method for determining reliable pitting potentials on stainless steels in crevice-free conditions, Corrosion science, 45 (2003) 2769-2786.
[57] I.M. Comotti, M. Trueba, S.P. Trasatti, The pit transition potential in the repassivation of aluminium alloys, Surface and interface analysis, 45 (2013) 1575-1584.
[58] A.-F.S.A. Malik Anees U, Pitting Behavior of Type 316L SS in Arabian Gulf Sea Water, Technical Report No.SWCC (RCD), (1992).
[59] B. Wilde, A critical appraisal of some popular laboratory electrochemical tests for predicting the localized corrosion resistance of stainless alloys in sea water, Corrosion, 28 (1972) 283-291.
[60] H. Böhni, Influence of temperature on the localized corrosion of stainless steels, Russian journal of electrochemistry, 36 (2000) 1122-1128.
[61] R. J Power, J. Shirokoff, Techniques for in situ corrosion studies of 316L stainless steel in sulfuric acid solutions, Recent Patents on Corrosion Science, 2 (2012) 2-21.
[62] D.N. Veritas, Risk based inspection of offshore topsides static mechanical equipment, (2002).

[63] L. Carpen, T. Hakkarainen, A. Sarpola, M. Riihimaki, J. Riimo, P. Kinnunen, P. Pohjanne, Localized corrosion risk of stainless steels under evaporative conditions, CORROSION 2007, (2007).
[64] H. Isaacs, G. Kissel, Surface preparation and pit propagation in stainless steels, Journal of the Electrochemical Society, 119 (1972) 1628-1632.
[65] S.F. Wika, Pitting and Crevice Corrosion of Stainless Steel under Offshore Conditions, in: Norwegian University of Science and Technology (NTNU), Norwegian University 2012.
[66] S. SH.M, Pitting Corrosion of Carbon Steel in Sodium Molybdate Solutions, in: University of Toronto, University of Toronto, U.T.O, 1990.
[67] R. Melchers, Modelling long term corrosion of steel infrastructure in natural marine environments, *Understanding Biocorrosion: Fundamentals and Applications*, **66** (2014) 213.
[68] M. Darmawan, Pitting corrosion model for reinforced concrete structures in a chloride environment, Magazine of Concrete Research, 62 (2010) 91-101.
[69] M. Darmawan, M. Stewart, Effect of pitting corrosion on capacity of prestressing wires, Magazine of Concrete Research, 59 (2007) 131-139.
[70] A. Davydov, Analysis of pitting corrosion rate, *Russian Journal of Electrochemistry*, **44** (2008) 835-839.
[71] C. Guedes Soares, Y. Garbatov, A. Zayed, Effect of environmental factors on steel plate corrosion under marine immersion conditions, Corrosion Engineering, Science and Technology, 46 (2011) 524-541.
[72] T. Nakai, H. Matsushita, N. Yamamoto, Effect of pitting corrosion on the ultimate strength of steel plates subjected to in-plane compression and bending, Journal of marine science and technology, 11 (2006) 52-64.
[73] P.A. Sørensen, S. Kiil, K. Dam-Johansen, C. Weinell, Anticorrosive coatings: a review, Journal of Coatings Technology and Research, 6 (2009) 135-176.
[74] R. Melchers, Effect of immersion depth on marine corrosion of mild steel, Corrosion, 61 (2005) 895-906.
[75] R. Melchers, Probabilistic modelling of immersion marine corrosion, Structural safety and reliability, 3 (1998) 1143-1149.
[76] A.U. Malik, S. Ahmad, I. Andijani, S. Al-Fouzan, Corrosion behavior of steels in Gulf seawater environment, Desalination, 123 (1999) 205-213.
[77] E. Ghali, W. Dietzel, K.-U. Kainer, General and localized corrosion of magnesium alloys: a critical review, Journal of Materials Engineering and Performance, 13 (2004) 7-23.
[78] N. Acuña-González, J.A. González-Sánchez, L.R. Dzib-Pérez, A. Rivas-Menchi, Early Corrosion Fatigue Damage on Stainless Steels Exposed to Tropical Seawater: A Contribution from Sensitive Electrochemical Techniques, (2012).
[79] R. Hadfield, The Corrosion of Iron and Steel, Proceedings of the Royal Society of London. Series A, Containing Papers of a Mathematical and Physical Character, (1922) 472-486.
[80] R. Melchers, Effect of temperature on the marine immersion corrosion of carbon steels, *Corrosion*, **58** (2002) 768-782.
[81] A. Younis, M. El-Sabbah, R. Holze, The effect of chloride concentration and pH on pitting corrosion of AA7075 aluminum alloy coated with phenyltrimethoxysilane, Journal of Solid State Electrochemistry, 16 (2012) 1033-1040.
[82] K.A. Chandler, Marine and offshore corrosion, (1985).

[83] R.W. Revie, Corrosion and corrosion control, John Wiley & Sons, 2008.
[84] P. Pistorius, G. Burstein, Growth of corrosion pits on stainless steel in chloride solution containing dilute sulphate, Corrosion science, 33 (1992) 1885-1897.
[85] K. Zakowski, M. Narozny, M. Szocinski, K. Darowicki, Influence of water salinity on corrosion risk—the case of the southern Baltic Sea coast, Environmental monitoring and assessment, (2014) 1-9.
[86] M. Yari, An Intro to Pipeline Corrosion in Seawater, in, corrosionpedia, 2014.
[87] A. Mercer, E. Lumbard, Corrosion of mild steel in water, British Corrosion Journal, 30 (1995) 43-55.
[88] R.E. Melchers, The effect of corrosion on the structural reliability of steel offshore structures, Corrosion Science, 47 (2005) 2391-2410.
[89] I.A.S.f.T. Materials, Annual book of ASTM standards, in, American Society for Testing & Materials, 2004.
[90] S. Qin, W. Cui, Effect of corrosion models on the time-dependent reliability of steel plated elements, Marine Structures, 16 (2003) 15-34.
[91] M. Salau, D. Esezobor, M. Omotoso, Reliability Assessment of Offshore Jacket Structures in Niger Delta, Petroleum & Coal, 53 (2011) 291-301.
[92] V. Zatkalíková, M. Bukovina, V. Škorík, L. Petreková, Pitting corrosion of aisi 316ti stainless steel with polished surface, Materials Engineering, 17 (2010) 15.
[93] R. Melchers, Effect of nutrient-based water pollution on the corrosion of mild steel in marine immersion conditions, Corrosion, 61 (2005) 237-245.
[94] S.A. Al-Fozan, A.U. Malik, Effect of seawater level on corrosion behavior of different alloys, *Desalination*, **228** (2008) 61-67.
[95] M. Zamanzadeh, E. Larkin, D. Gobbin, A re-examination of failure analysis and root cause determination, Pittsburgh, Pennsylvania, (2004).
[96] B.J. Little, J.S. Lee, R.I. Ray, The influence of marine biofilms on corrosion: a concise review, Electrochimica Acta, 54 (2008) 2-7.
[97] J.N. Friend, Deterioration of structures of timber, metal, and concrete exposed to the action of sea-water, (1940).
[98] J.R. Lewis, A.D. Mercer, Corrosion and marine growth on offshore structures, (1984).
[99] C. Southwell, A. Alexander, CORROSION OF METALS IN TROPICAL WATERS, STRUCTURAL FERROUS METALS, Materials Protection, 9 (1970).
[100] F. LaQue, Corrosion testing of electrodeposited coalings, in: Proc. AES, 1959, pp. 141.
[101] A. Malik, P. Mayan Kutty, N.A. Siddiqi, I.N. Andijani, S. Ahmed, The influence of pH and chloride concentration on the corrosion behaviour of AISI 316L steel in aqueous solutions, Corrosion science, 33 (1992) 1809-1827.
[102] A. Pardo, E. Otero, M. Merino, M. López, M. Utrilla, F. Moreno, Influence of pH and chloride concentration on the pitting and crevice corrosion behavior of high-alloy stainless steels, *Corrosion*, **56** (2000) 411-418.
[103] A.U. Malik, I.N. Andijani, N.A. Siddiqi, CORROSION BEHAVIOR OF SOME CONVENTIONAL AND HIGH ALLOY STAINLESS STEELS IN GULF SEAWATER1, in, Technical report, Saline Water Conversion Corporation, KSA, 1992.
[104] R. Newman, 2001 WR Whitney Award Lecture: Understanding the Corrosion of Stainless Steel, Corrosion, 57 (2001) 1030-1041.

[105] R. Melchers, Examples of mathematical modelling of long term general corrosion of structural steels in sea water, *Corrosion engineering, science and technology*, **41** (2006) 38-44.
[106] C. Thomas, R. Edyvean, R. Brook, Biologically enhanced corrosion fatigue, Biofouling, 1 (1988) 65-77.
[107] D. Schiffrin, S. De Sanchez, The effect of pollutants and bacterial microfouling on the corrosion of copper base alloys in seawater, Corrosion, 41 (1985) 31-38.
[108] W. Schultze, C.v.d. Wekken, Influence of alloying elements on the marine corrosion of low alloy steels determined by statistical analysis of published literature data, British Corrosion Journal, 11 (1976) 18-24.
[109] O.S. Ting, N.S. Potty, M. Shahir Liew, Prediction of corrosion rates in marine and offshore structures, in: National Postgraduate Conference (NPC), 2011, IEEE, 2011, pp. 1-6.
[110] R. Melchers, Modeling of marine immersion corrosion for mild and low-alloy steels-part 1: phenomenological model, *Corrosion*, **59** (2003) 319-334.
[111] A. Malik, N. Siddiqi, S. Ahmad, I. Andijani, The effect of dominant alloy additions on the corrosion behavior of some conventional and high alloy stainless steels in seawater, Corrosion science, 37 (1995) 1521-1535.
[112] P. Manning, D. Duquette, W. Savage, Technical Note: the effect of retained ferrite on localized corrosion in duplex 304L stainless steel, Weld. J, 59 (1980) 260-262.
[113] D.N. Veritas, Recommended practice DNV‐RP‐G 101: risk based inspection of offshore topside static mechanical equipment, Det Norske Veritas, Høvik, (2009).
[114] M. Norsok, 501: Surface preparation and protective coating, Norsok Standard M-501, Rev, 5 (2004).
[115] G.T. Bayer, M. Zamanzadeh, Failure analysis of paints and coatings, published internally by Matco Associates SUR FAC EPRE PA R AT IONANDC OAT INGAPPLI CAT IONPR AC TICES, 331 (2004).
[116] S. Xiong, Z. Zhu, L. Jing, Influence of Cl-ions on the pitting corrosion of boiler water-wall tube and its principle, Anti-Corrosion Methods and Materials, 59 (2012) 3-9.
[117] R. Jargelius-Pettersson, Application of the pitting resistance equivalent concept to some highly alloyed austenitic stainless steels, Corrosion, 54 (1998) 162-168.
[118] K. Lorenz, G. Medawar, Über das Korrosionsverhalten austenitischer Chrom-Nickel-(Molybdän-) Stähle mit und ohne Stickstoffzusatz unter besonderer Berücksichtigung ihrer Beanspruchbarkeit in chloridhaltigen Lösungen, Thyssenforschung, 1 (1969) 97-108.
[119] N.A. Johansen, Korrosjon på AISI 316‐rør. Utfordringer og tiltak, in, STATOIL, 2011.
[120] A. International, ASM handbook: Friction, lubrication, and wear technology, ASM International, 1992.
[121] S. Nešić, Key issues related to modelling of internal corrosion of oil and gas pipelines–A review, *Corrosion Science*, **49** (2007) 4308-4338.
[122] A. Stand, G46-94 (2005),“, Standard Guide for Examination and Evaluation of Pitting Corrosion,” ASTM International, West Conshohocken, PA.
[123] H. Kros, Performing detailed level 1 pipeline inspection in deep water with a remotely operated vehicle (ROV), in: offshore technology conference, Offshore Technology Conference, 2011.

[124] S. Jana, Non-destructive in-situ replication metallography, Journal of materials processing technology, 49 (1995) 85-114.
[125] D.S. Forsyth, –NON-DESTRUCTIVE TESTING FOR CORROSION, Corrosion Fatigue and Environmentally Assisted Cracking in Aging Military Vehicles (RTO-AG-AVT-140), (2011).
[126] D.S. Forsyth, H.T. Yolken, G.A. Matzkanin, A Brief Introduction to Nondestructive Testing, in, AMMTIAC Quarterly, 2006.
[127] E. Souza, S. Correa, A. Silva, R. Lopes, D. Oliveira, Methodology for digital radiography simulation using the Monte Carlo code MCNPX for industrial applications, Applied Radiation and Isotopes, 66 (2008) 587-592.
[128] W. Zhu, J. Rose, J. Barshinger, V. Agarwala, Ultrasonic guided wave NDT for hidden corrosion detection, Journal of Research in Nondestructive Evaluation, 10 (1998) 205-225.
[129] J. Riviere, Auger electron spectroscopy, Contemporary Physics, 14 (1973) 513-539.
[130] J.F. Watts, X-ray photoelectron spectroscopy, Vacuum, 45 (1994) 653-671.
[131] P. Williams, Secondary ion mass spectrometry, Annual Review of Materials Science, 15 (1985) 517-548.
[132] G. Engelhardt, D. Macdonald, Deterministic prediction of pit depth distribution, Corrosion, 54 (1998) 469-479.
[133] T. Shibata, T. Takeyama, Stochastic theory of pitting corrosion, Corrosion, 33 (1977) 243-251.
[134] G.A. Henshall, Modeling pitting corrosion damage of high-level radioactive-waste containers using a stochastic approach, Journal of Nuclear Materials, 195 (1992) 109-125.
[135] A. Valor, F. Caleyo, L. Alfonso, J. Velázquez, J. Hallen, Markov chain models for the stochastic modeling of pitting corrosion, Mathematical Problems in Engineering, 2013 (2013).
[136] A.G. Wilson, A statistical theory of spatial distribution models, Transportation research, 1 (1967) 253-269.
[137] P. Aziz, Application of the statistical theory of extreme values to the analysis of maximum pit depth data for aluminum, *Corrosion*, **12** (1956) 35-46.
[138] I.A. Chaves, R.E. Melchers, Extreme value analysis for assessing structural reliability of welded offshore steel structures, *Structural Safety*, **50** (2014) 9-15.
[139] R. Melchers, Statistical Characterization of pitting corrosion-part 2: probabilistic modeling for maximum pit depth, Corrosion, 61 (2005) 766-777.
[140] R. Melchers, M. Ahammed, R. Jeffrey, G. Simundic, Statistical characterization of surfaces of corroded steel plates, Marine Structures, 23 (2010) 274-287.
[141] R.E. Melchers, Extreme value statistics and long-term marine pitting corrosion of steel, *Probabilistic Engineering Mechanics*, **23** (2008) 482-488.
[142] P. Scheers, The effects of flow velocity and pH on the corrosion rate of mild steel in a synthetic minewater, Journal of the South African Institute of Mining and Metallurgy(South Africa), 92 (1992) 275-281.
[143] R.E. Melchers, R. Jeffrey, Probabilistic models for steel corrosion loss and pitting of marine infrastructure, *Reliability Engineering & System Safety*, **93** (2008) 423-432.
[144] R.E. Melchers, R. Jeffrey, Bacteria have transient influences on marine corrosion of steel, in: T.U.o. Newcastle (Ed.), The University of Newcastle, NSW Australia, 2011.

[145] R.E. Melchers, T. Wells, Models for the anaerobic phases of marine immersion corrosion, *Corrosion Science*, **48** (2006) 1791-1811.
[146] R.E. Melchers, Probabilistic models for corrosion in structural reliability assessment—Part 1: empirical models, Journal of Offshore Mechanics and Arctic Engineering, 125 (2003) 264-271.
[147] R.E. Melchers, Advances in Mathematical Probabilistic Modelling of the Atmospheric corrosion of Structural Steels in Ocean Environments, in: *3rd International ASRANet Colloquium*, Glasgow, UK, 2006, pp. 1-12.
[148] R.E. Melchers, Development of new applied models for steel corrosion in marine applications including shipping, *Ships and Offshore Structures*, **3** (2008) 135-144.
[149] R.E. Melchers, Microbiological and abiotic processes in modelling longer-term marine corrosion of steel, *Bioelectrochemistry*, **97** (2014) 89-96.
[150] R.E. Melchers, Modeling and Prediction of Long-Term Corrosion of Steel in Marine Environments, *International Journal of Offshore and Polar Engineering*, **22** (2012) 257-263.
[151] R. Melchers, Modeling of marine immersion corrosion for mild and low-alloy steels-part 2: uncertainty estimation, Corrosion, 59 (2003) 335-344.
[152] R. Melchers, Pitting corrosion of mild steel under marine anaerobic conditions-Part 1: Experimental observations, Corrosion, 62 (2006) 981-988.
[153] R. Melchers, R. Jeffrey, Modeling of long-term corrosion loss and pitting for chromium-bearing and stainless steels in seawater, *Corrosion*, **64** (2008) 143-154.
[154] R.E. Melchers, Probabilistic models of corrosion for reliability assessment and maintenance planning, in: 20th International Conference on Offshore Mechanics and Arctic Engineering, 2001, pp. 3-8.
[155] B. Rajani, Y. Kleiner, Comprehensive review of structural deterioration of water mains: physically based models, Urban water, 3 (2001) 151-164.
[156] Y. Katano, K. Miyata, H. Shimizu, T. Isogai, Predictive model for pit growth on underground pipes, *Corrosion*, **59** (2003) 155-161.
[157] C. Guedes Soares, Y. Garbatov, A. Zayed, G. Wang, R. Melchers, J. Paik, Non-linear corrosion model for immersed steel plates accounting for environmental factors. Discussion, *Transactions-Society of Naval Architects and Marine Engineers*, **113** (2005) 306-329.
[158] D. Mao, Bayesian modeling of pitting corrosion in steam generators, (2007).
[159] S. Paul, Modeling to Study the Effect of Environmental Parameters on Corrosion of Mild Steel in Seawater Using Neural Network, International Scholarly Research Notices, 2012 (2012).
[160] S. Jain, J.A. Beavers, F. Ayello, N. Sridhar, Probabilistic Model for Stress Corrosion Cracking of Underground Pipelines using Bayesian Networks, in: *CORROSION 2013, Paper No, 2616*, NACE International, Orlando, Florida, USA, 2013.
[161] A. Kolios, S. Srikanth, K. Salonitis, Numerical Simulation of Material Strength Deterioration due to Pitting Corrosion, Procedia CIRP, 13 (2014) 230-236.
[162] R.E. Melchers, Probabilistic model for marine corrosion of steel for structural reliability assessment, Journal of Structural Engineering, 129 (2003) 1484-1493.
[163] M. Kowaka, H. Tsuge, Introduction to life prediction of industrial plant materials: Application of the extreme value statistical method for corrosion analysis, Allerton Pr, 1994.

[164] H.M. Mohammad, N.J. Hammadi, R.M. Lafta, Prediction of Pitting Corrosion Characteristics using Artificial Neural Networks, International Journal of Computer Applications, 60 (2012).
[165] F.I. Khan, M.R. Haddara, Risk-based maintenance of ethylene oxide production facilities, Journal of Hazardous Materials, 108 (2004) 147-159.
[166] F.I. Khan, S. Abbasi, Analytical simulation and PROFAT II: a new methodology and a computer automated tool for fault tree analysis in chemical process industries, Journal of Hazardous Materials, 75 (2000) 1-27.
[167] L. Krishnasamy, F. Khan, M. Haddara, Development of a risk-based maintenance (RBM) strategy for a power-generating plant, Journal of Loss Prevention in the Process Industries, 18 (2005) 69-81.
[168] N. Arunraj, J. Maiti, Risk-based maintenance—Techniques and applications, Journal of Hazardous Materials, 142 (2007) 653-661.
[169] S. Yang, A condition-based preventive maintenance arrangement for thermal power plants, Electric Power Systems Research, 72 (2004) 49-62.
[170] M. Bertolini, M. Bevilacqua, F. Ciarapica, G. Giacchetta, Development of risk-based inspection and maintenance procedures for an oil refinery, Journal of Loss Prevention in the Process Industries, 22 (2009) 244-253.
[171] F.I. Khan, M. Haddara, Risk‐based maintenance (RBM): A new approach for process plant inspection and maintenance, Process Safety Progress, 23 (2004) 252-265.
[172] T. Suwanasri, R. Phadungthin, C. Suwanasri, Risk‐based maintenance for asset management of power transformer: practical experience in Thailand, International Transactions on Electrical Energy Systems, 24 (2014) 1103-1119.
[173] M. Abimbola, F. Khan, N. Khakzad, S. Butt, Safety and risk analysis of managed pressure drilling operation using Bayesian network, *Safety science*, **76** (2015) 133-144.
[174] P.K. Dey, A risk-based model for inspection and maintenance of cross-country petroleum pipeline, Journal of Quality in Maintenance Engineering, 7 (2001) 25-43.
[175] P. Hagemeijer, G. Kerkveld, A methodology for risk-based inspection of pressurized systems, Proceedings of the Institution of Mechanical Engineers, Part E: Journal of Process Mechanical Engineering, 212 (1998) 37-47.
[176] J.A. Harnly, Risk based prioritization of maintenance repair work, Process Safety Progress, 17 (1998) 32-38.
[177] F.I. Khan, M.M. Haddara, Risk-based maintenance (RBM): a quantitative approach for maintenance/inspection scheduling and planning, Journal of Loss Prevention in the Process Industries, 16 (2003) 561-573.
[178] N. Khakzad, F. Khan, P. Amyotte, Risk-based design of process systems using discrete-time Bayesian networks, Reliability Engineering & System Safety, 109 (2013) 5-17.
[179] F. Khan, R. Sadiq, M. Haddara, Risk-based inspection and maintenance (RBIM): multi-attribute decision-making with aggregative risk analysis, Process Safety and Environmental Protection, 82 (2004) 398-411.
[180] N. Siu, Risk assessment for dynamic systems: an overview, Reliability Engineering & System Safety, 43 (1994) 43-73.
[181] N. Khakzad, F. Khan, P. Amyotte, Safety analysis in process facilities: Comparison of fault tree and Bayesian network approaches, Reliability Engineering & System Safety, 96 (2011) 925-932.
[182] N. Khakzad, F. Khan, P. Amyotte, Quantitative risk analysis of offshore drilling operations: A Bayesian approach, Safety science, 57 (2013) 108-117.

[183] B. Jones, I. Jenkinson, Z. Yang, J. Wang, The use of Bayesian network modelling for maintenance planning in a manufacturing industry, Reliability Engineering & System Safety, 95 (2010) 267-277.
[184] P. Weber, G. Medina-Oliva, C. Simon, B. Iung, Overview on Bayesian networks applications for dependability, risk analysis and maintenance areas, Engineering Applications of Artificial Intelligence, 25 (2012) 671-682.
[185] B. Cai, Y. Liu, Z. Liu, X. Tian, Y. Zhang, R. Ji, Application of Bayesian networks in quantitative risk assessment of subsea blowout preventer operations, Risk Analysis, 33 (2013) 1293-1311.
[186] R. Neapolitan, Learning Bayesian Networks Pearson Prentice Hall, Upper Saddle River, New Jersey, (2004).
[187] N. Khakzad Rostami, Dynamic safety analysis using advanced approaches, in, Memorial University of Newfoundland, 2012.
[188] S. Jain, F. Ayello, J. Beavers, N. Sridhar, Probabilistic model for stress corrosion cracking of underground pipelines using Bayesian networks, in: Proc. of the NACE Int. Corros. Conf. Series, Corrosion, 2013, pp. 579-592.
[189] O. Participants, OREDA Offshore Reliability Data Handbook, in, DNV, PO Box, 2002.
[190] F. Lees, Loss prevention in CPI, in, London: Butterworths, 1996.
[191] I. Chaves, R. Melchers, Long term localised corrosion of marine steel piling welds, *Corrosion Engineering, Science and Technology*, **48** (2013) 469-474.
[192] G. Saville, S. Richardson, P. Barker, Leakage in ethylene pipelines, *Process Safety and Environmental Protection*, **82** (2004) 61-68.
[193] J. Bhandari, S. Lau, R. Abbassi, V. Garaniya, R. Ojeda, D. Lisson, F. Khan, Accelerated pitting corrosion test of 304 stainless steel using ASTM G48; experimental investigation and concomitant challenges, *Journal of Loss Prevention in the Process Industries*, **47** (2017) 10-21.
[194] O. Yevtushenko, D. Bettge, S. Bohraus, R. Bäßler, A. Pfennig, A. Kranzmann, Corrosion behavior of steels for CO 2 injection, *Process Safety and Environmental Protection*, **92** (2014) 108-118.
[195] J. Bhandari, F. Khan, R. Abbassi, V. Garaniya, R. Ojeda, Modelling of Pitting Corrosion in Marine and Offshore Steel Structures-A Technical Review, *Journal of Loss Prevention in the Process Industries*, **37** (2015) 39-62.
[196] J. Bhandari, F. Khan, R. Abbassi, V. Garaniya, R. Ojeda, Reliability assessment of offshore asset under pitting corrosion using Bayesian Network, in: *CORROSION 2016*, Paper No 7070, NACE International Houston, TX, Vancouver Canada, March 2016.
[197] H.-Y. Ha, H.-S. Kwon, Effects of pH levels on the surface charge and pitting corrosion resistance of Fe, *Journal of The Electrochemical Society*, **159** (2012) C416-C421.
[198] M.P. Ryan, D.E. Williams, R.J. Chater, B.M. Hutton, D.S. McPhail, Why stainless steel corrodes, *Nature*, **415** (2002) 770-774.
[199] R.E. Melchers, Using models to interpret data for monitoring and life prediction of deteriorating infrastructure systems, *Structure and Infrastructure Engineering*, **11** (2015) 63-72.
[200] W. Hou, C. Liang, Atmospheric corrosion prediction of steels, *Corrosion*, **60** (2004) 313-322.

[201] B.S. Phull, S.J. Pikul, R.M. Kain, Seawater corrosivity around the world: results from five years of testing, *ASTM special technical publication*, **1300** (1997) 34-73.
[202] T.D.J. Nielsen, Finn Verner, *Bayesian networks and decision graphs*, Springer Science & Business Media, Aalborg, Denmark, 2009.
[203] R.E. Neapolitan, *Learning bayesian networks*, Pearson Prentice Hall, Upper Saddle River, NJ, 2004.
[204] J. Pearl, S. Russell, Bayesian networks, *Computer Science Department, University of California*, Department of Statistics, UCLA (2011), 1998.
[205] M. Yang, F. Khan, P. Amyotte, Operational risk assessment: A case of the Bhopal disaster, *Process Safety and Environmental Protection*, **97** (2015) 70-79.
[206] J. Bhandari, R. Abbassi, V. Garaniya, F. Khan, Risk analysis of deepwater drilling operations using Bayesian network, *Journal of Loss Prevention in the Process Industries*, **38** (2015) 11-23.
[207] N. Khakzad, F. Khan, P. Amyotte, Dynamic safety analysis of process systems by mapping bow-tie into Bayesian network, *Process Safety and Environmental Protection*, **91** (2013) 46-53.
[208] M. Abimbola, F. Khan, N. Khakzad, Dynamic safety risk analysis of offshore drilling, *Journal of Loss Prevention in the Process Industries*, **30** (2014) 74-85.
[209] J. Bhandari, E. Arzaghi, R. Abbassi, V. Garaniya, F. Khan, Dynamic risk‐based maintenance for offshore processing facility, *Process Safety Progress*, **35** (2016) 399-406.
[210] B.W. Silverman, *Density estimation for statistics and data analysis*, CRC press, Florida, United States, 1986.
[211] Z.I. Botev, J.F. Grotowski, D.P. Kroese, Kernel density estimation via diffusion, *The Annals of Statistics*, **38** (2010) 2916-2957.
[212] E.L. Lehmann, Model specification: the views of Fisher and Neyman, and later developments, *Statistical Science*, **5** (1990) 160-168.
[213] F.I. Khan, M.M. Haddara, S.K. Bhattacharya, Risk‐Based Integrity and Inspection Modeling (RBIIM) of Process Components/System, *Risk analysis*, **26** (2006) 203-221.
[214] W. Zhu, An investigation into reliability based methods to include risk of failure in life cycle cost analysis of reinforced concrete bridge rehabilitation, in: *School of Civil, Environmental and Chemical Engineering RMIT University*, Victoria, Australia, 2008.
[215] C. Southwell, B. Forgeson, A. Alexander, Corrosion of Metals in Tropical Environments (Part 2-Atmospheric Corrosion of Ten Structural Steels), *Corrosion*, **14** (1958) 55-59.
[216] G. Sowinski, Sprowls, DO, *Atmospheric corrosion*, in: John Wiley and Sons, New York, USA, 1982, pp. 297-328.
[217] P. Aziz, H.P. Godard, Pitting Corrosion Characteristics of Aluminum-Influence of Magnesium and Manganese, *Industrial & Engineering Chemistry*, **44** (1952) 1791-1795.
[218] A.B. Tesler, P. Kim, S. Kolle, C. Howell, O. Ahanotu, J. Aizenberg, Extremely durable biofouling-resistant metallic surfaces based on electrodeposited nanoporous tungstite films on steel, Nature communications, 6 (2015).
[219] N.J. Laycock, D.P. Krouse, S.C. Hendy, D.E. Williams, Computer simulation of pitting corrosion of stainless steels, The Electrochemical Society Interface, 23 (2014) 65-71.

[220] R.B. Ribeiro, J. Silva, L. Hein, M. Pereira, E. Codaro, N. Matias, Morphology Characterisation of Pitting Corrosion on Sensitized Austenitic Stainless Steel by Digital Image Analysis, ISRN Corrosion, 2013 (2013).
[221] C. Lee, B. Batchelor, S.H. Park, D.S. Han, A. Abdel-Wahab, T.A. Kramer, Perchlorate reduction during electrochemically induced pitting corrosion of zero-valent titanium (ZVT), Journal of hazardous materials, 197 (2011) 183-189.
[222] W. Tian, N. Du, S. Li, S. Chen, Q. Wu, Metastable pitting corrosion of 304 stainless steel in 3.5% NaCl solution, Corrosion Science, 85 (2014) 372-379.
[223] A. Krzemień, A. Więckol-Ryk, A. Smoliński, A. Koteras, L. Więcław-Solny, Assessing the risk of corrosion in amine-based CO 2 capture process, Journal of Loss Prevention in the Process Industries, 43 (2016) 189-197.
[224] A.A. Khadom, A.F. Hassan, B.M. Abod, Evaluation of environmentally friendly inhibitor for galvanic corrosion of steel–copper couple in petroleum waste water, Process Safety and Environmental Protection, 98 (2015) 93-101.
[225] R. Murata, J. Benaquisto, C. Storey, A methodology for identifying and addressing dead-legs and corrosion issues in a Process Hazard Analysis (PHA), Journal of Loss Prevention in the Process Industries, 35 (2015) 387-392.
[226] D. Ward, Correlation of accelerated corrosion testing with natural exposure after 6+ years in a coastal environment, in: CORROSION 2008, NACE International, 2008.
[227] J.W. Oldfield, Test techniques for pitting and crevice corrosion resistance of stainless steels and nickel-base alloys in chloride-containing environments, International Materials Reviews, 32 (1987) 153-172.
[228] S. Kavitha, P.C. Stella, S. Kaliappan, I.T. Yeom, J.R. Banu, Enhancement of anaerobic degradation of sludge biomass through surfactant-assisted bacterial hydrolysis, Process Safety and Environmental Protection, 99 (2016) 207-215.
[229] S. Caines, F. Khan, J. Shirokoff, W. Qiu, Experimental design to study corrosion under insulation in harsh marine environments, Journal of Loss Prevention in the Process Industries, 33 (2015) 39-51.
[230] X. Tang, Y. Cheng, Quantitative characterization by micro-electrochemical measurements of the synergism of hydrogen, stress and dissolution on near-neutral pH stress corrosion cracking of pipelines, Corrosion Science, 53 (2011) 2927-2933.
[231] D.O. Thompson, D.E. Chimenti, Review of progress in quantitative nondestructive evaluation, Springer Science & Business Media, 2012.
[232] T. Mathiesen, P. Alle, A. Andersen, Challenges in Pre-Qualification Corrosion Testing of CRAs based on ASTM G48, in: CORROSION 2014, NACE International, 2014.
[233] J.R. Maurer, Optimizing surface quality of stainless alloys and using a modified ASTM G 48B procedure for acceptance testing, Materials performance, 38 (1999).
[234] A. G48-11, Standard Test Methods for Pitting and Crevice Corrosion Resistance of Stainless Steels and Related Alloys by Use of Ferric Chloride Solution, ASTM International, (2009).
[235] N. Nagaswami, M. Streicher, Accelerated Laboratory Tests for Crevice Corrosion of Stainless Alloys, Corrosion83, (1983) 1983.
[236] V. Salinas-Bravo, R. Newman, An alternative method to determine critical pitting temperature of stainless steels in ferric chloride solution, Corrosion science, 36 (1994) 67-77.
[237] A. Garner, Crevice corrosion of stainless steels in sea water: correlation of field data with laboratory ferric chloride tests, Corrosion, 37 (1981) 178-184.

[238] L. Garfias-Mesias, S. Taylor, In-situ Pitting of UNS S32550 Duplex Stainless Steel in Artificial Seawater below and above the Critical Pitting Temperature, (2016).
[239] R. Corbett, Problems in Utilizing ASTM G 48 to Evaluate High-Alloy Stainless Steels, R. A. Corbett, Paper, (1992).
[240] M. Hoseinpoor, M. Momeni, M. Moayed, A. Davoodi, EIS assessment of critical pitting temperature of 2205 duplex stainless steel in acidified ferric chloride solution, Corrosion Science, 80 (2014) 197-204.
[241] P. Woollin, Ferric chloride testing for weld procedure qualification of duplex stainless steel weldments, UK Corrosion and Eurocorr 94., 3 (1994) 51-60.
[242] A. ASTM, 262-93a: Standard Practices for Detecting Susceptibility to Intergranular Attack in Austenitic Stainless Steels, ASTM International, West Conshohocken, (2004) 42.
[243] G.W. Byrne, G Wilson, J Francis, R, Fabrication of superduplex stainless steel for optimum seawater corrosion resistance, in: World Congress/Perth Convention and Exhibition Centre (PCEC), Perth, Western Australia September 4-9, 2011, 2011.
[244] H. Zitter, G. Mori, G. Hochörtler, H. Wieser, Evaluation of CPT values determined by ASTM G48 practice. Report on round robin tests of the Corrosion Committee of the Austrian Society of Metallurgy, Materials and Corrosion, 53 (2002) 37-43.
[245] E. Bakrachevska, Analysis of corrosion resistance property of cold bended 316L and 6Mo stainless steel pipes, (2014).
[246] F.-Y. Ma, Corrosive effects of chlorides on metals, INTECH Open Access Publisher, 2012.
[247] G.S. Haynes, Laboratory corrosion tests and standards: a symposium by ASTM Committee G-1 on Corrosion of Metals, Bal Harbour, FL, 14-16 Nov. 1983, ASTM International, 1985.
[248] A. Standard, G61-86:'Conducting Cyclic Potentiodynamic Polarization Measurements for Localized Corrosion Susceptibility in Iron, Nickel-, or Cobalt-Based Alloys', ASTM Standards, ASTM, Philadelphia, PA, USA, (1986).
[249] W. Wang, Q. Wang, C. Wang, J. Yi, Experimental studies of crevice corrosion for buried pipeline with disbonded coatings under cathodic protection, Journal of Loss Prevention in the Process Industries, 29 (2014) 163-169.
[250] Y. Wang, G. Cheng, Y. Li, Observation of the pitting corrosion and uniform corrosion for X80 steel in 3.5 wt.% NaCl solutions using in-situ and 3-D measuring microscope, Corrosion Science, (2016).
[251] R. Brigham, E. Tozer, Temperature as a pitting criterion, Corrosion, 29 (1973) 33-36.
[252] E. Hibner, Evaluation of Test Procedures for Critical Crevice Temperature Determination for Nickel Alloys in a Ferric Chloride Environment, E. L. Hibner, Inco Alloys International, Inc. Huntington, WV 25720, Corrosion 86/181 NACE Houston, (1987).
[253] J.J. Moloney, W.Y. Mok, C.M. Menendez, In situ assessment of pitting corrosion and its inhibition using a localized corrosion monitoring technique, Corrosion, 66 (2010) 065003-065003-065018.
[254] J. Thompson, R. McKay, The Control of Motion and Aeration in Corrosion Tests, Industrial & Engineering Chemistry, 15 (1923) 1114-1118.
[255] S.H. Mameng, A. Bergquist, E. Johansson, Corrosion of Stainless Steel in Sodium Chloride Brine Solutions, in: CORROSION 2014, NACE International, 2014.

[256] M.T. Woldemedhin, R.G. Kelly, Evaluation of the maximum pit size model on stainless steel under atmospheric conditions, ECS Transactions, 58 (2014) 41-50.
[257] E. Otero, A. Pardo, M. Utrilla, E. Sáenz, F. Perez, Influence of microstructure on the corrosion resistance of AISI type 304L and type 316L sintered stainless steels exposed to ferric chloride solution, Materials characterization, 35 (1995) 145-151.
[258] D. Rivas, F. Caleyo, A. Valor, J. Hallen, Extreme value analysis applied to pitting corrosion experiments in low carbon steel: Comparison of block maxima and peak over threshold approaches, Corrosion Science, 50 (2008) 3193-3204.
[259] M. Khalifa, F. Khan, M. Haddara, A methodology for calculating sample size to assess localized corrosion of process components, Journal of Loss Prevention in the Process Industries, 25 (2012) 70-80.
[260] F. Caleyo, J. Velázquez, A. Valor, J. Hallen, Probability distribution of pitting corrosion depth and rate in underground pipelines: A Monte Carlo study, Corrosion Science, 51 (2009) 1925-1934.
[261] F. Caleyo, J. Velázquez, A. Valor, J. Hallen, Markov chain modelling of pitting corrosion in underground pipelines, Corrosion Science, 51 (2009) 2197-2207.
[262] Y. Mori, B.R. Ellingwood, Reliability-based service-life assessment of aging concrete structures, Journal of Structural Engineering, 119 (1993) 1600-1621.
[263] J.K. Paik, J.M. Lee, M.J. Ko, Ultimate shear strength of plate elements with pit corrosion wastage, Thin-Walled Structures, 42 (2004) 1161-1176.
[264] Z.H. Mohammad, E. Nouri, M.R. Khedmati, M.M. Roshanali, Degradation of the compressive strength of unstiffened/stiffened steel plates due to both-sides randomly distributed corrosion wastage, Latin American Journal of Solids and Structures, 7 (2010) 335-367.
[265] P. Sharma, H. Roy, Pitting corrosion failure of an AISI stainless steel pointer rod, Engineering Failure Analysis, 44 (2014) 400-407.
[266] E.M. Zahrani, A. Saatchi, A. Alfantazi, Pitting of 316L stainless steel in flare piping of a petrochemical plant, Engineering Failure Analysis, 17 (2010) 810-817.
[267] H. Liu, F. Khan, P. Thodi, Revised burst model for pipeline integrity assessment, Engineering Failure Analysis, (2017).
[268] Y. Wang, J.A. Wharton, R.A. Shenoi, Ultimate strength analysis of aged steel-plated structures exposed to marine corrosion damage: A review, Corrosion Science, 86 (2014) 42-60.
[269] D. Ok, Y. Pu, A. Incecik, Computation of ultimate strength of locally corroded unstiffened plates under uniaxial compression, Marine Structures, 20 (2007) 100-114.
[270] T.E. Dunbar, N. Pegg, F. Taheri, L. Jiang, A computational investigation of the effects of localized corrosion on plates and stiffened panels, Marine Structures, 17 (2004) 385-402.
[271] S. Arun, A.H. Sherry, M.C. Smith, M. Sheikh, Finite element simulation of a circumferential through-thickness crack in a cylinder, in: ASME 2014 Pressure Vessels and Piping Conference, American Society of Mechanical Engineers, 2014, pp. V003T003A086-V003T003A086.
[272] X. Jiang, C.G. Soares, Ultimate compressive capacity of rectangular plates with partial depth pits, Journal of Offshore Mechanics and Arctic Engineering, 135 (2013) 021401.
[273] J. Paik, J. Lee, M. Ko, Ultimate compressive strength of plate elements with pit corrosion wastage, Proceedings of the Institution of Mechanical Engineers, Part M: Journal of Engineering for the Maritime Environment, 217 (2003) 185-200.

[274] J.K. Paik, A.K. Thayamballi, Ultimate limit state design of steel-plated structures, John Wiley & Sons, 2003.
[275] H.K. Amlashi, T. Moan, Ultimate strength analysis of a bulk carrier hull girder under alternate hold loading condition–A case study: Part 1: Nonlinear finite element modelling and ultimate hull girder capacity, Marine structures, 21 (2008) 327-352.
[276] J. Silva, Y. Garbatov, C.G. Soares, Ultimate strength assessment of ageing steel plates subjected to random non-uniform corrosion wastage, Advances in Marine Structures, (2011) 213-220.
[277] Y. Huang, Y. Zhang, G. Liu, Q. Zhang, Ultimate strength assessment of hull structural plate with pitting corrosion damnification under biaxial compression, Ocean Engineering, 37 (2010) 1503-1512.
[278] J. Silva, Y. Garbatov, C.G. Soares, Ultimate strength assessment of rectangular steel plates subjected to a random localised corrosion degradation, Engineering Structures, 52 (2013) 295-305.
[279] J. Paik, A. Thayamballi, Ultimate strength of ageing ships, Proceedings of the Institution of Mechanical Engineers, Part M: Journal of Engineering for the Maritime Environment, 216 (2002) 57-77.
[280] A.P. Teixeira, C.G. Soares, Ultimate strength of plates with random fields of corrosion, Structure and Infrastructure Engineering, 4 (2008) 363-370.
[281] Y. Sharifi, J.K. Paik, Ultimate strength reliability analysis of corroded steel-box girder bridges, Thin-Walled Structures, 49 (2011) 157-166.
[282] Y. Garbatov, M. Tekgoz, C.G. Soares, Experimental and numerical strength assessment of stiffened plates subjected to severe non-uniform corrosion degradation and compressive load, Ships and Offshore Structures, (2016) 1-13.
[283] Y. Garbatov, C.G. Soares, J. Parunov, J. Kodvanj, Tensile strength assessment of corroded small scale specimens, Corrosion science, 85 (2014) 296-303.
[284] M. Cerit, K. Genel, S. Eksi, Numerical investigation on stress concentration of corrosion pit, Engineering Failure Analysis, 16 (2009) 2467-2472.
[285] T. Nakai, H. Matsushita, N. Yamamoto, H. Arai, Effect of pitting corrosion on local strength of hold frames of bulk carriers (1st report), Marine structures, 17 (2004) 403-432.
[286] S. Sultana, Y. Wang, A. Sobey, J. Wharton, R. Shenoi, Influence of corrosion on the ultimate compressive strength of steel plates and stiffened panels, Thin-Walled Structures, 96 (2015) 95-104.
[287] S. Rahmdel, K. Kim, S. Kim, S. Park, A novel stepwise method to predict ultimate strength reduction in offshore structures with pitting corrosion, Advances in Mechanical Engineering, 7 (2015) 1687814015600677.
[288] A. Standard, Metallic materials—tensile testing at ambient temperature, AS 1391-2007, Australia, (2007).
[289] T. Lyman, Metals handbook, American Society for Metals, 1967.
[290] D. ASTM, 882, Standard test methods for tensile, properties of thin plastic sheeting, (2002).
[291] O.C. Zienkiewicz, R.L. Taylor, O.C. Zienkiewicz, R.L. Taylor, The finite element method, McGraw-hill London, 1977.
[292] R. Blandford, D. Morton, S. Snow, T. Rahl, Tensile stress-strain results for 304L and 316L stainless steel plate at temperature, in: ASME 2007 Pressure Vessels and Piping Conference, American Society of Mechanical Engineers, 2007, pp. 617-628.

[293] D.K. Morton, R.K. Blandford, S.D. Snow, Impact Testing of Stainless Steel Material at Cold Temperatures, in: ASME 2008 Pressure Vessels and Piping Conference, American Society of Mechanical Engineers, 2008, pp. 183-193.
[294] H. Wang, G. Wang, F. Xuan, S. Tu, Numerical investigation of ductile crack growth behavior in a dissimilar metal welded joint, Nuclear Engineering and Design, 241 (2011) 3234-3243.
[295] C.W. Solbrig, J. Andrus, C. Pope, ZPPR Fuel Element Thermal Stress-Strain Analysis, World Journal of Nuclear Science and Technology, 2014 (2014).
[296] W.A. Poling, Grain size effects in micro-tensile testing of austenitic stainless steel, in, Colorado School of Mines. Arthur Lakes Library, 2007.
[297] S. Moaveni, Finite Element Analysis Theory and Application with ANSYS, 3/e, Pearson Education India, 2008.
[298] E. Gutman, G. Solovioff, D. Eliezer, The mechanochemical behavior of type 316L stainless steel, Corrosion science, 38 (1996) 1141-1145.